Institute of Geophysics
Polish Academy of Sciences

IAHR AIRH International Association for Hydro-Environment Engineering and Research
Hosted by Spain Water and IWHR, China

IAHR YPN Young Professionals Network
Hosted by Spain Water and IWHR, China

PUBLICATIONS OF THE INSTITUTE OF GEOPHYSICS POLISH ACADEMY OF SCIENCES

Geophysical Data Bases, Processing and Instrumentation

434 (E-11)

BOOK OF EXTENDED ABSTRACTS

Webinar
on Experimental Methods
and Laboratory Instrumentation in Hydraulics,
13-15 April 2021

Warsaw 2021 (Issue 3)

INSTITUTE OF GEOPHYSICS
POLISH ACADEMY OF SCIENCES

PUBLICATIONS
OF THE INSTITUTE OF GEOPHYSICS
POLISH ACADEMY OF SCIENCES

Geophysical Data Bases, Processing and Instrumentation

434 (E-11)

BOOK OF EXTENDED ABSTRACTS

Webinar
on Experimental Methods
and Laboratory Instrumentation in Hydraulics,
13-15 April 2021

Warsaw 2021

Published by the Institute of Geophysics, Polish Academy of Sciences

ISBN 978-83-66254-06-0 eISSN-2299-8020
DOI: 10.25171/InstGeoph_PAS_Publs-2021-039

Editorial Office
Instytut Geofizyki Polskiej Akademii Nauk
ul. Księcia Janusza 64, 01-452 Warszawa

C O N T E N T S

Publications of the Institute of Geophysics, Polish Academy of Sciences
Geophysical Data Bases, Processing and Instrumentation
vol. 434 (E-11), 2021, pp. 3-4
DOI: 10.25171/InstGeoph_PAS_Publs-2021-003
Webinar on Experimental Methods and Laboratory Instrumentation in Hydraulics, 13-15 April 2021

Experimental Methods and Laboratory Instrumentation in Hydraulics

PREFACE

The recent development of equipment and software for hydraulic measurements, data analysis, and visualization, has introduced new opportunities but also new challenges for research and technical cadre.

The advanced methods and techniques are significantly contributing to a more comprehensive approach in analyzing research problems, enabling testing new theories and adding new study possibilities. Such advancements are particularly important for experimental studies which rely on good data quality and reliable methodology. The set-up of new equipment often requires the development of custom solutions, acquisition of new skills and experience to be able to interpret the data. In the multitude of available equipment, laboratory setups, and techniques, it is necessary to exchange knowledge and experience to identify the best solutions to solve challenging research problems. This information is rarely covered in scientific communication. Thus, this webinar was designed to serve as a platform for academics, technicians, and practitioners from the industry to share their experience in modern hydraulic experimental approaches. Presentations were then specifically chosen to tackle state-of-the-art and well-established methods employed for measuring e.g. the water velocity, density, particle tracking, quantification of acting forces in water, numerical description of bed geometry.

The main aim of this webinar was therefore to bring together young and experienced researchers, who are often pioneers in implementing some methods, and specialists from the industry. The former group is also connected with IAHR Young Professionals Network, which gathers both students and scientists and is a part of this webinar. We believe the participation of young people is especially important to foster their professional development, to help them in seeking the newest, most optimal methods for their investigations and to build a community of future specialists. This would not be possible without the participation of experienced researchers and practitioners who often operate with top-grade equipment. We hope that the webinar will spark a meaningful discussion, initiate new ideas and promote collaboration between participants in the near future.

The present work is summarizing the outcomes of a webinar on Experimental Methods and Laboratory Instrumentations in Hydraulics, co-organized by the Institute of Geophysics of the Polish Academy of Sciences, the IAHR Committee on Experimental Methods and Instrumentation and the IAHR Poland Young Professional Network. During the webinar, six keynote lectures will combine with three speeches from industry representatives and 27 technical contributions, mainly coming from young researchers.

In terms of the geographical distribution of the abstracts, around 15 countries are represented, showing the importance of the topic in the actual literature, and the willingness for developing international and transdisciplinary connections.

We would like to acknowledge the contribution of the Scientific Committee, which helped us in judging the abstracts, suggesting changes and future directions that, hopefully, can contribute to new outcomes and in filling gaps in the understanding of fluid dynamics at the laboratory scale.

Local Organizing Committee

Giulio Dolcetti
Łukasz Przyborowski
Magdalena Mrokowska
Michael Nones
Slaven Conevski

Publications of the Institute of Geophysics, Polish Academy of Sciences
Geophysical Data Bases, Processing and Instrumentation
vol. 434 (E-11), 2021, pp. 5-7
DOI: 10.25171/InstGeoph_PAS_Publs-2021-004
Webinar on Experimental Methods and Laboratory Instrumentation in Hydraulics, 13-15 April 2021

Hydro-acoustic Techniques in Hydraulics Engineering

Massimo GUERRERO

Department of Civil, Chemical, Environmental and Materials Engineering, University of Bologna, Bologna, Italy

✉ massimo.guerrero@unibo.it

A b s t r a c t

Underwater sound techniques began since Leonardo Da Vinci which listened to approaching ships by using a tube in water and placing its outer extremity to hear. The sound speed into water was firstly measured on Lake Geneva in 1826 whereas the modern acoustics is due to Lord Rayleigh which lived in the late 19th and early 20th century. In spite of these well consolidated bases, the using of acoustic techniques in hydraulics is pretty recent and developed in parallel for laboratory and field applications. Ultrasound techniques are particularly relevant in case of opaque fluids and for no optical access through boundaries. This talk delineates important features of hydro-acoustics and the instruments used. Some experiences show the acoustic investigation of sediment transport, which has always been a challenging task in riverine environment, and sea waves tests carried out at the hydraulic laboratory of the University of Bologna.

Keywords: hydro-acoustics, Doppler effect, backscatter, sediment transport, waves impact.

1. INTRODUCTION

Hydro-acoustics is a quite novel discipline which is the application of underwater sound to investigate a variety of parameters in hydraulics (e.g., water depth, flow discharge, suspended sediment concentration, bedforms). The using of underwater sound began since centuries but technical advancement were mainly produced while aiming at locating submarine targets during the world wars which gave rise to SOund Navigation And Ranging technology (i.e., SONAR) and has laid the foundation for following environmental, engineering and medical applications. Particularly relevant for the hydraulic engineers, the development of the Acoustic Doppler Current Profiler – ADCP (Gordon 1996) and the Ultrasound Velocity Profiler – UVP (Takeda 1986) enabled the velocity profiling of a water column in the field and in laboratory, respectively. Both these technologies relies on the scattering back of sound from particles transported

by the fluid flow. The projected sound by active transducers is then received at the same transducers that is typical for mono-static configuration. The receivers and the projector are different transducers in the bistatic configuration which was evenly implemented for punctual measurement, the Acoustic Doppler Velocimeter – ADV, and more recently for velocity profiling: the Acoustic Doppler Velocity Profiler – ADVP (UBERTONE 2019). Emitted and received signals differs of the Doppler shift that is linearly correlated with the particles velocity by means of speed of sound into the fluid. While this represents a direct velocity measurement (i.e., with no need for calibration) a number of physical limitations must be carefully considered when designing an experimental campaign. These affect the measurable range, the resolution and accuracy and undermine the reliability of measured velocity profiles. This combines with the signal modulation and following processing adopted by instrumental developers. As a matter of fact different technologies developed depending on the targeted application. For example the ADCP uses the broadband technology which enables accurate and detailed profiling in a variety of field conditions but makes the returning signal uncorrelated in case of extreme conditions. Differently, the UVP typically applies two pulse coherent technique which is subjected to Aliasing but allows a larger control to end users.

2. EXPERIENCES IN USING HYDROACOUSTC TECHNIQUES

Laboratory and field applications parallelly developed and a number of acoustically based methodologies thrived aiming at measuring specific parameters and for well-defined ranges. In any case, hydro-acoustics is particularly relevant in case of opaque fluids that is exactly the case of sediment transport measurement in the turbid river flow, and for no optical access through boundaries that may be the case of many experimental set-ups in the hydraulic laboratory (e.g., wavy water surface). Therefore, we aimed at characterizing the suspended sediment transport and bedload in rivers by using the ADCP that is usually available in the field for river flow discharge measurement. This research effort entailed the testing of backscattering, mono-static and bi-static technologies (i.e., UVP and ADVP) under controlled condition in different laboratories which produced some methodologies for the profiling of suspended sand from river bed in large rivers (Guerrero and Lamberti 2011; Guerrero et al. 2013; Szupiany et al. 2019), the continuous monitoring of suspended sediment transport at river channel stream (Guerrero and Di Federico 2018; Aleixo et al. 2020) and the estimation of bedload rate at riverbed (Conevski et al. 2019, 2020). Furthermore, we applied the UVP in experimental set-ups characterized with wavy surface and transient conditions partially disabling optical methods deploying from water surface. These were the cases of reconstructing the hydraulic conditions which mobilized coastal mega boulders (Bressan et al. 2018) and the testing of overtopping processes at scaled dikes (Gaeta et al. 2020).

Acknowledgments. I greatly acknowledge all my co-authors: the mentioned results would not have been possible without their valuable and prevalent contributes.

References

Aleixo, R., M. Guerrero, M. Nones, and N. Ruther (2020), Applying ADCPs for long-term monitoring of SSC in rivers, *Water Resour. Res.* **56**, 1, e2019WR026087, DOI: 10.1029/2019WR026087.

Bressan, L., M. Guerrero, A. Antonini, V. Petruzzelli, R. Archetti, A. Lamberti , and S. Tinti (2018), A laboratory experiment on the incipient motion of boulders by high-energy coastal flows, *Earth Surf. Process. Landforms*, **43**, 14, 2935–2947, DOI: 10.1002/esp.4461.

Conevski, S., M. Guerrero, N. Ruther, and C.D. Rennie (2019), Laboratory investigation of apparent bedload velocity measured by ADCPs under different transport conditions, *ASCE J. Hydraul. Eng.* **145**, 11, 04019036, DOI: 10.1061/(ASCE)HY.1943-7900.0001632.

Conevski, S., R. Aleixo, M. Guerrero, and N. Ruther (2020), Bedload velocity and backscattering strength from mobile sediment bed: A laboratory investigation comparing bistatic versus monostatic acoustic configuration, *Water* **12**, 12, 3318, DOI: 10.3390/w12123318.

Gaeta, M.G., M. Guerrero, S.M. Formentin, G. Palma, and B. Zanuttigh (2020), Non-intrusive measurements of wave-induced flow over dikes by means of a combined ultrasound Doppler velocimetry and videography, *Water* **12**, 11, 3053, DOI: 10.3390/w12113053.

Gordon, R.L. (1996), *Acoustic Doppler Current Profiler. Principles of Operation: A Practical Primer*, 2nd ed., R.D. Instruments, San Diego.

Guerrero, M., and V. Di Federico (2018), Suspended sediment assessment by combining sound attenuation and backscatter measurements – analytical method and experimental validation, *Adv. Water Resour.* **113**, 167–179, DOI: 10.1016/j.advwatres.2018.01.020.

Guerrero, M., and A. Lamberti (2011), Flow field and morphology mapping using ADCP and multibeam techniques: Survey in the Po River, *ASCE J. Hydraul. Eng.* **137**, 12, 1576–1587, DOI: 10.1061/(ASCE)HY.1943-7900.0000464.

Guerrero, M., R.N. Szupiany, and F. Latosinski (2013), Multi-frequency acoustics for suspended sediment studies: an application in the Parana River, *J. Hydraul. Res.* **51**, 6, 696-707, DOI: 10.1080/00221686.2013.849296.

Szupiany, R.N., C. Lopez Weibel, M. Guerrero, F. Latosinski, M. Wood, L. Dominguez Ruben, and K. Oberg (2019), Estimating sand concentrations using ADCP-based acoustic inversion in a large fluvial system characterized by bi-modal suspended-sediment distributions, *Earth Surf. Process. Landforms*, **44**, 6, 1295–1308, DOI: 10.1002/esp.4572.

Takeda, Y. (1986), Velocity profile measurement by ultrasound Doppler shift method, *Int. J. Heat Fluid Flow* **7**, 4, 313–318, DOI: 10.1016/0142-727X(86)90011-1.

UBERTONE (2019), *ADVP Measurement Principle—User Manual*, UBERTONE, Schiltigheim, France.

Received 22 March 2021
Accepted 12 April 2021

Publications of the Institute of Geophysics, Polish Academy of Sciences
Geophysical Data Bases, Processing and Instrumentation
vol. 434 (E-11), 2021, pp. 9-10
DOI: 10.25171/InstGeoph_PAS_Publs-2021-005
Webinar on Experimental Methods and Laboratory Instrumentation in Hydraulics, 13-15 April 2021

Automating Hydraulic Engineering Experiments

Stuart CAMERON

University of Aberdeen, School of Engineering, Aberdeen, United Kingdom

✉ s.cameron@abdn.ac.uk

A b s t r a c t

Automating hydraulic engineering experiments may allow an increased number of scenarios or repetitions to be studied within a research programme and additionally increase measurement precision by reducing human errors. Several aspects of the Aberdeen Open Channel Facility (AOCF) have already been automated, including flow configuration and control and stereoscopic particle image velocimetry deployment and calibration. We expect these developments to contribute to scientific progress through enabling larger systematic data sets in future studies.

Keywords: automation, particle image velocimetry, open-channel flume.

1. INTRODUCTION

Hydraulic engineering research often involves a large parameter space requiring systematic experiments to fully uncover underlying physical mechanisms. For example, uniform, steady, open-channel flow over a rough bed may be characterised by the flow depth (H), the shear velocity (u_*), the depth averaged velocity (U), the channel width (B), the bed slope (S_b), the fluid density and viscosity (ρ and ν), the roughness height or particle size (Δ), and potentially additional length scales describing the roughness geometry. To study hydraulic resistance or turbulence structure, for example, the number of experiments required to explore the relevant parameter space may be unachievable with traditional laboratory flumes and measurement technologies. These restrictions on the amount of data that can be captured during a research programme ultimately limit scientific progress. In this paper, we explore how automating aspects of hydraulic engineering experiments can address this shortfall, with particular focus on automating PIV deployment and flume setup and configuration.

2. AUTOMATING HYDRAULIC FLUMES AND INSTRUMENTATION

Automation in this context means to bring aspects of an experiment under the control of a computer software programme. One reason to attempt this is to reduce experiment setup time and reduce down-time between experiments. Automation, however, has additional benefits in that experiment methodology is precisely defined by a computer programme. Therefore, results are highly repeatable, human error is minimised and produced data is of higher quality. At the University of Aberdeen we have been exploring how automation can support our research projects. In the following, a few examples of our progress to date are outlined.

2.1 Particle image velocimetry

Stereoscopic particle image velocimetry poses several challenges that must be overcome before it can be programmatically controlled to deploy across a sequence of measurement positions. Firstly, "water prisms" attached to flume sidewalls are conventionally used to limit internal reflection and image distortion, however, they prevent the measurement plane from being traversed. Secondly, a typical calibration procedure involves creating near still-water conditions in the channel, then taking pictures of a dot grid calibration plate manually positioned at several different points within the camera field of view. We have addressed these challenges by designing a "semi immersible" camera lens and implementing a single point calibration technique. The semi-immersible lens was designed such that a prism at the tip of the lens just penetrates the water surface. The camera can then be traversed within the channel, free from the constraints of the water prisms. The calibration plate in our setup was replaced with a height-adjustable back-lit pinhole that can be deployed through the flume bed, even when the flow is running. We then traverse the cameras, taking pictures of the pinhole to generate the data required to compute a pinhole camera calibration model. This calibration approach can be run automatically after an experiment without manual intervention. We have used this setup in the AOCF to measure double averaged velocity field statistics over rough beds.

2.2 Open-channel flume

Establishing a uniform flow in a laboratory open-channel flume with a prescribed flow depth (H) and shear velocity (u_*) involves calculating and setting the required bed slope $S_b = u_*^2/[gH]$, where g is acceleration due to gravity, and then experimentally adjusting the flowrate and weir setting until uniform flow at the correct water level is found. Automating this procedure involves firstly bringing the pumps, flume slope, and weir mechanisms under computer control. This can be achieved using relatively simple hardware and software systems. To measure flow depth profiles along the channel and check flow uniformity, we measure both bed and water surface profiles with an array of confocal chromatic sensors attached to a traverse mechanism. This instrument has a footprint of around 20 microns, sub-micron resolution, and very little drift making it ideal to capture precise flow depth measurements. The final step to automate flow setup is the software control loops to adjust pump speed and weir setting based on the feedback from the confocal sensors. We hope to bring this last step online within 2021.

Received 22 March 2021
Accepted 12 April 2021

Publications of the Institute of Geophysics, Polish Academy of Sciences
Geophysical Data Bases, Processing and Instrumentation
vol. 434 (E-11), 2021, pp. 11-13
DOI: 10.25171/InstGeoph_PAS_Publs-2021-006
Webinar on Experimental Methods and Laboratory Instrumentation in Hydraulics, 13-15 April 2021

Uni and Bi-directional Exchange Flows in a Large Scale Rotating Channel

Claudia ADDUCE[1,✉], Maria Chiara DE FALCO[1], Alan CUTHBERTSON[2], Maria Eletta NEGRETTI[3], Janek LAANEARU[4], Daniela MALCANGIO[5], and Joel SOMMERIA[3]

[1]University Roma Tre, Rome, Italy
[2]University of Dundee, Dundee, UK
[3]LEGI, UGA/CNRS, Grenoble, France
[4]Tallinn University of Technology, Tallinn, Estonia
[5]Polytechnic University of Bari, Bari, Italy

✉ claudia.adduce@uniroma3.it

A b s t r a c t

Laboratory experiments were performed at the Coriolis Rotating Platform to study uni and bi-directional exchange flows in a trapezoidal channel. PIV and conductivity probes were used to measure velocity fields and density profiles. The rotation rate and the freshwater flowrate were varied. The stratified flow dynamics was found to depend on the Burger number, Bu, and for Bu < 0.5 unsteady exchange flows develop. Both the ambient rotation and freshwater flowrate affect the transverse velocity distribution and leads to the partial blockage of the lower saline outflow for the largest freshwater inflows. In addition, shear-driven interfacial instabilities are analysed and for larger rotation rates the mixing layer thickness increases.

Keywords: stratified exchange flows, rotating flows, interfacial instabilities.

1. INTRODUCTION

Uni- and bi-directional exchange flows occur within estuaries and sea straits when horizontal density differences or pressure gradients are present between the adjacent water bodies. The

nature of these flows depends on both Coriolis effects due to the Earth's rotation and the topographic controls imposed by seafloor bathymetry and channel shape. These factors have a significant influence on both internal mixing and secondary circulations generated by exchange flows (De Falco et al. 2021). Understanding of these uni- and bi-directional flow processes is relevant in coastal regions, where water and nutrient exchanges between estuaries and open marine waters are regulated by channel topography (Cuthbertson et al. 2006) with significant implications for the intrusion of saline marine waters (Matthäus and Lass 1995).

2. EXPERIMENTAL DETAILS

Laboratory experiments were conducted in the Coriolis Rotating Platform at LEGI, which consists of a 13 m diameter and 1.2 m deep circular tank that can be rotated at a constant angular velocity. A trapezoidal cross-section channel of length 6.5 m was positioned in the tank. The trapezoidal section had a 2 m top width, 1 m bottom width and 0.5 m total depth, with side slopes of $\alpha_s = 45°$. A saline water flowrate Q_1 and a fresh water flowrate Q_2 , with $q^* = Q_2/Q_1$, were fed into the channel with opposite directions and a uni- or two-layer exchange flow was developed. The rotation rate, Ω, of the tank and the freshwater flowrate Q_2 were varied. Velocity fields, in eleven sections spanning the trapezoidal cross section, and density profiles were measured by PIV and conductivity probes, respectively. Figure 1 shows the effect of the varied parameters on the interface between the salty and freshwater flow.

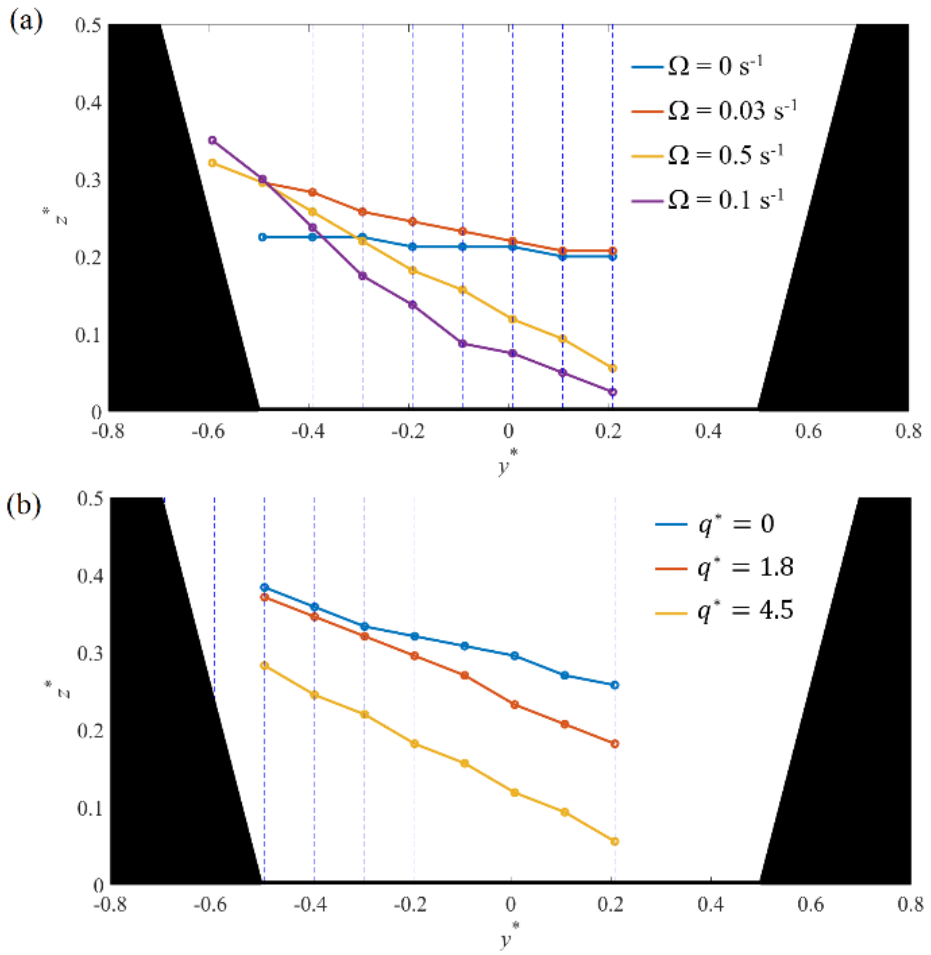

Fig. 1. Cross channel variation of zero-velocity elevation in all the measured PIV sections: (a) rotating experiments with $q^* = 4.5$, (b) rotating experiments with $\Omega = 0.05\ s^{-1}$.

References

Cuthbertson, A.J.S., J. Laanearu, and P.A. Davies (2006), Buoyancy-driven two-layer exchange flows across a slowly submerging barrier, *Environ. Fluid Mech*. **6**, 133–151, DOI: 10.1007/s10652-005-5460-6.

De Falco, M.C., C. Adduce, A. Cuthbertson, M.E. Negretti, J. Laanearu, D. Malcangio, and J. Sommeria (2021), Experimental study of uni-and bi-directional exchange flows in a large-scale rotating trapezoidal channel, *Phys. Fluids* **33**, 3, 036602, DOI: 10.1063/5.0039251.

Matthäus, W., and H.U. Lass (1995), The recent salt inflow into the Baltic Sea, *J. Phys. Oceanogr*. **25**, 2, 280–286, DOI: 10.1175/1520-0485(1995)025<0280:TRSIIT>2.0.CO;2.

Received 22 March 2021
Accepted 12 April 2021

Publications of the Institute of Geophysics, Polish Academy of Sciences
Geophysical Data Bases, Processing and Instrumentation
vol. 434 (E-11), 2021, pp. 15-15
DOI: 10.25171/InstGeoph_PAS_Publs-2021-007
Webinar on Experimental Methods and Laboratory Instrumentation in Hydraulics, 13-15 April 2021

The Use of Experimental Measurements for the Validation of Transient Models

David FERRAS

IHE Delft Institute for Water Education, Delft, The Netherlands

✉ d.ferras@un-ihe.org

A b s t r a c t

Experimental research of pressurized hydraulic transients is conditioned to pressure (water-hammer) waves, which are usually characterized for having high celerity values and involving high pressures. Reservoir-pipe-valve systems are the usual experimental rigs to carry out such analyses. Flow rate and pressures at specific points of the pipe system are standard measurements from which water-hammer solvers are consequently verified and validated. During this webinar first a brief introduction is provided concerning the standard numerical model and the subsequent experimental validation approach. Then the talk evolves to more advanced numerical models, where not only the transients in the fluid but also their interaction with the structure are considered. Additional lab measurements are therefore required to capture the associated structure behaviour which, additionally, involve transient waves propagating even at a higher velocity. Finally, some remarks are provided pointing out the importance of a good understanding of the physical phenomena, especially in terms of time-scale, to experimentally capture fast transient phenomena in pressurized pipe flows.

Keywords: pipe systems, pressurized pipe flows.

Received 22 March 2021
Accepted 12 April 2021

Publications of the Institute of Geophysics, Polish Academy of Sciences
Geophysical Data Bases, Processing and Instrumentation
vol. 434 (E-11), 2021, pp. 17-19
DOI: 10.25171/InstGeoph_PAS_Publs-2021-008
Webinar on Experimental Methods and Laboratory Instrumentation in Hydraulics, 13-15 April 2021

Advancing the Frontier of Hydraulics Experimentation using Ferrofluids

Laura Maria STANCANELLI

Delft University of Technology TU-Delft, Faculty of Civil Engineering and Geosciences, Delft, The Netherlands

✉ e-mail: L.M.Stancanelli@tudelft.nl

A b s t r a c t

Ferrofluids (FFs) are colloid liquids susceptible to magnetic field. Although they represent a novelty in Hydraulics, they have been widely used in engineering sciences since the eighties, with different industrial and biomedical applications. Here, a collection of experiences carried out in hydraulic laboratories is presented. Indeed, FFs have been exploited to measure key hydraulic quantities (e.g. wall friction). Moreover, their interaction with flow have been investigated with original techniques (optical methods, microfluidics) observing the rise of novel phenomena (e.g. lubrication).

Keywords: ferrofluids, wall shear stress, lubrication, PTV, microfluidics.

1. INTRODUCTION

Ferrofluids (FFs) are formed by magnetic nanoparticles coated with a surfactant (preventing agglomeration) and dispersed in a liquid carrier (water or oil). One of their most important characteristics is their susceptibility to the magnetic field. FFs are very flexible due to: i) their tunable rheology; ii) the possibility of controlling their shape through their responsiveness to a magnetic field; iii) the fluid state, whereby the particles are free to move, showing lubricant properties; iv) the capability to hold the FF in place using an externally applied magnetic field.

The dynamics of ferrofluids have been extensively studied since the seventies (Shliomis 1972; Patel et al. 2013). Because of these peculiar characteristics, ferrofluids have been widely used in different applications (i.e. loudspeakers, bearings, micro valves, drug targeting, cancer therapy). In the following, a series of laboratory experiments carried out with ferrofluids are described. In particular, it is shown how ferrofluids can be exploited to measure wall friction and how their interaction with the surrounding flow gives rise to novel phenomena (e.g. lubrication) that can be investigated with original techniques (optical methods, microfluidics).

2. EXPERIENCES WITH FERROFLUIDS IN HYDRAULIC LABS

2.1 The development of an innovative wall shear stress measurement technique

The measurement technique takes advantage of the above described properties of ferrofluids to measure fluid-wall shear stresses, with possible applications on sandy bottoms (Stancanelli et al. 2020). The principle of operation is really simple (Musumeci et al. 2015a,b; 2018). A ferrofluid drop, O (1 mm) high, is placed on the wall and exposed to a permanent magnetic field. Therefore, this drop takes a conical shape that deforms under the action of the flow impacting on it. The measure of shear stresses exerted by the flow is performed by evaluating the ferrofluid drop deformation (i.e. the drop apex displacement) acquired by a camera. The technique is capable to measure changes in flow resistance induced by either skin friction and form drag. Experimental results demonstrated the capability to measure small shear stress variations (less than 0.001 N/m^2), as those associated with the change in roughness of the bimodal mixture composing the sediment bed.

2.2 Ferrofluid-flow interaction investigated with PTV and in microfluidics

Pressure-driven channel-flow experiments (square cross section 1 cm × 1 cm) have been carried out for investigating the ferrofluid-flow interaction. A stable ferrofluid layer is placed on one of the confining walls. This layer interacts with the fluid flowing within the channel, leading to a slip boundary condition. The ferrofluid layer is shaped and stabilized at the wall using an array of permanent magnets. Different steady flow regimes, characterized by Re numbers in the laminar, transitional and turbulent regime, have been tested. The flow field has been investigated by means of optical techniques (i.e., PIV, PTV). Flow velocity profiles and flow patterns within the channel have been extracted and compared with the flow regime observed in the absence of ferrofluid. The comparison demonstrates significant drag reduction (>60%) in both laminar and turbulent regimes. Moreover, in order to further understand ferrofluid-flow interactions, as well as ferrofluids rheology, a series of experiments has been carried out at the micron scale. Microfluidic chips, such as straight channel (rectangular section 1500 μm × 110 μm), and Y-junction channels (rectangular section 1100 μm × 50 μm), have been used for this aim. In these specific settings, it was possible to study the reorganization of the ferrofluid structure under the action of different magnetic fields (i.e. chains formation composed of magnetite particles) and the phenomena acting at the interface of the ferrofluid and a co-flowing fluid (a mineral oil).

Acknowledgments. The work on the measurement technique has been funded by the EU project HYDRALAB PLUS (proposal number 64110) and was carried out at the University of Catania under the supervision of Prof. Rosaria Musumeci and Prof. Enrico Foti. The work on the analysis of ferrofluid-flow interaction has received funding from the European Union's Horizon 2020 research and innovation programme under the Maria Skłodowska-Curie grant agreement No. 841259 hosted at Swiss Federal Institute for Forest, Snow, and Landscape Research (WSL). The experimental research activity has been carried out at the ETH Zurich under the supervision of Prof Markus Holzner and in close collaboration with Eleonora Secchi. The author wish to thank members of the GIC group (UNICT) and of the EFM group (WSL, Birmendorf), and Prof Stefano Lanzoni (University of Padua) for the fruitful discussions, the useful comments and suggestions.

References

Musumeci, R.E., V. Marletta, B. Andò, S. Baglio, and E. Foti (2015a), Ferrofluid measurements of bottom velocities and shear stresses, *J. Hydrodyn*. **27**, 1, 150–158, DOI: 10.1016/S1001-6058(15)60467-X.

Musumeci, R.E., V. Marletta, B. Andò, S. Baglio, and E. Foti (2015b), Measurement of wave near-bed velocity and bottom shear stress by ferrofluids, *IEEE Trans. Instrum. Meas*. **64**, 5, 1224–1231, DOI: 10.1109/TIM.2014.2359521.

Musumeci, R.E., V. Marletta, A. Sanchez-Arcilla, and E. Foti (2018), A ferrofluid-based sensor to measure bottom shear stresses under currents and waves, *J. Hydraul. Res*. **56**, 5, 630–647, DOI: 10.1080/00221686.2017.1397779.

Patel, R., R.V. Upadhyay, and R.V. Mehta (2003), Viscosity measurements of a ferrofluid: comparison with various hydrodynamic equations, *J. Colloid Interface Sci*. **263**, 2, 661–664, DOI: 10.1016/S0021-9797(03)00325-4.

Shliomis, M.I. (1972), Effective viscosity of magnetic suspensions, *Sov. J. Exp. Theor. Phys*. **34**, 6, 1291–1294.

Stancanelli, L.M., R.E. Musumeci, M. Stagnitti, and E. Foti (2020), Optical measurements of bottom shear stresses by means of ferrofluids, *Exp. Fluids* **61**, 52, DOI: 10.1007/s00348-020-2890-3.

Received 22 March 2021
Accepted 12 April 2021

Publications of the Institute of Geophysics, Polish Academy of Sciences
Geophysical Data Bases, Processing and Instrumentation
vol. 434 (E-11), 2021, pp. 21-23
DOI: 10.25171/InstGeoph_PAS_Publs-2021-009
Webinar on Experimental Methods and Laboratory Instrumentation in Hydraulics, 13-15 April 2021

Clogging of Riverbeds – from Complex Field Conditions to Isolated Processes in the Laboratory

Markus NOACK

Faculty of Architecture and Civil Engineering, Karlsruhe University of Applied Science, Karlsruhe, Germany

✉ markus.noack@hs-karlsruhe.de

A b s t r a c t

The complex phenomenon riverbed clogging constitutes one reason for degraded riverine ecosystems. However, measuring or monitoring of clogging is challenging because of its multifaceted character. This keynote addresses clogging from different perspectives including field and laboratory aspects and shows recent developments in measuring techniques to gather relevant involved parameters and processes.

Keywords: riverbed clogging, colmation, field and laboratory methods, MultiPAC, gamma ray attenuation.

1. INTRODUCTION

Although clogging of riverbeds, also referred to colmation, has been studied for decades in the field as well as in hydraulic laboratories significant knowledge gaps exist to fully understand the complex and interacting physical and biogeochemical processes. The relevance of studying colmation and its single processes becomes obvious as it can have a tremendous impact on the hyporheic zone and the biotic community living there. In fact, riverbed clogging is suspected to be one reason for failing the target of the European Water Framework Directive in achieving the "good ecological status".

Riverbed clogging is also a matter of overlapping scales including macro-scale aspects on river basin level such as sediment delivery and hydrology but also micro-scale characteristics such as local topography, particle size/shape and the compaction of the riverbed. Moreover, clogging is a highly dynamic process.

These multifaceted issues are highly interesting but also challenging to cope with riverbed clogging, especially because of its high temporal and spatial variability but also because of the

numerous multifaceted parameters and processes that need to be considered in measuring and monitoring riverbed clogging.

This keynote addresses the phenomena riverbed clogging from different perspectives and presents different methods to assess clogging in the field and in hydraulic laboratories.

2. METHODS AND RESULTS

For field applications, a so-called Multiparameter Approach for Colmation (MultiPAC) was developed to capture four key parameters in describing riverbed clogging on a local scale including particle size distribution, porosity, hydraulic conductivity and dissolved oxygen (Seitz 2020). The first results are very promising and prove that riverbed clogging cannot be described by single parameters. Especially the capability to gather vertical profiles allows the identification of clogged layers in the riverbed. However, to study the influence of single processes and parameters the complexity of riverbed clogging need to be simplified to be studied in hydraulic laboratories under controlled boundary conditions.

Therefore, a laboratory flume was designed to focus on sediment infiltration and accumulation only using a simplified bed made of spheres that can be arranged in different packings. Main objective of the experiments is to explore interactions between turbulences at the water-sediment interface, interstitial flows and the progressive occlusion of pores with fine sediments that are fundamental to understand the dynamic behaviour of colmation processes. Therefore, the gamma ray attenuation method (GRA) was adapted and successfully tested to allow for non-intrusive measurements of sediment infiltration masses in vertical profiles (Mayar et al. 2020), which represents a precondition to study the dynamics of clogging processes. In future experiments, the measuring setup will be complemented by PIV measurements of surface flow and endoscopic PIV measurements of pore flow. These combined non-intrusive and simultaneously conducted measurements will lead to a unique dataset in describing the sediment infiltration and accumulation behaviour and allows for derivations of functional relationships between surface and subsurface processes to describe the interactions and dynamics of clogging processes on a fundamental and physical basis.

3. CONCLUSIONS

Despite the complicated phenomenon riverbed clogging, both the field and laboratory methods represents important advancements in studying the involved parameters and processes. While MultiPAC represents a step forward in measuring riverbed clogging in the field on a quantitative basis, the laboratory experiments with the GRA method enabled for the first time to study the dynamics of clogging given to its non-intrusive character. The combination with advanced PIV-techniques will further allow in-depth investigation, especially in quantifying interacting processes at the water-sediment interface.

Acknowledgments. The author presents his gratitude to Lydia Seitz and M. Assem Mayar for their work within their Ph.D. Thesis' and the Institute for Modelling Hydraulic and Environmental Systems at the University of Stuttgart, Germany where all the work and experiments have been realized.

References

Mayar, M.A., G. Schmid, S. Wieprecht, and M. Noack (2020), Proof-of-concept for non-intrusive and undisturbed measurement of sediment infiltration masses using gamma-ray attenuation, *J. Hydraul. Eng.* **146**, 5, DOI: 10.1061/(ASCE)HY.1943-7900.0001734.

Seitz, L. (2020), Development of new methods to apply a multiparameter approach – a first step towards the determination of colmation, Ph.D. Thesis No. 276, University of Stuttgart, Stuttgart, Germany, DOI: 10.18419/opus-11249.

Received 22 March 2021
Accepted 12 April 2021

Publications of the Institute of Geophysics, Polish Academy of Sciences
Geophysical Data Bases, Processing and Instrumentation
vol. 434 (E-11), 2021, pp. 25-27
DOI: 10.25171/InstGeoph_PAS_Publs-2021-010
Webinar on Experimental Methods and Laboratory Instrumentation in Hydraulics, 13-15 April 2021

Hydrodynamic Forces Generated on a Coarse Spherical Particle Beneath a Tidal Bore

Muhammad Zain Bin RIAZ✉, Shu-Qing YANG, and Muttucumaru SIVAKUMAR

School of Civil, Mining and Environmental Engineering, University of Wollongong, NSW, Australia
✉ mzbr518@uowmail.edu.au

A b s t r a c t

The development of a bore in an open channel creates a sudden change in water surface elevation propagating upstream. In this study, physical modelling was performed to investigate both horizontal and vertical components of velocity and forces to clarify the mechanism of sediment initiation beneath a tidal bore. A laser Doppler anemometer, a highly sensitive force transducer, and ultrasonic displacement meters accompanied by video recordings were used to provide some quantitative data in terms of various force and velocity terms measured simultaneously acting on a targeted sphere. According to the experimental results, upward vertical force was the main force in destabilizing the particles however, a large upstream longitudinal force was found to be the dominant cause promoting upstream particle motion during the breaking roller passage. Furthermore, the forces were not only due to velocity but also to the sudden discontinuity in free water surface.

Keywords: tidal bore, drag force, lift force, laser Doppler anemometer, force transducer.

1. INTRODUCTION

It is common that when a tide starts to rise, a series of waves propagate upstream in some river mouths as a tidal bore. Some field observations and physical modelling highlighted that sediment incipient motion is likely to occur due to horizontal pressure gradient introduced by free stream velocity gradient (Foster et al. 2006; Frank et al. 2015). Khezri and Chanson (2015) investigated the incipient sediment motion beneath the tidal bore by estimating only the longitudinal forces that are responsible for sediment entrainment and took no account of the role of vertical forces. In waves, the vertical pressure gradient is mostly associated with variations in water depth. Whereas, how the uplift force caused by the vertical pressure gradient modifies sediment transport still needs to be investigated (Berni et al. 2017). The main aim of this study

is to verify the newly designed experimental setup and relative impact of drag and lift force during a tidal bore.

2. EXPERIMENTAL SETUP AND INSTRUMENTATION

The experiments were conducted in a 10.5 m long, 0.4 m deep, and 0.3 m wide rectangular flume. The laser Doppler anemometer (LDA) was used to measure point velocity and turbulence. More detail of setup can be found in Yang et al. (2020) and Riaz et al. (2020). A highly sensitive force transducer was used to measure forces on the target sphere. A fast fully closing Tainter gate was installed at $x = 10$ m and a force transducer was fixed at $x = 6$ m, where x is the distance from the channel upstream inlet end. Two ultrasonic displacement meter were installed to measure water elevation fluctuation. Spheres of 38 mm average diameter were fixed by glue into a Perspex sheet in a hexagonal-shaped structure over a 10 m length of the flume. In the test section, a target sphere of 36.6 mm diameter was surrounded by a group of 3D printed spheres filled with small steel spheres which were not glued, in order to allow them to stay in place due to their own weight. Thus, the force sensor recorded the hydrodynamic forces on the sphere only due to water flow. All instruments were synchronized to within ± 0.5 ms.

For all observations, the initial flow conditions were $Q = 0.033$ m^3/s, $h_0 = 0.135$ m, and $V_0 = 0.815$ m/s where h_0 and V_0 are the flow depth and depth averaged velocity. Videos were recorded between $x = 6$ and 7 m with a handy camera Zoom™ (60 fps) for a tidal bore, for which the bore celerity was $U \approx 0.85$ m/s, corresponding to a Froude number = 1.35 to 1.45.

3. RESULTS AND DISCUSSION

The water surface, instantaneous velocities and forces were measured over fixed rough bed. The propagation of breaking roller was linked with strong longitudinal deceleration and some negative instantaneous vertical velocities as reported by Reungoat et al. (2018) (see Fig. 1a). Two different trends of forces were observed. Stage 1 was the smooth rise of free surface (point 1) to the roller toe (point 2) while, roller toe to peak of the first wave crest (point 3) was stage 2 (Fig. 1). At stage 1, lift force (≈ 85% of submerged weight) was the predominant force however, behind the bore during stage 2, the increasing trend of drag force (i.e., along the bore, upstream) had a significant role in maintaining motion and determining its extent. Both drag and lift forces acted on the particle in the negative direction due to flow reversal through transient recirculation and the sudden increase in free water surface at the arrival of the breaking

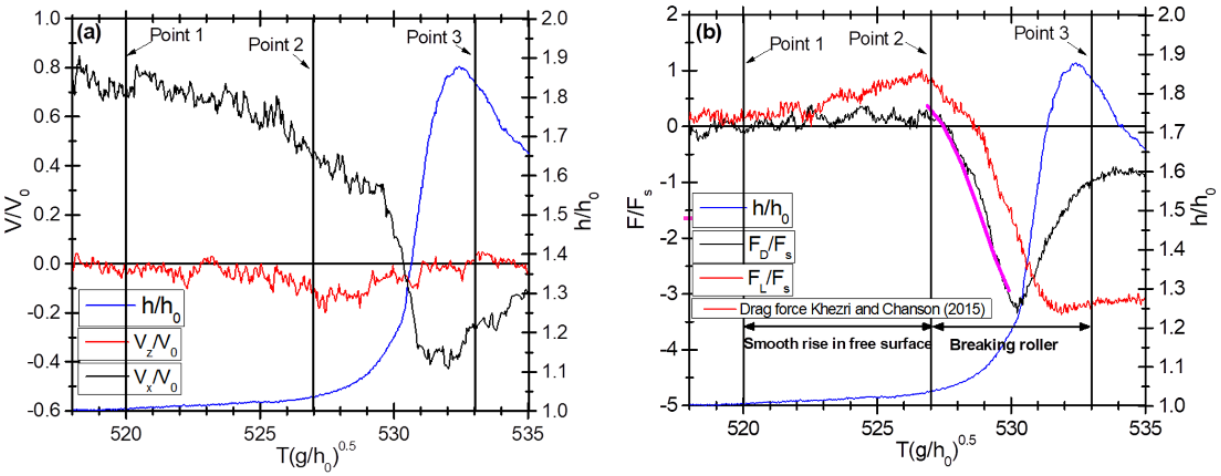

Fig. 1. Dimensionless Median EA water depth, horizontal velocity and vertical velocity, drag force and lift force beneath breaking bore at $x = 6$ m, $z/h_0 = 0.037$.

bore. The directly measured drag force findings were consistent with Khezri and Chanson's (2015) estimated drag force data (Fig. 1b). The forces acting on the target particle were median ensemble-averaged over 25 test runs to find the main trend, which is shown in Fig. 1b.

4. CONCLUSION

During the smooth rise of free-surface in a tidal breaking bore, the increase in forces indicates the importance of lift force which is necessary for particle movement. For the most part, drag force was the main influencing force prompting the inception of upstream particle motion.

A c k n o w l e d g m e n t s. The authors acknowledge the technical assistance of Gavin Bishop and Peter Ihnat (The University of Wollongong).

R e f e r e n c e s

Berni, C., H. Michallet, and E. Barthélemy (2017), Effects of horizontal pressure gradients on bed destabilization under waves, *J. Fluid Mech.* **812**, 721–751, DOI: 10.1017/jfm.2016.805.

Foster, D.L., A.J. Bowen, R.A. Holman, and P. Natoo (2006), Field evidence of pressure gradient induced incipient motion, *J. Geophys. Res. Oceans* **111**, C05004, DOI: 10.1029/2004JC002863.

Frank, D., D. Foster, I.M. Sou, and J. Calantoni (2015), Incipient motion of surf zone sediments, *J. Geophys. Res. Oceans* **120**, 8, 5710–5734, DOI: 10.1002/2014JC010424.

Khezri, N., and H. Chanson (2015), Turbulent velocity, sediment motion and particle trajectories under breaking tidal bores: simultaneous physical measurements, *Environ. Fluid Mech*. **15**, 633–650, DOI: 10.1007/s10652-014-9358-z.

Reungoat, D., P. Lubin, X. Leng, and H. Chanson (2018), Tidal bore hydrodynamics and sediment processes: 2010–2016 field observations in France, *Coastal Eng. J.* **60**, 4, 484–498, DOI: 10.1080/21664250.2018.1529265.

Riaz, M.Z.B., S.-Q. Yang, and M. Sivakumar (2020), Simultaneous measurement of horizontal and vertical velocities and forces beneath a tidal bore, Coastlab20, IAHR, Zhoushan, China, 8 pp.

Yang, S.-Q., M.Z.B. Riaz, M. Sivakumar, K. Enever, and N.S. Miguntanna (2020), Three-dimensional velocity distribution in straight smooth channels modeled by modified log-law, *J. Fluids Eng.* **142**, 1, 011401, DOI: 10.1115/1.4044183.

Received 22 March 2021
Accepted 12 April 2021

Publications of the Institute of Geophysics, Polish Academy of Sciences
Geophysical Data Bases, Processing and Instrumentation
vol. 434 (E-11), 2021, pp. 29-30
DOI: 10.25171/InstGeoph_PAS_Publs-2021-011
Webinar on Experimental Methods and Laboratory Instrumentation in Hydraulics, 13-15 April 2021

An Advanced Measurement Method to Investigate the Dynamic Development of Sediment Infiltration in an Artificial Riverbed

Assem MAYAR[1,✉], Stefan HAUN[1], Markus NOACK[2], and Silke WIEPRECHT[1]

[1]Institute for Modelling Hydraulic and Environmental Systems, University of Stuttgart, Germany

[2]Faculty of Architecture and Civil Engineering, Karlsruhe University of Applied Science, Germany

✉ assem.mayar@iws.uni-stuttgart.de

Abstract

The dynamic development of sediment infiltration in gravel-bed rivers is not entirely understood yet because existing methods are unable to cope with the high spatio-temporal variability of the involved processes. Therefore, high-resolution and non-intrusive measurements of governing parameters are required to unravel the interactions of the multifaceted processes involved in the clogging or colmation phenomenon. This study presents high-resolution measurements of the dynamic process of sediment infiltration and the development of sediment accumulations in an artificial riverbed under laboratory conditions using an advanced non-intrusive and undisturbed method.

Keywords: gamma-ray attenuation, dynamic sediment infiltration, sediment accumulation, clogging, colmation.

1. INTRODUCTION

Excessive sediment infiltration and accumulation in gravel-bed rivers, intensified by anthropogenic activities, reduce pore space, conductivity, and dissolved oxygen supply, leading to severe consequences for aquatic species (Schälchli 1992; Noack et al. 2016). Owing to the several physical and bio-geo-chemical parameters involved in colmation, existing methods are unable to cope with the complex and highly dynamic behavior of the involved processes. Therefore, this study develops an advanced laboratory method for measuring the dynamic development of infiltrating sediments in an artificial riverbed with high spatial and temporal resolution.

The artificial gravel-bed was developed from 0.040 m and 0.026 m spheres in a combined cubic and rhombohedral arrangement in a laboratory flume with 0.24 m width, 0.30 m height, 8.0 m length, and 1.35% slope. The spheres were situated in 16 blocks with fixation from the

top. Each block consisted of six 0.04 m spheres in lateral and horizontal directions and four 0.04 m spheres on the vertical axis leading to a total length of 3.84 m. The 0.026 m spheres were glued in the concave of 0.04 m spheres in the cubic set up at the middle layer of the bed.

Two sediment mixtures (Fine = 1.0–1.8 mm, Coarse = 2.0–3.5 mm), with two supply rates (1.4 and 3.7 kg/min) and a total mass of 20 kg, are supplied to the flume for observing the dynamic development of the sediment infiltration and accumulation processes.

The gamma-ray attenuation (GRA) method (Mayar et al. 2020) is used for non-intrusive and undisturbed continuous measurement of infiltration masses at a specific position (one-point measurement with a 15 mm diameter) during the entire experiments (temporal resolution of 60 seconds) and for measurements of the vertical infiltration profiles in two different intervals: (i) at the end of the sediment supply (T1), and (ii) 28 minutes after the start of the experiment (T2) with a 7 mm spatial resolution.

2. RESULTS

The results showed that the infiltrated sediment masses strongly depend on the infiltrated particle sizes. According to the vertical profiles measurement results and visual observations, the infiltrated fine sediments started filling from the bottom, while the infiltrating coarse sediment mixture resulted in a clogging layer, and subsequently, less coarse sediments penetrated to the bottom. The second time-step vertical profile measurements show that dynamic changes mostly occur in the top section due to washing of the sediments by the flow. The one-point dynamic measurement indicates higher infiltrated sediment thickness for the fine sediment mixture compared to coarse particles as a result of the clogging in the upper section. Further, the one-point measurement of the dynamic development of sediment accumulation shows that a higher supply rate leads to an earlier start of the infiltration and a more rapid filling than the lower supply rate.

3. CONCLUSIONS

The results proved that the GRA method is capable of non-intrusive and undisturbed measurements of sediment infiltration's dynamic development with a high spatial and temporal resolution. Within future studies, the experimental setup can be adapted (e.g., design to more nature-like conditions) to further unravel parameters involved in the highly dynamic process of sediment infiltration. Moreover, the GRA method can be coupled with other advanced flow measurement devices for an in-depth investigation of the riverbed clogging phenomenon.

Acknowledgments. The first author is funded by a scholarship from DAAD.

References

Mayar, M.A., G. Schmid, S. Wieprecht, and M. Noack (2020), Proof-of-concept for nonintrusive and undisturbed measurement of sediment infiltration masses using gamma-ray attenuation, *J. Hydraul. Eng.* **146**, 5, 04020032, DOI: 10.1061/(ASCE)HY.1943-7900.0001734.

Noack, M., J. Ortlepp, and S. Wieprecht (2016), An approach to simulate interstitial habitat conditions during the incubation phase of gravel-spawning fish, *River Res. Appl.* **33**, 2, 192–201, DOI: 10.1002/rra.3012.

Schälchli, U. (1992), The clogging of coarse gravel river beds by fine sediment, *Hydrobiologia* **235**, 1, 189–197, DOI: 10.1007/BF00026211.

Received 22 March 2021
Accepted 12 April 2021

Publications of the Institute of Geophysics, Polish Academy of Sciences
Geophysical Data Bases, Processing and Instrumentation
vol. 434 (E-11), 2021, pp. 31-33
DOI: 10.25171/InstGeoph_PAS_Publs-2021-012
Webinar on Experimental Methods and Laboratory Instrumentation in Hydraulics, 13-15 April 2021

Breach Geometry Studies Using Depth Detection Technology

Rubens Gomes Dias CAMPOS✉ and Aloysio Portugal Maia SALIBA

UFMG, Hydraulic Engineering and Water Resources Department, Belo Horizonte, MG, Brazil

✉ rubensengenheiro2004@yahoo.com.br

A b s t r a c t

The use of a 3D Scanner allowed the acquisition of dam breach geometry on a physical model. This technique is widely used in interactive movement entertainment and was adapted for this study's aims. The conceived apparatus collected breach geometry from a physical model built to evaluate a channel's cascade dam break. The 3D Scanner mapped breach surfaces and allowed the input on image processing software to generate its digital surface and elevation contours, reducing measurement errors since it is a non-contact method. An apparatus was then developed to enable accurate scanning since this feature's original function was motion detection. The apparatus consisted of a platform assembled on rails, installed over channel walls, supporting a Kinect II (Microsoft Corporation ® 3D Scanner), connected to a notebook.

Keywords: 3D Scanner, physical models, cascade dam breach geometry, breach equation, breach formation time.

1. INTRODUCTION

Obtaining undisturbed test geometries surfaces in physical models is an arduous task, as incautious measurement can disturb the surface, and a non-contact method is preferred. Also, breach geometry characterization needs three-dimensional (3D) scanning, many times too expensive, especially in developing countries' hydraulic laboratories. This research used a low-cost 3D scanning technique in this regard. The overall cost of the scanning apparatus was about US$ 2 000, including the notebook.

2. SCANNING METHODOLOGY

The scanning equipment used for surveying dams' models and their breaches was the Kinect II 3D scan sensor (Microsoft Corporation ®), similar to developed by Marinello et al. (2015).

The Kinect II 3D scanning sensor includes an infrared laser emitter, an infrared camera, and a RGB camera. Depth information came from a triangulation process, where a diffraction grid divides the infrared laser into a specific pattern projected into the scene. The pattern is collected by the infrared camera and compared to the projected one. Local offsets generate a disparity map, where larger displacement values correspond to the sensor's farther positions and, conversely, smaller values correspond to positions closer to the sensor.

According to Gonzalez-Jorge et al. (2015), the Kinect II 3D scanning sensor has an accuracy ranging from 0.3 to 7.5 mm for a surveying distance from 1.0 to 4.0 m. The scanning survey distance on this research was between 1.0 and 2.0 m, with depth measurements' errors between 0.3 and 0.4 mm. Scanning measurements showed values precisely equal to scale measured channel width, demonstrating that errors were below 1 mm (the smallest scale division). This error interval is quite reasonable for these dam breach geometry analyses. Figure 1a shows a physical model breach resulting from a cascade dam break, and Fig. 1b shows this breach 3D scanned (Campos 2020).

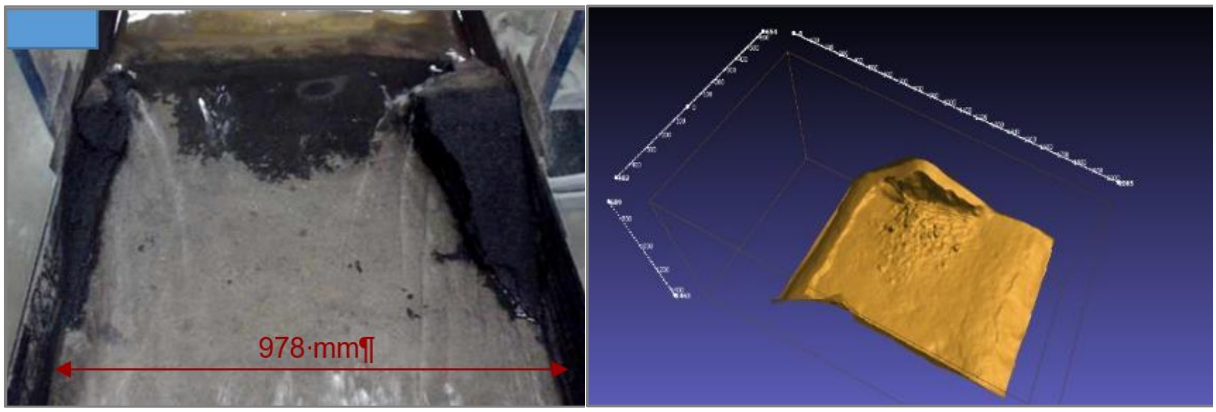

Fig. 1. Physical model cascade breach at time 4 minutes 16 seconds: (a) downstream view, and (b) final developed breach 3D scanned (Campos 2020).

A few software must be installed in a microcomputer to use Kinect II 3D as a scanning device, such as 3D Builder (Microsoft Corporation ®) for scanning input, Kinect SDK 1.8, OpenNI 2, NiTE 2.2, and Skanect for notebook compatibility. A Scanner 3D Kinect II adapter cable was purchased to connect this sensor to the notebook's USB input.

Acknowledgments. We express our gratitude to Professor Márcio Benedito Baptista (*In memoriam*) and to the Hydraulics Research Center (Centro de Pesquisas Hidráulicas – CPH) of the Federal University of Minas Gerais (UFMG) that had held this research.

References

Campos, R.G.D. (2020), Proposta de uma metodologia para obtenção de parâmetros de brechas em rupturas de barragens em cascata utilizando modelagem física, Ph.D. Thesis, UFMG, 230 pp. (in Portuguese).

Gonzalez-Jorge, H., P. Rodríguez-Gonzálvez, J. Martínez-Sánchez, D. González-Aguilera, P. Arias, M. Gesto, and L. Díaz-Vilariño (2015), Metrological comparison between Kinect I and Kinect II sensors, *Measurement* **70**, 21–26, DOI: 10.1016/j.measurement.2015.03.042.

Marinello, F., A. Pezzuolo, F. Gasparini, J. Arvidsson, and L. Sartori (2015), Application of the Kinect sensor for dynamic soil surface characterization, *Precision Agric*. **16**, 601–612, DOI: 10.1007/s11119-015-9398-5.

Received 22 March 2021
Accepted 12 April 2021

Publications of the Institute of Geophysics, Polish Academy of Sciences
Geophysical Data Bases, Processing and Instrumentation
vol. 434 (E-11), 2021, pp. 35-37
DOI: 10.25171/InstGeoph_PAS_Publs-2021-013
Webinar on Experimental Methods and Laboratory Instrumentation in Hydraulics, 13-15 April 2021

3-D Velocities in a Bore: Comparison of an Electromagentic Current Meter (ECM) and an Acoustic Doppler Velocimeter (ADV)

Suresh Kumar THAPPETA[1, ✉], Joel P.L. JOHNSON[2], Eran HALFI[3], Yael STORZ PERETZ[4], and Jonathan B. LARONNE[1]

[1]Ben-Gurion University of the Negev, Beer Sheva, Israel
[2]The University of Texas at Austin, Austin, USA
[3]Dead Sea and Arava Science Center, Masada, Israel
[4]Israel Hydrological Service, Israel Water Authority, Jerusalem, Israel
✉ sthappeta@gmail.com

A b s t r a c t

An experimental flume study was undertaken to compare water velocity in a bore for a given cross section using an Acoustic Doppler Velocimeter (ADV) and an Electromagnetic Current Meter (ECM). We present a comparison of two among nine elevations above the flume bed. Average and standard deviation of ECM velocities are somewhat higher than those of ADV. However, ADV vertical velocities showed an unexpected trend for the first 4 s after bore arrival when turbulent intensity (TI) from ECM varied from 8% to 2%.

Keywords: flash flood, velocimeter, time-averaged velocity.

1. INTRODUCTION

Measuring of water velocity allows characterizing the hydro-dynamics of flood bores. Acoustic Doppler Velocimeters (ADV) and Electromagnetic Current Meters (ECM) are the most widely used instruments for velocity measurements (Buffin-Belanger and Roy 2005). These instruments respectively operate on the Doppler shift and Faraday principle of electromagnetic induction.

A bore over a dry bed was generated in a $32 \times 0.5 \times 0.8$ m flume by sudden release of water using a computer-controlled lift gate. Water velocity was measured using down-looking ADV (N4000-72, Nortek, USA) and ECM (ACM3-RS, Alec Electronics, Japan) at 0.04 and 0.10 m above the bed at 27.1 m downstream from the gate. The ADV and ECM data were collected at respective sampling frequencies and voulmes of 50 Hz/0.03 m, 40 Hz/0.34 m at the same cross section. Measurements at each elevation were obtained by repeating the hydrograph. Water depth was monitored using temperature-corrected ultrasonic distance transducers (M-5000, Massa, USA).

2. RESULTS

Unsteady flow occurred during the first ~30 s, quasi-steady flow followed during ~30 to ~60 s after bore arrival, with a following recession. Respective time-averaged velocities (using Fourier Component Method) Uavg, Vavg, and Wavg were monitored in the streamwise, vertical and lateral directions (Fig. 1). As reported elsewhere ECM velocities were considerably larger than comparable ones by ADV. A significant inconsistency occurred between the ADV and the ECM time-averaged vertical velocities during the initial 4 seconds (Fig. 1; Table 1), when flow was very unsteady. Turbulent intensity (TI) was calculated using turbulent fluctuations and time-averaged velocities; a difference in TI (~5–7.8%) was observed between ADV and ECM data at the same elevation, which can be due to (i) different measurement principles and (ii) low correlation of ADV measurements. For example: ADV data are based on velocities of small particles passing through a sampling volume and based on two correlated measurements for a time interval. At high turbulent intensities, the correlation can be reduced (MacVicar et al. 2007), thus measurement accuracy is reduced.

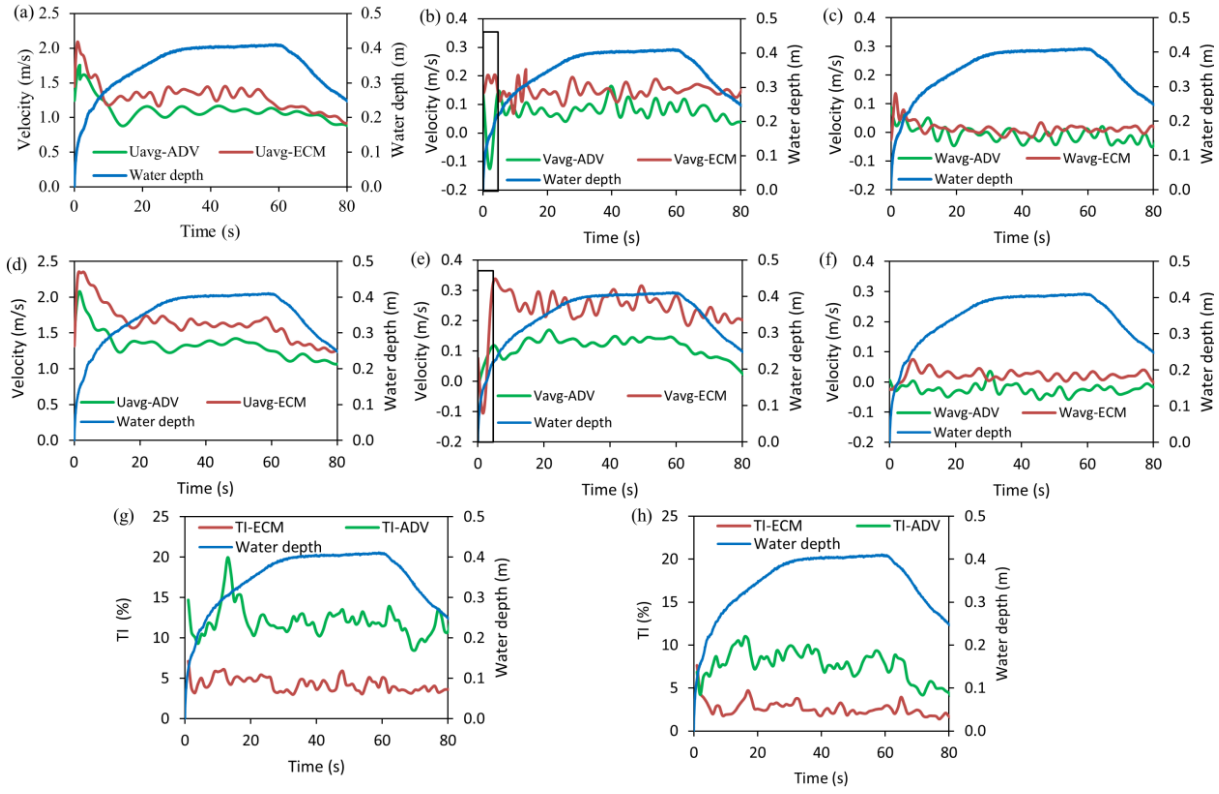

Fig. 1. ADV and ECM three dimensional time averaged velocities at: (a)–(c) 0.04 m, (d)–(f) 0.10 m, and turbulent intensity –TI at: (g) 0.04 m, and (h) at 0.10 m.

A similar inconsistency with ADV signals at high turbulent intensities for field data were observed elsewhere (MacVicar et al. 2007). The standard deviations about the average velocities are shown in Table 1.

Table 1
Average and standard deviation of ADV and ECM

Height above bed	Velocimeter	Average ± standard deviation			
		Uavg	Vavg	Wavg	TI
		m/s			%
0.04 m	ADV	1.10±0.20	0.10±0.04	–0.01±0.02	12.01±1.87
	ECM	1.20±0.30	0.15±0.02	0.01±0.02	4.23±0.85
0.10 m	ADV	1.30±0.20	0.10±0.06	–0.02±0.02	7.73±1.68
	ECM	1.50±0.30	0.20±0.06	0.02±0.02	2.64±0.88

Acknowledgments. This project was funded by the Israel Science Foundation grant 834/14 to JBL. YS-P and JPLJ were supported by The University of Texas at Austin Jackson School of Geosciences.

References

Buffin-Bélanger, T., and A.G. Roy (2005), 1 min in the life of a river: selecting the optimal record length for the measurement of turbulence in fluvial boundary layers, *Geomorphology* **68**, 1–2, 77–94, DOI: 10.1016/j.geomorph.2004.09.032.

MacVicar, B.J., E. Beaulieu., V. Champagne., and A.G. Roy (2007), Measuring water velocity in highly turbulent flows: field tests of an electromagnetic current meter (ECM) and an acoustic Doppler velocitmeter (ADV), *Earth Surf. Process. Lanforms* **32**, 9, 1412–1432, DOI: 10.1002/esp.1497.

Received 22 March 2021
Accepted 12 April 2021

Publications of the Institute of Geophysics, Polish Academy of Sciences
Geophysical Data Bases, Processing and Instrumentation
vol. 434 (E-11), 2021, pp. 39-41
DOI: 10.25171/InstGeoph_PAS_Publs-2021-014
Webinar on Experimental Methods and Laboratory Instrumentation in Hydraulics, 13-15 April 2021

Videography Modelling of the Wave-structure Interaction Processes through Cluster Analysis

Sara Mizar FORMENTIN✉, Maria Gabriella GAETA, Giuseppina PALMA, Massimo GUERRERO, Roberto DE VECCHIS and Barbara ZANUTTIGH

DICAM, University of Bologna, Italy

✉ saramizar.formentin2@unibo.it

A b s t r a c t

This contribution presents the application of the videography as a low-cost, non-intrusive alternative to measure the wave-structure interaction processes. To this purpose, a full-HD camera was used to film laboratory tests of wave overtopping against a sea-dike. From the image processing, the flow depths over the dikes, the wave celerities, the wave spectra and the amount of the air entrapped in the overtopping tongue were estimated. The results of this analysis were successfully compared to the measurements from traditional techniques.

Keywords: videography, cluster analysis, wave-structure interaction, wave overtopping, air entrainment.

1. INTRODUCTION

The modelling of the interaction processes between waves and coastal structures is a key-element for the assessment of the safety of the coastland areas. Despite simultaneous measurements of the parameters involved in the interaction processes (run-up, overtopping, reflection, loads, etc. induced by waves) would be essential for an integrated analysis, the use of numerous techniques during the same campaign (resistant gauges, velocimeters, water volume trapping in tanks, pressure sensors) is unaffordable for economic and practical reasons and, especially at small scales of laboratory tests, not recommendable due to the their disturbance of the investigated processes (Soares-Frazão et al. 2009). The videography has been already demonstrated to be a reliable alternative to the traditional techniques in the coastal engineering (i.a., Den Bieman et al. 2020). Following these examples, this paper investigates the effectiveness of the

videography as a low-cost and non-intrusive tool to model the wave-structure interaction processes during laboratory tests of wave overtopping at sea-dikes (Formentin et al. 2019).

2. METHODOLOGY

To the authors' purpose, a full-HD camera was installed in correspondence of the dike crest to film the wave run-up and overtopping processes with an acquisition frequency of 30 Hz. The records were elaborated with the image processing technique developed by Gaeta et al. (2020) based on the clusters analysis (K-means method). Pre- and post-processing filtering techniques were implemented to ease the clustering phase and to achieve a more realistic recognition of the patterns. An example of the cluster mapping is shown in Fig. 1. Here, the magenta and white colours are associated to the "classes" 3 and 5, which can be used to, respectively, track the free surface and estimate the aerated portion of the water body. The association class-object relies on human supervision in a training phase of the technique. The trained method (i.e., the class-object association) remains valid for unchanged light condition during following phases.

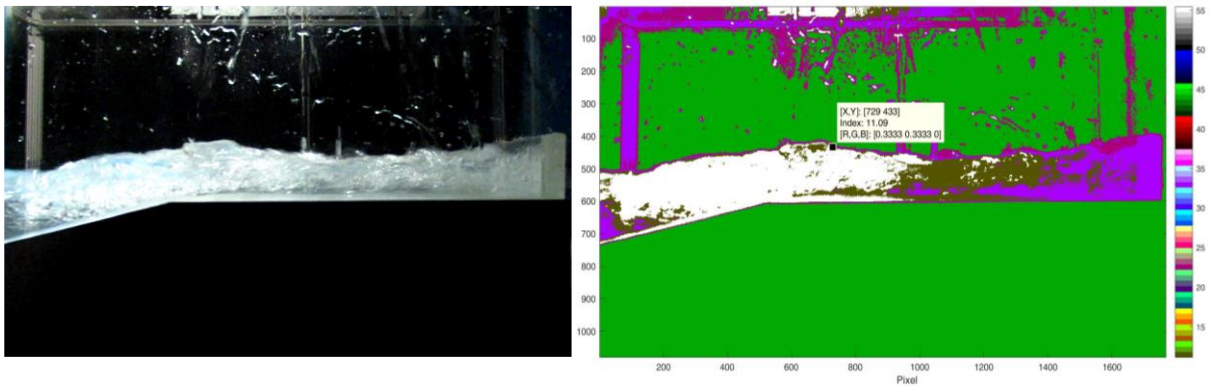

Fig. 1. Wave overtopping event at the dike (left) and corresponding clusters mapping (right).

3. PRELIMINARY RESULTS

The results of the image processing were elaborated to reconstruct the overtopping flow depths, the water front celerities and the wave spectra and to get an estimation of the amount of the air entrainment associated to the overtopping events. Comparisons with laboratory measurements of the overtopping flow characteristics derived from gauges (water levels, spectra) and ultra-

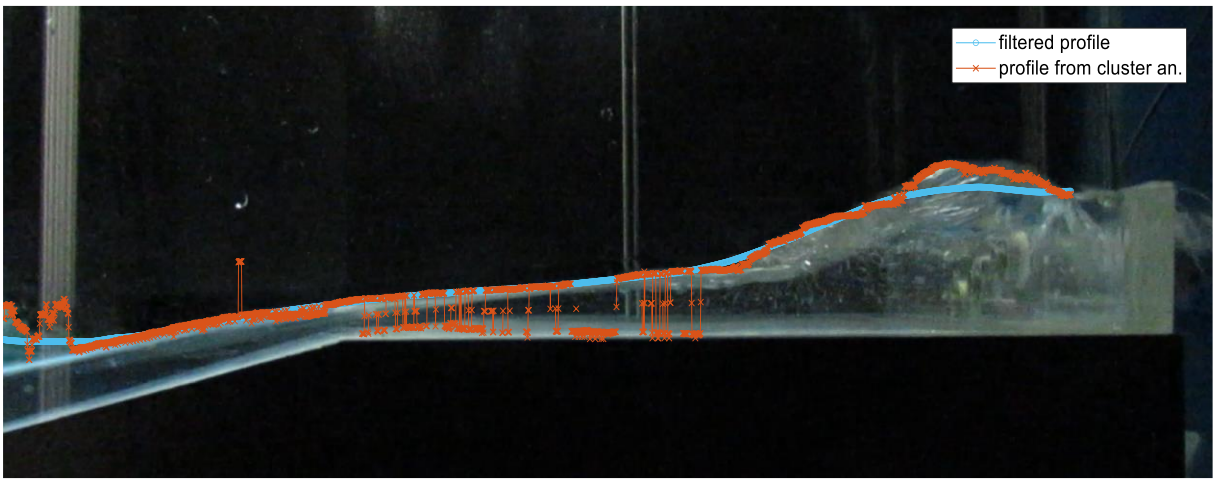

Fig. 2. Reconstruction of the free surface from the cluster analysis of an overtopping event at the dike.

sonic Doppler velocimeters (depths, velocities, and air amount) are carried out and discussed. Figure 2 shows the water surface elevation resulted from the cluster analysis (orange) and optimized with the filtering techniques (cyan) during an overtopping event.

References

Den Bieman, J.P., M.P. de Ridder, and M.R.A. van Gent (2020), Deep learning video analysis as measurement technique in physical models, *Coastal Eng.* **158**, 103689, DOI: 10.1016/j.coastaleng.2020.103689.

Formentin, S.M., M.G. Gaeta, G. Palma, B. Zanuttigh, and M. Guerrero (2019), Flow depths and velocities across a smooth dike crest, *Water* **11**, 10, 2197, DOI: 10.3390/w11102197.

Gaeta, M.G., M. Guerrero, S.M. Formentin, G. Palma, and B. Zanuttigh (2020), Non-intrusive measurements of wave-induced flow over dikes by means of a combined ultrasound Doppler velocimetry and videography, *Water* **12**, 11, 3053; DOI: 10.3390/w12113053.

Soares-Frazão, S., Y. Zech, and F. Alcrudo (2009), Laboratory experiments. **In:** D. de Wrachien and S. Mambretti (eds.), *Dam-break Problems, Solutions, and Case Studies*, Ch. 2, 51-84, WIT Press, Ashurst Lodge, UK.

Received 22 March 2021
Accepted 12 April 2021

Publications of the Institute of Geophysics, Polish Academy of Sciences
Geophysical Data Bases, Processing and Instrumentation
vol. 434 (E-11), 2021, pp. 43-45
DOI: 10.25171/InstGeoph_PAS_Publs-2021-015
Webinar on Experimental Methods and Laboratory Instrumentation in Hydraulics, 13-15 April 2021

How Can We Investigate What We Cannot Scale? Introducing the Concept of Synoptic Models for Fluvial Processes

Ivo BASELT

Universität der Bundeswehr München, Hydromechanics and Hydraulic Engineering, Neubiberg, Germany

✉ ivo.baselt@unibw.de

Abstract

To investigate fluvial processes under laboratory conditions the application of similarity laws is a well-accepted experimental method. Studying natural systems in scaled physical models is usually limited by the laboratory's infrastructure and by similarity validities, which confines the model's realisable geometric dimension. Using similarity laws becomes barely feasible if complex geomorphic fluvial events are studied with physical laboratory models, especially due to the steep slope and broad grain size distribution. Nevertheless, computational models predicting the outcomes of these hazard events require reliable data sets for calibration and validation. In this work, we present a synoptic model approach to overcome this dilemma. Derived from other research disciplines, we will discuss, how the synoptic functionality could be applied to fluvial problems based on the example of the 2017 Piz Cengalo–Bondo landslide.

Keywords: similarity laws, geomorphic fluvial systems, physical laboratory models, analogue models, synoptic model approach.

EXTENDED ABSTRACT

Using similarity laws to investigate research questions in the field of hydromechanics and morphodynamic is a well-known experimental method. By transferring the properties of the investigated prototype to a downsized physical laboratory model the associated workflow usually begins by identifying an appropriate length scale. In general, the design of physical laboratory models is limited by several conditions. The model's geometric dimensions cannot be too large

because the lab infrastructure (space, discharge) is restricted. Other limits are the model's cost, its manageability, or safety at work. On the contrary, the model's dimension can also not be too small without violating specific similarity validities (state of flow, surface tension, transcendence of cohesive grain size, similarity of sediment transport). Normally, a possible range of length scale factors can be determined that allows the realisation of models under laboratory conditions, which becomes much more difficult when geomorphic fluvial events should be studied with laboratory models. Landslides, torrential flows, and debris flows normally occur in areas with large topographic inclinations. The total elevation difference from flow initiation until deposition is often from a similar magnitude than the horizontal runout distance in these fluvial events. An appropriate realisation of the real system in a scaled model often fails due to the available vertical space. Furthermore, downscaling the flow depth and the grains size induce insurmountable problems of surface tension and cohesive effects because gravitational multiphase mass flows often contain a noticeable amount of fine sediments, which cannot be scaled properly. Moreover, despite requiring only a few dimensionless numbers for scaling river systems (Fr, Re, We), additional dimensional numbers like Savage, Bagnold, or Friction must be considered in gravitational mass flows, which impedes the realisation.

Nevertheless, there is an essential need to study complex geomorphic fluvial processes. Computational models are used to create hazard maps, adjusting prewarning systems, and implementing effective countermeasures to reduce the risk of such hazard events. Detailed data sets are therefore essentially required for calibration and validation. Unfortunately, field data is rare and former laboratory experiments were mainly conducted in straight flumes under very idealized conditions. To overcome this dilemma, novel experimental methods for complex geomorphic fluvial processes are needed to create data sets for calibration and validation of holistic computational models. Already applied in meteorology, product design, or electric mobility systems synoptic model approaches help to find isomorph conclusions by studying relevant attributes in one or more interrelated analogue systems (replacement systems) instead of upscaling measured physical variables from a model to the prototype. This synoptic approach could include physical models, computational models, analytical solutions, empirical approaches or laboratory and field measurements. The finding from all interrelated replacement systems must be finally merged in a conclusion of the studied problem.

In this work, we present some first conceptual ideas on how to transfer the concept of synoptic models to a potential application for fluvial processes. After we give an overview of the techniques and functionality of synoptic models, the concept is explained exemplary based on the 2017 Piz Cengalo–Bondo landslide cascade. Since the total original system cannot be scaled to a physical laboratory model, we identify relevant attributes in the original system which might serve as analogue sources. This could be the type of failure (rockfall), the overall terrain characteristic and sectionwise slopes, areas for erosion and deposition, and mobility. Then, we propose to split the total system for the Bondo landslide cascade into four analogue subsystems to investigate the relevant attributes in interrelated replacement systems. Because the initial rockfall and the following fragmentation follow stochastic behaviour, this process might be investigated with data from field surveys or with empirical approaches. How the fragments entrain the glacier's ice and how the ice is liquefied due to shearing could be studied in laboratory rheological tests. An existing computational multi-phase mass flow model should be used to study the flow properties of the evolved channelized debris flow in the narrow valley. Finally, a sophisticated scaled laboratory model could represent the last part of the Bondo landslide and enable studying the deposition morphology in the city of Bondo. Following the principles of synoptic modelling, specific model parameters can be set unleashed in the interrelated replacement systems, like length scale, particle size, or bathymetry. The combined results from all analogue models create a suitable data set serving for calibration and validation of holistic simu-

lations. Even if a real application is still pending, this work provides some first novel ideas on how to create calibration and validation test cases for computational models by deducing isomorph conclusions from a synoptic model approach.

Received 22 March 2021
Accepted 12 April 2021

Publications of the Institute of Geophysics, Polish Academy of Sciences
Geophysical Data Bases, Processing and Instrumentation
vol. 434 (E-11), 2021, pp. 47-49
DOI: 10.25171/InstGeoph_PAS_Publs-2021-016
Webinar on Experimental Methods and Laboratory Instrumentation in Hydraulics, 13-15 April 2021

A Novel Shear Plate for Direct Measurements of Bottom Shear Stress Induced by a Model Ship Propeller

Stephan NIEWERTH[1,✉], Francisco NÚÑEZ-GONZÁLEZ[1], Toni LLULL[2], and Sebastian LEMPA[1]

[1]Leichtweiß-Intstitut für Wasserbau, Technische Universität Braunschweig, Braunschweig, Germany

[2]Maritime Engineering Laboratory, Universitat Politècnica de Catalunya, Barcelona, Spain

✉ s.niewerth@tu-braunschweig.de

A b s t r a c t

The high rotational speed of ship propellers generates a strongly turbulent jet which can impact the stability of channel, river and ocean beds, as well as harbour structures. For the design of protective measures against scouring, the boundary shear stresses induced by propeller jets must be estimated. However, so far there is no general method available for such estimations. This is partly related to the intrinsic difficulties to perform direct measurements of boundary shear stress. We present preliminary results of measurements of bottom shear stresses generated by a ship propeller. To this end a novel shear plate which operates with strain gauges was developed. The measurements result in the expected quadratic relation between bed shear stress and the propeller rotational speed, and also give evidence of a good reproducibility. The new shear plate shows to be an affordable and reliable tool for the measurement of submerged boundary shear stresses.

Keywords: shear stress measurements, ship propeller, scouring, bed stability.

1. INTRODUCTION

The design of stable revetments to protect alluvial beds from the scouring action of ship propellers requires a reliable estimate of the expected forces that would act over the bottom. Different methods are used in hydraulics and river engineering to calculate these forces through indirect estimation of the bottom shear stress (e.g., Rowiński et al. 2005). However, such

methods are mostly restricted to normal flow conditions or contain a large degree of uncertainty. Therefore, they cannot be applied to the strongly turbulent jets generated by ship propellers. Semi-empirical formulas are available to describe the velocity field in the propeller wake, but no general accurate methods have been developed to relate the jet near-boundary flow velocity to the bottom shear stress. This knowledge gap is in part related to the intrinsic difficulties to perform direct measurements of bed shear stress induced by ship propellers, either in laboratory or field.

The objective of this work is to present the design of a novel system for the direct measurement of bottom shear stresses. Although similar devices exist and have been described in previous literature (e.g., Tinoco and Cowen 2013), they are normally based on expensive technology, while the system here presented is made of relatively low-cost components. The general characteristics of the new system are described and preliminary results of measurements of bed shear stress induced by a ship propeller are presented.

2. CHARACTERISTICS OF THE SHEAR PLATE AND PRELIMINARY TESTS

The shear measurement system is composed of a rectangular head plate (HP) resting upon a jointed support (JS) and upon a force measurement system (DFS) (Fig. 1) used by Schoneboom et al. (2008) to measure drag forces of single vegetation elements. The DFS is based on the employment of four double strain gauges mounted on a stainless steel beam. The strain gauges are connected to an amplifier and the corresponding signal is logged by a PC. The function of the JS is to allow a horizontal displacement of HP, and in turn of the head of the DFS, as a reaction to the shear forces exerted by the flow on the HP. The displacement induces deformation of the steel beam embedded in the DFS, generating bending moments and compression strains, which are measured directly by the strain gauges.

To test the novel system, the bottom shear stress was measured for six different rotational speeds of a model propeller. The results are shown in Fig. 2. As expected, the measured shear stresses correlated well with the square of the propeller rotational speed. Moreover, for 6 repetitions of the measurements for each speed, the standard deviation of the measured forces (considering an area of the HP of 0.093 m^2) was in average 0.032 N, giving evidence of the high sensibility of the system and of the good reproducibility in terms of the complex turbulent flow field. These preliminary results show that the new shear plate is a promising device for reliable measurements of submerged boundary shear stress under a wide range of environments and flow conditions.

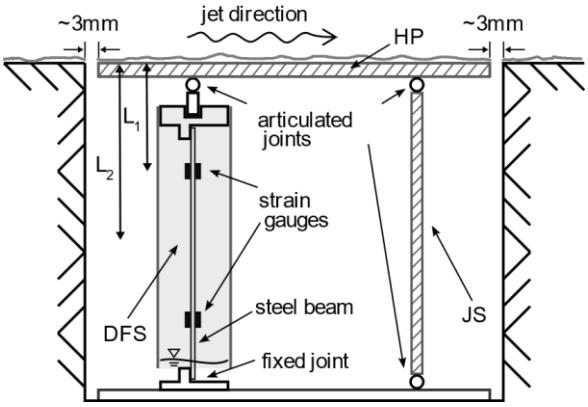

Fig. 1. Components of the new shear plate.

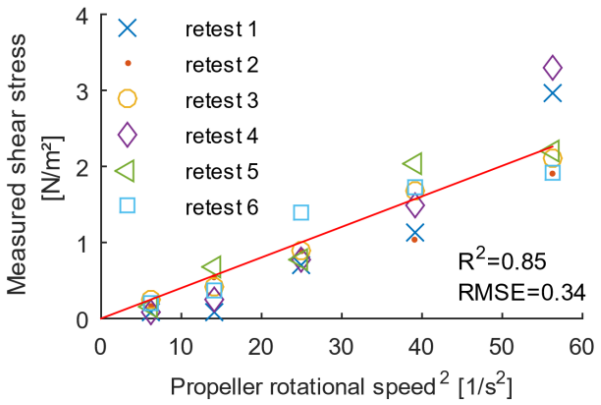

Fig. 2. Variation of bed shear stress with the square of the propeller rotational speed.

References

Rowiński, P., J. Aberle, and A. Mazurczyk (2005), Shear velocity estimation in hydraulic research, *Acta Geophys. Pol*. **53**, 4, 567-583.

Schoneboom, T., J. Aberle, C. Wilson, and A. Dittrich (2008), Drag force measurements of vegetation elements. **In:** *Proc. 8th Int. Conf. on Hydro-Science and Engineering (ICHE*), *8-12 September 2008, Nagoya, Japan.*

Tinoco, R.O., and E.A. Cowen (2013), The direct and indirect measurement of boundary stress and drag on individual and complex arrays of elements, *Exp. Fluids* **54**, 4, 1509, DOI: 10.1007/s00348-013-1509-3.

Received 22 March 2021
Accepted 12 April 2021

Publications of the Institute of Geophysics, Polish Academy of Sciences
Geophysical Data Bases, Processing and Instrumentation
vol. 434 (E-11), 2021, pp. 51-53
DOI: 10.25171/InstGeoph_PAS_Publs-2021-017
Webinar on Experimental Methods and Laboratory Instrumentation in Hydraulics, 13-15 April 2021

High Resolution Measurements of the Scour Hole Induced by a Ski-bucket Jet by Means of Structure from Motion

Elsa CARVALHO[1], Suzana ROSA[1], Maria Manuela LIMA[2], and Rui ALEIXO[3,✉]

[1]Department of Civil Engineering, Faculty of Engineering, University of Porto, Porto, Portugal

[2]Department of Civil Engineering/School of Engineering, University of Minho, Guimarães, Portugal

[3]CERIS – Instituto Superior Técnico, Universidade de Lisboa, Lisboa, Portugal

✉ rui.aleixo@tecnico.ulisboa.pt

A b s t r a c t

In this article a low-cost high-resolution photogrammetric method is presented to characterize the 3D geometry of scour cavity and bar induced by a ski jump jet. From the obtained 3D model all the main characteristics of the scour cavity and bar: the central longitudinal and transversal scour profiles, maximum scour depth and maximum bar height were determined with resolutions up to 0.0049 m. This technique allowed also to analyse the time evolution of the scour volume.

Keywords: photogrammetry, scour cavity and bar, high resolution bed model.

1. INTRODUCTION

Photogrammetry is based on a solid mathematical foundation and its details can be found in many textbooks (Konecny 2002). Within photogrammetry, structure from motion (SfM) is a technique to estimate 3 dimensional structures from two-dimensional images, which in a sense, mimics the biological vision of humans (and other animals) that perceive the 3D shapes from the retina projected 2D motion field of a moving object or scene. To the authors' best knowledge there are no applications of SfM to the study of jet induced scour.

2. EXPERIMENTAL SETUP AND RESULTS

The scour experiments were made in the Hydraulics Laboratory of the Faculty of Engineering of Porto University. A stepped spillway equipped with a ski-jump bucket defined by an angle $\alpha = 10^{o}$, drives the water from an upstream reservoir to a dissipation basin (1.5 m long, 0.705 m wide, and 0.70 m deep). The sand used on these experiments had a $d_{50} = 9.92\times10^{-3}$ m, and its density was $\rho_s = 2650$ kgm^{-3}. Four conditions made of two flow rates (0.51 and 0.85 Ls^{-1}) and two tailwater depths (0.03 and 0.05 m) were tested. Detailed information about the experimental setup can be found in Sá Machado et al. (2019). The bed was scanned with a Canon 7D Mark II, with a sensor of 20 Mpix, and equipped with a 50 mm f1.8 lens, and 50 photos were taken, corresponding to the maximum images that the free version of the software Zephyr 3D could handle. It was verified that scanning the bed with a cell phone camera hold similar results (Rosa 2018). The obtained 3D model as further processed in Meshlab and using an in-house built software. Figure 1a–c depicts the results for $Q = 0.85$ Ls^{-1} and $h_0 = 0.05$ m. Repeating the same experiment for different times, it was possible to analyse the evolution of the scour volume with time (Fig. 1d). The comparison of the longitudinal profiles with direct physical measurements showed differences in the range of 0.0049 to 0.0073 m (Rosa 2018).

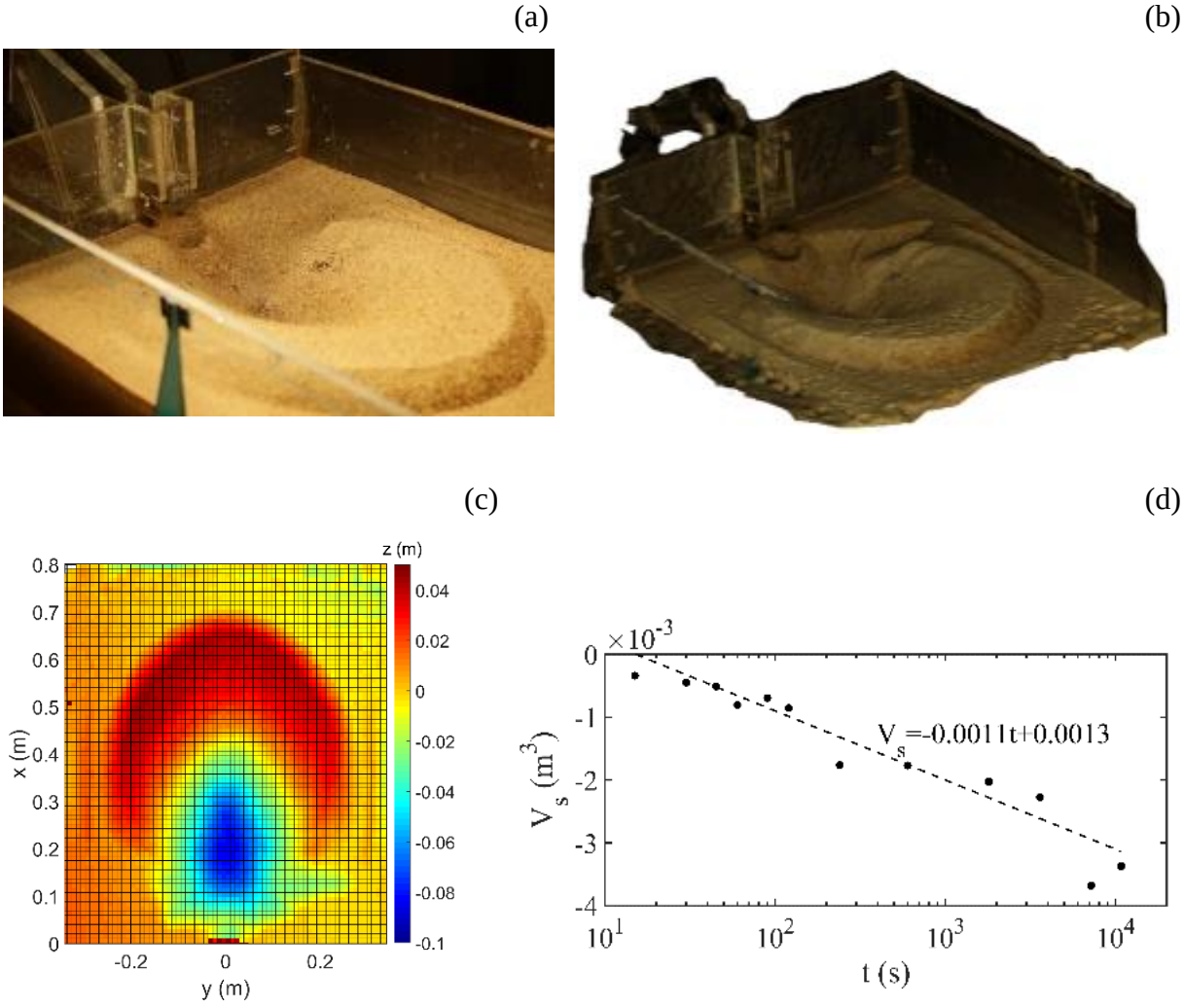

Fig. 1: (a) Photo of the spillway and dissipation basin, (b) obtained 3D model, (c) quantitative results of scour cavity and bar topography, (d) time evolution of the scour for $Q = 0.85$ Ls^{-1} and $h = 0.05$ m.

3. CONCLUSIONS

A low-cost, yet accurate and fast, structure from motion photogrammetry technique was applied to the jet induced scour. This technique used the free version of a SfM software (Zephyr 3D), an open-source mesh visualization software (Meshlab) and in-house developed software for post-processing and data analysis. The achieved resolution ranged from 0.0049 to 0.0073 m or about 5 to 8 grain diameters. Repeating the experiment and applying the same methodology it as possible to determine the time evolution of the scour hole volume and it was observed that it follows a log-law.

References

Konecny, G. (2002), *Geoinformation: Remote Sensing, Photogrammetry and Geographic Information Systems*, CRC Press, Boca Raton.

Rosa, S. (2018), Analysis of the ski-bucket angle influence on the erosion downstream of a stepped spillway, MSc. Thesis, Faculty of Engineering of University of Porto (in Portuguese).

Sá Machado, L., M.M.C.L. Lima, R. Aleixo, and E. Carvalho (2020), Effect of the ski jump bucket angle on the scour hole downstream of a converging stepped spillway, *Int. J. River Basin Manage.* **18**, 3, 383–394, DOI: 10.1080/15715124.2019.1586717.

Received 22 March 2021
Accepted 12 April 2021

Publications of the Institute of Geophysics, Polish Academy of Sciences
Geophysical Data Bases, Processing and Instrumentation
vol. 434 (E-11), 2021, pp. 55-57
DOI: 10.25171/InstGeoph_PAS_Publs-2021-018
Webinar on Experimental Methods and Laboratory Instrumentation in Hydraulics, 13-15 April 2021

Assessing the Transport of Pollutants by Means of Imaging Methods

Francisco MOLTENI[1], Patricio WINCKLER[1], Mauricio REYES[1], Alejandra GUBLER[2], Jorge SANDOVAL[3], and Rui ALEIXO[4,✉]

[1]Escuela de Ingeniería Civil Oceánica, Universidad de Valparaíso, Chile

[2]Centro de Investigación y Gestión de Desastres Naturales (CIGIDEN-PUC), Chile

[3]Departamento de Ingeniería Hidráulica y Ambiental, Pontificia Universidad Católica de Chile, Chile

[4]Civil Engineering Research and Innovation for Sustainability, Universidade de Lisboa, Portugal

✉ rui.aleixo@tecnico.ulisboa.pt

A b s t r a c t

Tragic oil spills such as the Exxon Valdez episode in the 1989 are a reminder of such events and their consequences. It is therefore important to have tools capable of detecting and tracking the fate of such spills. This paper presents some imaging-based tools developed to track the evolution of pollutant spills and tested in laboratory environment with two types of pollutants: a liquid and a dust-type pollutant.

Keywords: pollutants, imaging techniques, tracking, rhodamine, coal.

1. INTRODUCTION

Imaging methods have a range of application in many fields of science, and in hydraulics, where imaging-based methods such as PIV and PTV are often used (Muste et al. 2017). Imaging methods offer the possibility of analysing a significant area with enough resolution and so are particularly suited to field applications. In this study, imaging techniques were applied to determine the spill geometry and its evolution, of two different materials: rhodamine (liquid) and coal (dust). To extract the spill geometry a threshold analysis is used. This threshold can be defined in terms of the pixel intensity or pixel color. A trial-and-error test is usually needed to define the threshold value to consider. The goal is to obtain a binary image where the spill is isolated as depicted in Fig. 1. This task is not always trivial when the contrast between the pollutant and

Fig. 1. Identifying the spill by imaging methods. From left to right: raw image, binary image, isolated spill.

the background is low. In the present case, the threshold was adapted to consider dilution and light changes along the flume. With the spill isolated, it is then possible to compute its geometrical characteristics, namely its perimeter and its area. With some assumptions regarding its thickness, it becomes also possible to calculate its volume. By applying this procedure to the whole footage, it is possible to estimate the evolution and fate of the spill.

2. RESULTS

Experiments were carried out in a 15 m long, 1.0 m wide, and 1.5 m deep flume at the School of Ocean Engineering of the University of Valparaíso (Fig. 2). Tests were carried for a flow rate of $Q = 0.0101$ m^{3}s^{-1}, corresponding to a bulk mean velocity of $U \approx 0.050$ m/s. Images of the rhodamine and coal ($d_{50} = 0.54$ mm) spills were acquired by means of GoPro cameras located above the flume. The obtained results for the tracking of the different spills are depicted in Fig. 2. Mean velocity of the spills was 0.17 and 0.09 m/s for rhodamine and coal, respectively. The heavier fraction of coal deposits, and the lighter is transported in suspension.

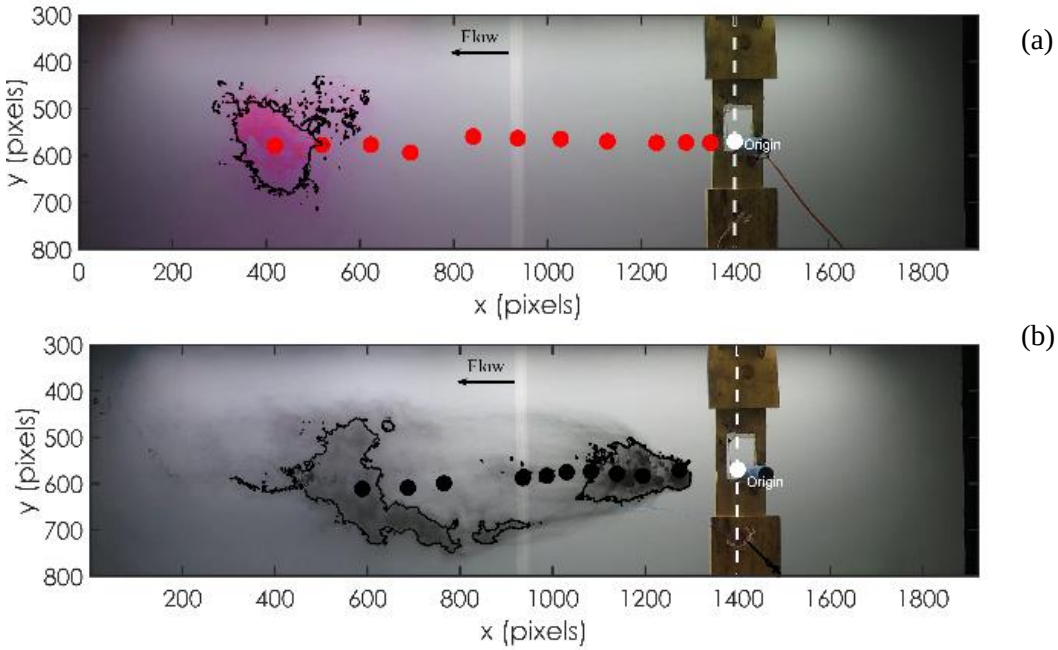

Fig. 2: (a) rhodamine spill tracked, (b) coal spill tracked. Flow is right to left. Dots indicate the center of mass of the spills at regular time intervals ($dt = 1.67$ s).

3. CONCLUSIONS

A detection and tracking algorithm was applied to spills made of different material at a laboratory scale. It was possible to track the evolution in time and space of the spill, allowing to track its trajectory, and ultimately its fate. It became also possible to determine the area and the velocity of the spill.

Acknowledgments. The authors would like to acknowledge Ecotecnos for providing the coal samples.

References

Muste, M., D.A. Lyn,, D. Admiraal, R. Ettema, V. Nikora, and M.H. Garcia (eds.) (2017), *Experimental Hydraulics: Methods, Instrumentation, Data Processing and Management: Volume I: Fundamentals and Methods*, CRC Press, Boca Raton.

Received 22 March 2021
Accepted 12 April 2021

Publications of the Institute of Geophysics, Polish Academy of Sciences
Geophysical Data Bases, Processing and Instrumentation
vol. 434 (E-11), 2021, pp. 59-61
DOI: 10.25171/InstGeoph_PAS_Publs-2021-019
Webinar on Experimental Methods and Laboratory Instrumentation in Hydraulics, 13-15 April 2021

Laboratory Experiments on Gravity Currents Interacting with Upslope and Overhang Barriers

Maria Rita MAGGI[1,✉],
Claudia ADDUCE[1], and Gregory Francis LANE-SERFF[2]

[1]Roma Tre University, Rome, Italy
[2]University of Manchester, Manchester, United Kingdom
✉ mariarita.maggi@uniroma3.it

A b s t r a c t

The dynamics of steady two-dimensional gravity currents interacting with slopes and overhangs are investigated by laboratory experiments. Parameters such as the initial volume of the dense fluid and the angle of the barrier positioned inside the tank are varied. An image analysis technique is adopted to evaluate the instantaneous density fields. The analysis performed showed how the nature of the barrier affects the dynamics of the dense current.

Keywords: gravity currents, laboratory experiments, image analysis technique, complex topography.

1. INTRODUCTION

Gravity currents are flows driven by a density difference due to a variation in salinity, temperature or the concentration of suspended particulates. These geophysical flows widely occur spontaneously in nature or for anthropogenic causes (Simpson 1997). Although gravity currents develop generally over more complex floor topographies involving slopes, submarine channels and seamounts (Lane-Serff et al. 1995), most laboratory investigations dealing with the dynamics of those currents considers flows over flat surfaces. These last investigations reveal a lack of knowledge on gravity currents interacting with a complex topography.

The aim of this work is to investigate how even simple variations of the geometry of the domain influence the dynamics of gravity currents by using laboratory experiments.

2. EXPERIMENTAL DETAILS

The laboratory experiments are conducted in a Perspex tank 3 m long, 0.2 m wide and 0.3 m deep. The experimental apparatus (Fig. 1) is similar to that described in Lane-Serff et al. (1995) which allows an incoming steady flow. The lock reservoir is realized with a fixed gate placed at $L_0 = 0.4$ m leaving a rectangular opening at the bottom of the tank. A removable gate covers the opening. A slope is located at $L_S = 0.85$ m from the fixed gate with different inclination θ, ranging from 15° and 165°, in order to represent up slopes (S runs), or overhanging barriers cases (O runs).

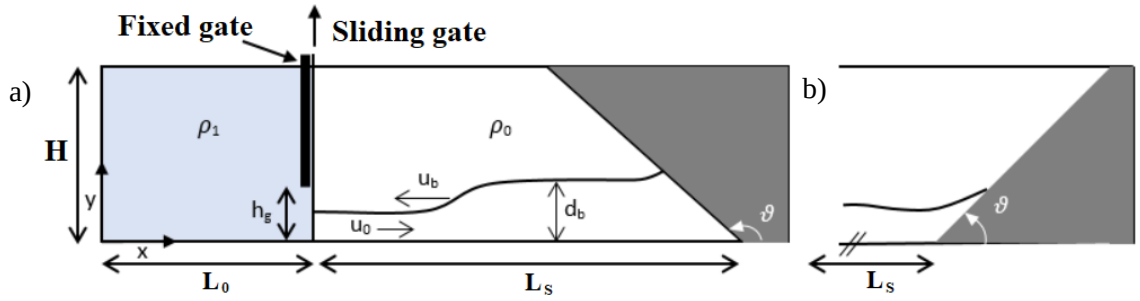

Fig. 1. Sketch of the tank used to perform laboratory experiments. Gravity current reflected back respectively by: a) overhang barrier (O runs); b) slope (S runs).

For each experiment the left part of the tank is filled with salty water with initial density ρ_1, while the rest of the tank is filled with an ambient fluid of density ρ_0 ($\Delta\rho = \rho_1 - \rho_0 = 40$ kg/m^3).

A controlled quantity of dye is added to the salty water in order to allow the visualization of the dense fluid. The run starts when the sliding gate is removed and stopped when the reflected dense flow, after the interaction with the slope, reached the position L_0. The Froude number $Fr = U_b/\sqrt{g_0'(h_g/2)} \cong 0.8$, where U_b is the bulk velocity and $g_0' = g * (\Delta\rho/\rho_0)$ is the initial reduced gravity. The experiments were recorded by a camera with an acquisition frequency of 25 Hz and spatial resolution of 1024×668 pixels. Images extracted from the acquired movie were converted into matrices of grey levels. The instantaneous density fields $\rho^*(x,y,t) = (\rho(x,y,t) - \rho_0)/(\rho_1 - \rho_0)$ was obtained by an image analysis technique (Nogueira et al. 2013). The pixel-based analysis of the density fields adopted here allows us to obtain the local density value and then the depth-averaged density, $\bar{\rho}_v$. From the $\bar{\rho}_v$ is possible to infer the main characteristics of the flow dynamics. Figure 2 shown $\bar{\rho}_v$ in the plane $x^* - t^*$ for the S

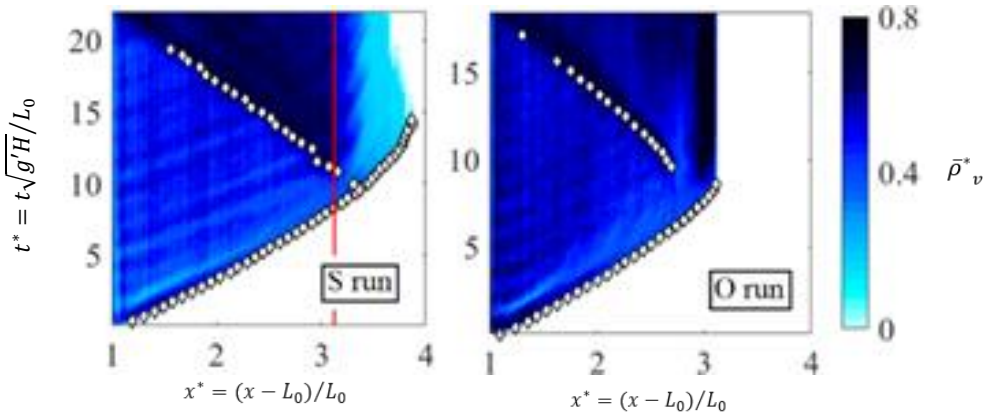

Fig. 2. Dimensionless $\bar{\rho}^*_v$, for the S run with $\theta = 15°$ and for the O run with $\theta = 150°$. The white markers mark the dimensionless front and reflected bore position. The red line represents the toe of the slope.

and O runs. In the up slope case the high values of $\bar{\rho}^*_v$ are identified in the area near the front of the current and in the outgoing bore, while for the overhang run high values of $\bar{\rho}^*_v$ can be also observed at the foot of the barrier. The presence of mixing associated with the reflection process is larger for the O run than the S run. The density fields emphasizes a more complex dynamics in the O run related to the presence of the barrier even before the current interacts with it.

References

Lane-Serff, G.F., L.M. Beal and T.D. Hadfield (1995), Gravity current flow over obstacles, *J. Fluid Mech.* **292**, 39–53, DOI: 10.1017/S002211209500142X.

Nogueira, H.I.S., C. Adduce, E. Alves, and M.J. Franca (2013), Image analysis technique applied to lock-exchange gravity currents, *Meas. Sci. Technol.* **24**, 4, 047001.

Simpson, J.E. (1997), *Gravity Currents: In the Environment and the Laboratory*, 2nd ed., Cambridge University Press, Cambridge, 258 pp.

Received 22 March 2021
Accepted 12 April 2021

Publications of the Institute of Geophysics, Polish Academy of Sciences
Geophysical Data Bases, Processing and Instrumentation
vol. 434 (E-11), 2021, pp. 63-65
DOI: 10.25171/InstGeoph_PAS_Publs-2021-020
Webinar on Experimental Methods and Laboratory Instrumentation in Hydraulics, 13-15 April 2021

In-situ Survey of an Unstructured Block Ramp

Ralph EIKENBERG✉ and Jochen ABERLE

Leichtweiß-Institute for Hydraulic Engineering and Water Resources,
Division of Hydraulic Engineering and River Morphology, Technische Universität Braunschweig,
Braunschweig, Germany

✉ r.eikenberg@tu-braunschweig.de

A b s t r a c t

This paper describes the in-situ survey of an unstructured block ramp to obtain a detailed topographical digital model for a research project focusing on the fish-based identification of migration corridors. The strategy to drain the block ramp in the field for the survey is described and the obtained digital model is presented. The digital model will be used in subsequent experiments with live fish in the field and laboratory to link fish trajectories, the local flow field, and the bed topography to improve the development of new and enhanced design criteria for nature-like unstructured block ramps.

Keywords: unstructured block ramps, structure from motion photogrammetry, terrestrial laser scan, ecohydraulics.

1. INTRODUCTION AND PROJECT OVERVIEW

Unstructured block ramps are nature-based hydraulic structures which are built in rivers for the restoration of the ecological connectivity. They are characterized by a spatially heterogeneous roughness structure and flow conditions due to the irregular arrangement of large stones and boulders. Compared to more geometrically defined structures with cross bars or regularly arranged boulders, unstructured ramps fit well into the appearance of the river landscape and provide additional habitat for the aquatic flora and fauna. Until today, the hydraulic design of these structures is based on empirical approaches considering only reach-averaged values of water depths and flow velocities. This means that local hydrodynamic flow conditions, which are important for fish passage, cannot be adequately quantified. It is therefore not possible to guarantee the existence of functioning migration corridors for fish, and this is why this type of block ramp is often not implemented despite its advantages.

The project MigRamp aims at identifying and quantifying migration corridors of ascending fish on such nature-based hydraulic structures by linking fish trajectories to bed topography and the local flow field. For this purpose, combined fish-biological and hydraulic studies will be carried out in cooperation with the river maintenance association Leineverband and Vattenfall Research and Development AB (Vattenfall R&D). The corresponding studies will be carried out on an existing nature-like unstructured block ramp in the river Ilme in Lower Saxony, Germany, and on a 1:1 partial model of this ramp in the "Laxelerator", a unique research facility for ethohydraulic experiments in the Vattenfall hydraulic engineering laboratory in Älvkarleby, Sweden. The purpose of this paper is to describe the topographical in-situ survey of the block ramp that was carried out in October 2020.

2. RAMP SCAN

The unstructured block ramp in the Ilme river, which is in the focus of MigRamp, was built after a weir removal to conduct water to a diverted historical mill channel (Fig. 1a). For the survey by structure-from-motion (SfM) photogrammetry and terrestrial laser scanning (TLS), it was necessary to drain the ramp for a few hours. Before starting the temporary construction works for diverting the flow (approx. 700 l/s on that day), the fish in the ramp area were professionally recovered by means of electrofishing and relocated upstream. The diversion of the water was achieved by constructing a temporary dam using gravel-filled big bags. The dam was additionally sealed with a plastic sheet and sandbags and seepage water was intercepted by pumps and fed back into the Ilme downstream of the ramp structure (Fig. 1b). A further pump installed upstream of the temporary dam provided a sufficient environmental flow (approx. 150 l/s) for the duration of the survey, so that the river did not run dry downstream of the ramp.

A total of 16 marker points were distributed on the drained ramp for SfM together with five fixed points for later measurements. The corresponding coordinates were recorded using differential GPS. Four photo sets were created with different cameras to ensure high data quality for SfM, and the ramp surface was additionally surveyed by TLS. After completion of the work, the dam was removed, and the original condition of the ramp was restored. The final result of the in-situ survey, in which about 15 people from different institutions were involved, was a GPS referenced point cloud (~85 million points on ~90 m² projected area) which will serve as the basis for a 1:1 partial model of the ramp in the "Laxelerator" (Fig. 1c).

Fig. 1: a) top view sketch of the water damming and diversion, b) dam and drained ramp, c) concept sketch for the 1:1 partial model in the "Laxelerator", based on a 3d mesh of the existing ramp.

Acknowledgments. We acknowledge the support of the Leineverband (Northeim, Germany) and everyone who contributed to the success of the ramp scan from TU Braunschweig, Federal Agency for Technical Relief (OV Einbeck), and the Fischereiverein Einbeck e.V. The MigRamp project is funded by the Deutsche Bundesstiftung Umwelt (DBU), Germany.

Received 22 March 2021
Accepted 12 April 2021

Publications of the Institute of Geophysics, Polish Academy of Sciences
Geophysical Data Bases, Processing and Instrumentation
vol. 434 (E-11), 2021, pp. 67-69
DOI: 10.25171/InstGeoph_PAS_Publs-2021-021
Webinar on Experimental Methods and Laboratory Instrumentation in Hydraulics, 13-15 April 2021

Non-intrusive Density Measurements Applied to Gravity Currents Interacting with an Obstacle

Maria Chiara DE FALCO✉, Claudia ADDUCE, and Maria Rita MAGGI

Department of Engineering, University Roma Tre, Rome, Italy

✉ mariachiara.defalco@uniroma3.it

A b s t r a c t

The dynamics of lock-release gravity currents interacting with a triangular barrier are investigated experimentally by applying non-intrusive density measurements based on image analysis, to measure the instantaneous density fields. The relevant parameter varied is the ratio between the height of the obstacle and the initial water depth. Results suggest that the image analysis based on a calibration curve is a suitable technique for the study of the gravity currents dynamics, which is strongly affected by the presence of a bottom obstacle depending on the relative obstacle height.

Keywords: gravity currents, image analysis technique, bottom obstacle, density fields.

1. INTRODUCTION

Gravity currents are density-driven flows caused by a density difference, which can be due to a temperature or salinity gradient or the presence of suspended sediments. In the latter case, these flows are known as turbidity currents and represent a geohazard to seafloor structures and offshore pipelines. For this reason, in lakes or in reservoirs, a barrier could be designed to stop or deviate the flow away from the structures, which can be damaged by an interaction with the current (De Cesare et al. 2001). Obstacles with a triangular cross-section are a good approximation to represent submerged barriers (Tokyay and Constantinescu 2015) and an accurate comprehension of the implications of the interference can help to improve the engineering models, depending on the parametric conditions characterizing these flows.

In the present study, an image analysis technique is used to evaluate the instantaneous density fields of a gravity current interacting with a triangular obstacle. Several experiments are performed with and without the obstacle and the effect of the relative obstacle height on the dynamics of the dense current is studied.

2. EXPERIMENTAL PROCEDURE

Lock-exchange gravity currents are produced in a Perspex tank 3 m long, 0.2 m wide, and 0.3 m deep (Fig. 1). A lock-release technique was applied to generate gravity currents, by dividing the tank in two different volumes with a removable gate, placed at a distance $x_0 = 0.4$ m from the left wall. The left part of the tank was filled with a saline mixture at density $\rho_1 = 1010$ kg/m^3 while the right part of the tank was filled with fresh tap water at a measured density $\rho_0 = 1000$ kg/m^3, where $\rho_1 > \rho_0$ with a constant $\Delta\rho = \rho_1 - \rho_0 = 10$ kg/m^3. Experiments were performed first on the horizontal bed and then with a triangular obstacle placed at a distance L_0 from the gate. The main parameter varied is the relative obstacle height $R_0 = h_c/d$ where d is the obstacle height and $h_c = H/2$ is the current height (Benjamin 1968).

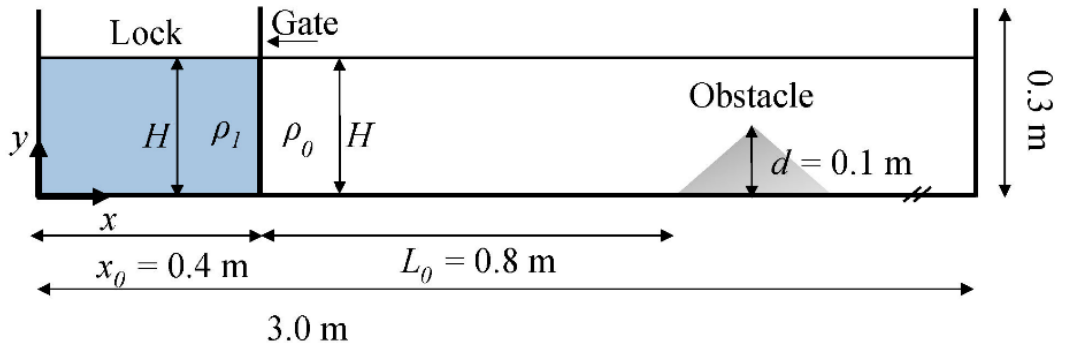

Fig. 1. Schematic representation of the experimental apparatus.

An image analysis technique is applied to evaluate the instantaneous density fields $\rho(x, y, t)$. The concentration of dye in the gravity current is considered linearly correlated to the salt concentration. A calibration technique is used to correlate the light intensity with the concentration of dye for each pixel of the acquired images. To this aim, nine controlled concentrations of dye were added and mixed to the fresh water in the tank in order to obtain a homogeneous dyed fluid and images were acquired to build a calibration curve. Figure 2a shows the calibration points obtained for a single pixel in the domain, considering nine images.

A snapshot of a gravity current with $R_0 = 1.28$ and the corresponding instantaneous non-dimensional density field $\rho^*(x, y) = (\rho(x, y) - \rho_0)/\Delta\rho$ are shown in Fig. 2b,c. The obtained density field gives insight into the gravity current's dynamics, which is strongly affected by the presence of the obstacle. A diluted current propagates downstream the obstacle, while part, denser, is retained by the obstacle.

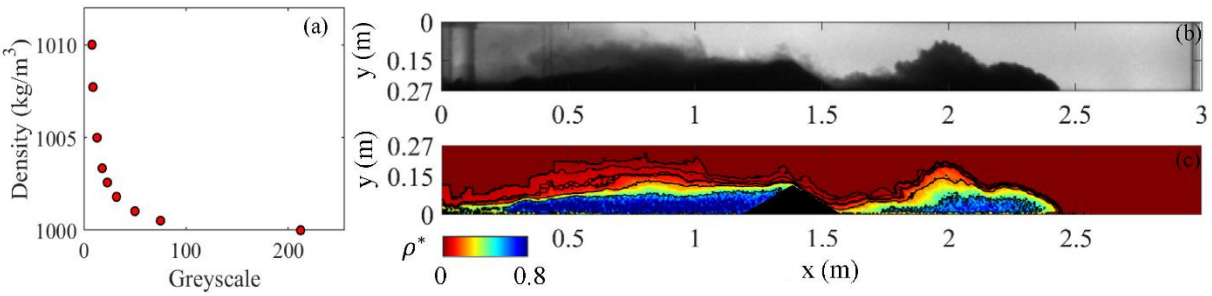

Fig. 2: (a) Calibration curve based on nine controlled quantities of dye, (b) snapshot of a gravity currents, and (c) corresponding non-dimensional density field after the interaction with the obstacle.

References

Benjamin, T.B. (1968), Gravity currents and related phenomena, *J. Fluid Mech*. **31**, 2, 209–248.

De Cesare, G., A. Schleiss, and F. Hermann (2001), Impact of turbidity currents on reservoir sedimentation, *J. Hydraul. Eng*. **127**, 1, 6–16, DOI: 10.1061/(ASCE)0733-9429(2001)127:1(6).

Tokyay, T., and G. Constantinescu (2015), The effects of a submerged non-erodible triangular obstacle on bottom propagating gravity currents, *Phys. Fluids* **27**, 5, 056601, DOI: 10.1063/1.4919384.

Received 22 March 2021
Accepted 21 April 2021

Publications of the Institute of Geophysics, Polish Academy of Sciences
Geophysical Data Bases, Processing and Instrumentation
vol. 434 (E-11), 2021, pp. 71-73
DOI: 10.25171/InstGeoph_PAS_Publs-2021-022
Webinar on Experimental Methods and Laboratory Instrumentation in Hydraulics, 13-15 April 2021

Turbulence Anisotropy in a Sinuous Channel with Downward Seepage

Jyotismita TAYE✉ and Bimlesh KUMAR

Indian Institute of Technology, Guwahati, Assam, India

✉ taye176104022@iitg.ac.in

Abstract

The study estimates the turbulence anisotropy for flow in a sinuous channel under the influence of downward seepage. Anisotropy provides the deviation from the isotropic turbulence. Given the complex flow processes in a sinuous channel, it is vital to investigate the turbulent flow characteristics.

Keywords: turbulence, anisotropy, sinuous channel, seepage.

1. INTRODUCTION

The geometry of the channel may have a significant effect on the flow characteristics around the sinuous bend. Lumley and Newman (1977) defined the Reynolds stress anisotropy tensor to evaluate the turbulence structure to different bed condition. The Reynolds stress anisotropy tensor (b_{ik}) is given as:

$$b_{ij} = \frac{\overline{u'_i u'_j}}{2k} - \frac{\delta_{ij}}{3} \tag{1}$$

where k is the average turbulent kinetic energy (TKE) and δ_{ij} is the Kronecker delta function, where $i, j = 1, 2, 3$ are the spatial components. The anisotropic invariant map (AIM) is constructed to examine the anisotropy of Reynolds stress. AIM is represented using the two principal independent invariants (II and III). The AIM by can also be presented by plotting ξ against η because it produces less distortion in forming a triangle. The detailed methodology can be found in Raushan et al. (2020). With seepage, the flow parameters are modified near the channel bed. With downward seepage, the magnitude of Reynolds shear stress increased (Taye et al. 2020), and with upward seepage, the Reynolds shear stress decreased (Herrera-Granados and Kostecki 2017).

The three-dimensional instantaneous velocities were recorded using a Nortek® Vectrino + Acoustic Doppler Velocimeter (4-beam probe down-looking). The velocimeter uses the Doppler shift principle for velocity measurement and delivers the velocities in three orthogonal directions (streamwise, transverse, and vertical). In the present study, the velocities were collected for 2 minutes with sampling frequency 100 Hz. The SNR (signal-to-noise) was greater than 15 decibels and the correlation greater than 60% during data collection. For good result, the SNR should be greater than 15 decibels (Nortek 1997) and the correlation should be at least 60% (McLelland and Nicholas 2000). The raw data was filtered by the acceleration threshold method, as it may sometimes be contaminated with spikes.

2. RESULTS AND DISCUSSIONS

The anisotropy at bend upstream and bend center tends to move towards the one-component isotropy for no seepage and seepage flows. At bend downstream, the anisotropy is reduced to two-component isotropy, as maximum points lie towards the left line, signifying the turbulence fluctuations to lead along two directions. At bend upstream and center, maximum points lie above the right line, which signify the fluctuations to dominate along one direction.

With seepage flows at bend upstream, the points reach one-component isotropy faster than at bend center, and further at bend downstream, the points are clustered near the two-component isotropy (Fig. 1).

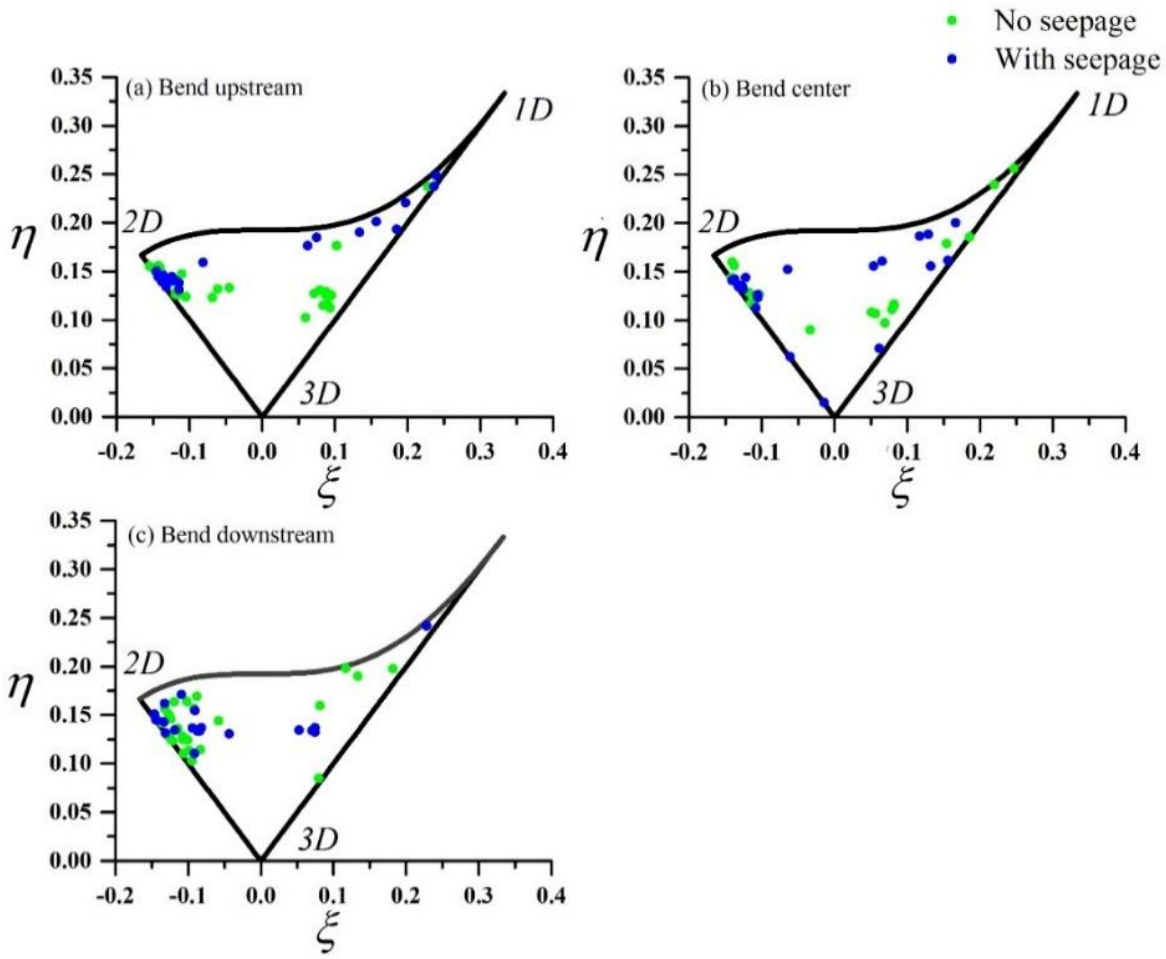

Fig. 1. Representation of Lumley triangle for no seepage and seepage flows at: (a) Bend upstream, (b) Bend center, and (c) Bend downstream.

References

Herrera-Granados, O. and S.W. Kostecki (2017), Experimental study of the influence of small upward seepage on open-channel flow turbulence, *J. Hydraul. Eng.* **143**, 8, 06017009, DOI: 10.1061/(ASCE)HY.1943-7900.0001312.

Lumley, J.L., and G.R. Newman (1977), The return to isotropy of homogeneous turbulence, *J. Fluid Mechanics* **82**, 1, 161–178, DOI: 10.1017/S0022112077000585.

McLelland, S.J., and A.P. Nicholas (2000), A new method for evaluating errors in high-frequency ADV measurements, *Hydrol. Processes* **14**, 2, 351–366, DOI: 10.1002/(SICI)1099-1085(20000215)14:2<351::AID-HYP963>3.0.CO;2-K.

Nortek (1997), ADV Operation manual, Nortek AS Inc.

Raushan, P.K., S.K. Singh, and K. Debnath (2020), Turbulence anisotropy with higher-order moments in flow through passive grid under rigid boundary influence, *Proc. Inst. Mech. Eng., Part C: J. Mech. Eng. Sci.*, DOI: 10.1177/0954406220969736.

Taye, J., A.D. Lade, A. Mihailović, D.T. Mihailović, and B. Kumar (2020), Information measures through velocity time series in a seepage affected alluvial sinuous channel, *Stoch. Environ. Res. Risk Assess*. **34**, 11, 1925–1938, DOI: 10.1007/s00477-020-01849-2.

Received 22 March 2021
Accepted 12 April 2021

Publications of the Institute of Geophysics, Polish Academy of Sciences
Geophysical Data Bases, Processing and Instrumentation
vol. 434 (E-11), 2021, pp. 75-77
DOI: 10.25171/InstGeoph_PAS_Publs-2021-023
Webinar on Experimental Methods and Laboratory Instrumentation in Hydraulics, 13-15 April 2021

Laboratory Investigation of Sediment Transport under Transient Flow – Preliminary Results

Łukasz PRZYBOROWSKI[1,✉], Michael NONES[1], Magdalena MROKOWSKA[1], Leszek KSIĄŻEK[2], PHAN Cong Ngoc[2], Andrzej STRUŻYŃSKI[2], and Maciej WYRĘBEK[2]

[1]Institute of Geophysics, Polish Academy of Sciences, Warszawa, Poland

[2]University of Agriculture in Kraków, Faculty of Environmental Engineering and Land Surveying, Kraków, Poland

✉ lprzyborowski@igf.edu.pl

A b s t r a c t

Flooding events in rivers are usually causing an increment in sediment transport. To investigate the relationships between bedload, bed shear stress and wave characteristics, laboratory experiments were performed in a 12-m-long flume at the University of Agriculture in Kraków, Poland. Three sets of experiments were conducted, imposing singular trapezoidal flood waves as forcing terms. The maximal wave height differed between runs, but the water volume and bed slope stayed the same. The bed was covered with mixed gravel, and the sediment was weighted using a trap at the end of the flume. The water level was measured at 5 points along the flume, while the velocity was measured in the middle of the flume by Acoustic Doppler Velocimeter at a point 7 cm above the bed. Preliminary results show that unsteadiness of flow induces the variation of bedload transport during the wave passage and that the total yield of sediment is positively correlated with the wave magnitude.

Keywords: ADV, laboratory experiments, sediment transport, unsteady flow.

1. INTRODUCTION

The studies of sediment transport in conditions most comparable to that of natural watercourses are essential in understanding the effects of naturally and accidentally occurring events. Such events are associated with abrupt unsteadiness of the river flow, which causes a higher rate at which sediments are moved within a river, resulting eventually in morphodynamic and water

quality changes (Michalik and Książek 2009). Recent laboratory experiments correlated bed shear stress, bedload rate and stream power, and pointed out that hysteresis is present in the relationship between sediment flux and flow rate, as well as between other process variables (Mrokowska et al. 2018; Phillips et al. 2018). Moving from such findings, the present experiments were designed to further investigate the characteristics of transient flows, and the influence of wave characteristics on the bedload dynamics.

2. EXPERIMENTAL SETUP

Experiments were performed in 12-m-long and 0.485-m-wide flume. The channel bottom was covered with a layer of mixed gravel with median grain size d_{50} = 3.52 mm and maximal grain size d_{max} = 12.50 mm. Trapezoidal waves were generated varying the maximum discharge. Water depth was measured using 5 resistive sensors placed along the flume. The flow velocity was measured at a point around 7 cm above the bed, using a Sontek ADV at 50 Hz placed in the middle of the flume. Before each run, the bed was manually smoothed, and the flume was slowly filled with water, initially to discharge equal to 6 m^3/h, then for 2 minutes increased to 80 m^3/h, which was estimated to correspond to incipient motion conditions.

3. RESULTS

Three series of experiments were conducted and repeated, obtaining 10 runs in total with three different wave magnitude. Accordingly, the average water depth during a wave peak was 13.0 cm with average discharge $Q = 176\ m^3h^{-1}$ and stream power $\omega = 2.34\ Nm^{-1}s^{-1}$ for the first set of tests; 11.9 cm with $Q = 150\ m^3h^{-1}$ and $\omega = 2.91\ Nm^{-1}s^{-1}$ for the second; 9.6 cm with $Q = 113\ m^3h^{-1}$ and $\omega = 1.49\ Nm^{-1}s^{-1}$ for the third test. The dimensionless shear stress derived from the ADV data exceeded the critical shields parameter. The bedload rate q [kgs^{-1}] was an order of magnitude higher during the highest discharge case (Fig. 1a) in comparison to the lowest discharge (Fig. 1b).

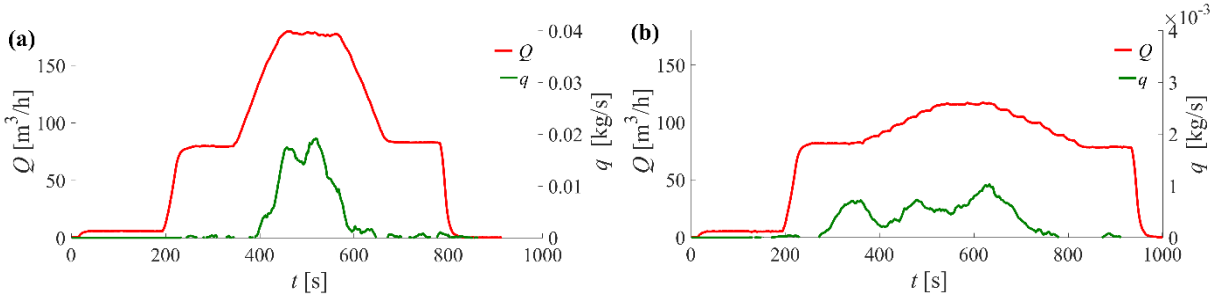

Fig. 1. Recorded hydrographs with discharge and bedload rate for a wave with a peak at: 180 m^3h^{-1} (a) and 115 m^3h^{-1} (b).

Acknowledgements. We express our gratitude to Szymon Wojak who was actively engaged in the process of laboratory data collection.

References

Michalik, A., and L. Książek (2009), Dynamics of water flow on degraded sectors of Polish mountain stream channels, *Pol. J. Environ. Stud.* **18**, 4, 665–672.

Mrokowska, M.M., P.M. Rowiński, L. Książek, A. Strużyński, M. Wyrębek, and A. Radecki-Pawlik (2018), Laboratory studies on bedload transport under unsteady flow conditions, *J. Hydrol. Hydromech*. **66**, 1, 23–31, DOI: 10.1515/johh-2017-0032.

Phillips, C.B., K.M. Hill, C. Paola, M.B. Singer, and D.J. Jerolmack (2018), Effect of flood hydrograph duration, magnitude, and shape on bed load transport dynamics, *Geophys. Res. Lett*. **45**, 16, 8264–8271, DOI: 10.1029/2018GL078976.

Received 22 March 2021
Accepted 12 April 2021

Publications of the Institute of Geophysics, Polish Academy of Sciences
Geophysical Data Bases, Processing and Instrumentation
vol. 434 (E-11), 2021, pp. 79-81
DOI: 10.25171/InstGeoph_PAS_Publs-2021-024
Webinar on Experimental Methods and Laboratory Instrumentation in Hydraulics, 13-15 April 2021

Laser Profilometry Technique for Nonintrusive and Subaquaous 3D Geometry Reconstructions

Ismail RIFAI[1,✉], Lydia KHELOUI[2], Sébastien E. BOURBAN[2], Sébastien ERPICUM[3], Pierre ARCHAMBEAU[3], Michel PIROTTON[3], Damien VIOLEAU[2], Benjamin DEWALS[3], and Kamal EL KADI ABDERREZZAK[2,✉]

[1]Egis, Flood Risks and Water Resources, Strategy and Innovation, Guyancourt, France
[2]EDF R&D, National Laboratory for Hydraulics and Environment, Chatou, France
[3]University of Liège, Hydraulics in Environmental and Civil Engineering, Liège, Belgium
✉ ismail.rifai@egis.fr; kamal.el-kadi-abderrezzak@edf.fr

A b s t r a c t

Laser Profilometry refers to a surface measurement by laser sheet projection on the geometry of interest. This technique is routinely used in industrial and in hydraulics laboratory applications. In this paper, we present a development of this technique for overtopping induced dike breaching experiments. The Laser Profilometry Technique (LPT) presented hereafter allows for high resolution continuous monitoring of the three-dimensional (3D) evolving breach in laboratory models of fluvial dikes. The reconstructions of submerged parts of the dike were allowed by use of a dedicated refraction correction module. The LPT was selected for this application as it is compatible with commercial cameras and standard sheet projecting lasers while offering accurate and sufficient spatiotemporal resolution of the 3D reconstructions. The method has also advantages in terms of flexibility and compatibility with different experimental configurations and could be used on different scale models.

Keywords: profilometry, DLT, subaqueous, dike breaching, nonintrusive.

1. INTRODUCTION

Nonintrusive reconstruction of highly evolving surfaces is a challenging task and a highly valuable feature in experimental setups, especially in erosion, scouring and morphodynamics related experiments. Recent advances in digital imaging and processing capabilities promoted

development of image processing based measurement technique. The Laser Profilometry Technique (LPT) presented in this paper is one of them as almost all the information needed for the geometry reconstruction is encapsulated in recorded images.

2. OVERALL ALGORITHM

The LPT applied to dike breaching experiments is structured in three main modules: (1) image processing, (2) reconstruction, and (3) refraction correction. The image processing module consists of a series of filters allowing to segregate the laser profile incident on the measured geometry (Fig. 1a). The reconstruction module transforms the laser profiles defined in image coordinates into 3D coordinates. This step is performed using the Direct Linear Transformation (DLT) algorithm (Abdel-Aziz and Karara 2015) (Fig. 1b). The refraction correction module allows for refraction bias correction for submerged reconstructed surfaces. The refraction correction is applied using the Snell-Descartes law (Glassner 1989) and assuming simplified planar approximations of the water surface. Detailed description of the algorithm is presented in Rifai et al. (2020).

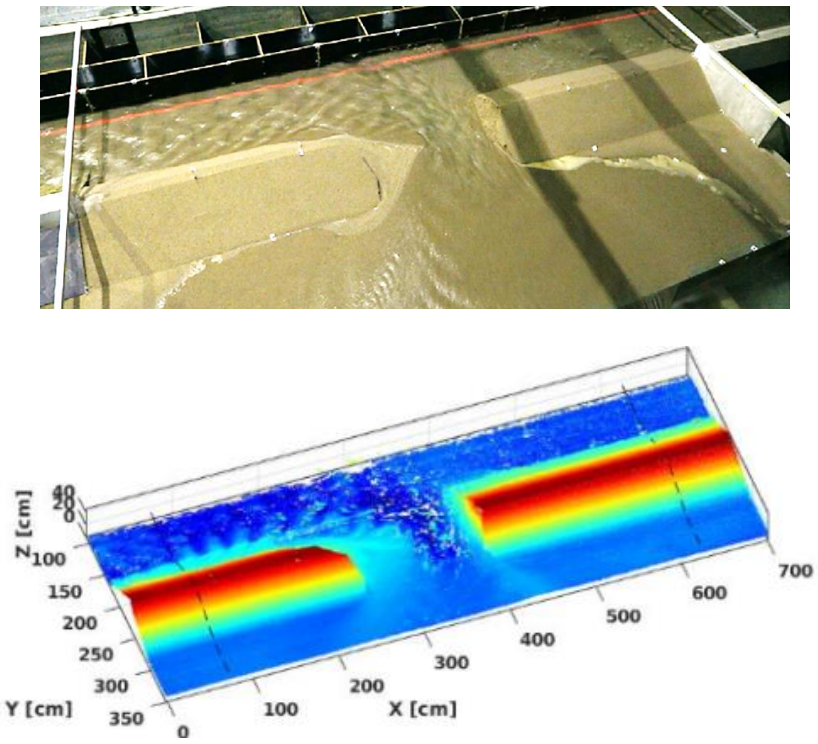

Fig. 1. Reconstruction of the breach geometry for a fluvial dike breaching test with erodible bottom.

3. LIMITS AND PERSPECTIVES

Although the method has proven its performance and allowed for satisfactory results on overs 50 dike breaching tests (Rifai et al. 2019), several limits were pinpointed and restricted the range of experimental configurations that could be studied.

Issues related to laser visibility, such as blind spots and water turbidity, can result in missing data in the reconstruction. Adding cameras with different point of views and different colour lasers can be a workaround of the first issue. Adaption of the laser power and enhancement of the image processing algorithm can allow improvement of the accuracy of reconstructions in high turbidity cases.

Other adaptations of the overall algorithm can be explored and can allow for complementary measurements. For hydraulics and/or morphodynamics related experiments, this enhancements could be particle tracking for flow trajectories and velocities, water height deduction from laser refraction measurements, colorized and texturized reconstructions allowing for tracking of bed forms migration, etc.

References

Abdel-Aziz, Y.I., and H.M. Karara (2015), Direct linear transformation from comparator coordinates into object space coordinates in close-range photogrammetry, *Photogramm. Eng. Remote Sens.* **81**, 2, 103–107, DOI: 10.14358/PERS.81.2.103.

Glassner, A.S. (ed.) (1989), *An Introduction to Ray Tracing*, Morgan Kaufmann Publ., San Francisco.

Rifai, I., K. El Kadi Abderrezzak, S. Erpicum, P. Archambeau, D. Violeau, M. Pirotton, and B. Dewals (2019), Flow and detailed 3D morphodynamic data from laboratory experiments of fluvial dike breaching, *Scien. Data* **6**, 53, DOI: 10.1038/s41597-019-0057-y.

Rifai, I., V. Schmitz, S. Erpicum, P. Archambeau, D. Violeau, M. Pirotton, B. Dewals, and K. El Kadi Abderrezzak (2020), Continuous monitoring of fluvial dike breaching by a laser profilometry technique, *Water Resour. Res.* **56**, 10, e2019WR026941, DOI: 10.1029/2019WR026941.

Received 22 March 2021
Accepted 12 April 2021

Publications of the Institute of Geophysics, Polish Academy of Sciences
Geophysical Data Bases, Processing and Instrumentation
vol. 434 (E-11), 2021, pp. 83-85
DOI: 10.25171/InstGeoph_PAS_Publs-2021-025
Webinar on Experimental Methods and Laboratory Instrumentation in Hydraulics, 13-15 April 2021

Some Thoughts on Assessing near Bed Surface Flow Hydrodynamics using Instrumented Particles

Khaldoon ALOBAIDI and Manousos VALYRAKIS✉

Water Engineering Lab, School of Engineering, University of Glasgow, Glasgow, UK

✉ Manousos.Valyrakis@glasgow.ac.uk

A b s t r a c t

A novel and low cost tool, namely the instrumented particle, that is potentially able to directly monitor the near bed surface flow hydrodynamics and can be used by researchers and practitioners alike is presented. The particle is fitted with micro-electro-mechanical-systems, MEMS, sensors that are able to quantify its inertial dynamics and detect the particle's incipient motion accurately. A well-controlled laboratory flume experiment for assessing the incipient entrainment of the instrumented particle which mimics the behaviour of a naturally rounded pebble resting on a riverbed for a range of flowrates near the threshold of motion is conducted. The logged acceleration readings, after appropriate post-processing, are used to assess the entrainement threshold of the instrumented particle. Appropriate theories that take into account the dynamic characteristics of particle's entrainment are considered to interpret these readings with an ultimate goal of back-estimating hydrodynamic drag which is representative of the hydrodynamic forces acting on the bed-surface.

Keywords: instrumented particle, impulses, MEMS sensors, incipient motion, turbulence.

1. INTRODUCTION

Sediment entrainment is considered to be the governing process in different applications around the fields of geoscience and engineering and therefore has gained a lot of attention in the literature for the past century (Buffington and Montgomery 1997). Therefore, extensive field and laboratory studies exist in the literature for assessing the conditions that can result in initiation of sediment entrainment, namely incipient motion. Different criteria for assessing the incipient entrainment of sediment particles have been suggested by different authors (Shields 1936; Bagnold 1966; Valyrakis *et al.* 2010). Among the different criteria, the impulse (or energy) criterion

is the only criterion that considers both the force magnitude of the near bed turbulent event and it duration are relevant in predicting sediment entrainment. The field and laboratory studies of sediment entrainment are usually performed using expensive tools like Acoustic Doppler Velocimetry (ADV) and particle image velocimetry (PIV). The recent technological advancement has provided researchers in the field of fluvial hydraulics with the ability to directly assess sediment entrainment using low cost tools like micro-electro-mechanical-systems, MEMS, sensors (Valyrakis and Pavlovskis 2014; Valyrakis and Alexakis 2016; Al-Obaidi *et al.* 2020; Al-Obaidi and Valyrakis 2021). Researchers and practitioners alike can benefit from using such low cost sensors in comparison to the expensive velocimetry techniques that indirectly offer estimates of shear stresses that could be linked to sediment entrainment via Shields diagram. Hence, the motivation of this work is to study the application of instrumented particles as low cost tools for assessing near-bed flow hydrodynamics with an ultimate goal of back-estimating hydrodynamic drag which is representative of the hydrodynamic forces acting on the bed-surface.

2. THE INSTRUMENTED PARTICLE

The instrumented particle used in this study is 7 cm in diameter that is embedded with microelectromechanical (MEMS) sensors (a tri-axial accelerometer, a tri-axial gyroscope, and a magnetometer) that record at the same frequency which is adjustable with a range of 100–500 Hz. Depending on the flow conditions and expected particle's response, one can define a sufficient logging frequency (for this study a logging frequency of 150 Hz is selected). The sensors are interconnected forming inertial measurement units (IMUs) with which the particle's inertial dynamics can be precisely quantified.

3. EXPERIMENTS AND RESULTS

A water recirculating flume that is 8 m in length, 0.9 m in width and is able to carry flows of up to 0.4 m deep is used for the study. The particle is placed on micro-topography made of 4 hemispheres forming a triangular arrangement in the test section that is located 2.5 m downstream the outlet and 5.5 m upstream the inlet of the flume. The location of the test section ensures having hydraulically rough fully developed turbulent flow. For a range of flowrate that represents the for near-critical flow conditions, six run are performed to investigate the incipient entrainment of the instrumented particle. A video camera is placed on one side of the flume near the test section in order to record the particle's movements accurately. The logged readings of the sensors (20 minutes for each run) are post-processed using inertial sensor fusion (Kalman filtering) to reduce the uncertainty (by using the readings from one sensor to correct the readings

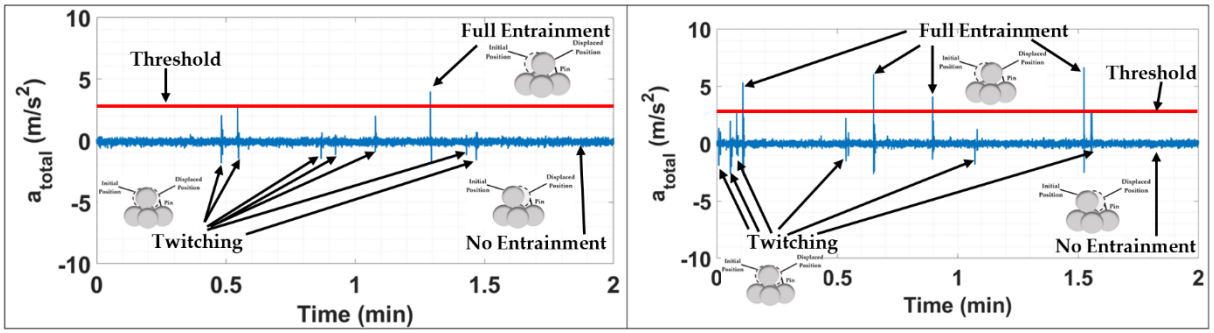

Fig. 1. The corrected total acceleration (estimated by inertial sensor fusion of the logged readings of the instrumented particle) for two runs of the experiment with the red line showing the threshold separating the full entrainments from the twitching events (or the partial entrainments) as validated by the visual assessment.

of the other sensor) and the corrected acceleration readings are used to estimate the total acceleration of the instrumented particle (samples of two minutes are shown in Fig. 1). The total acceleration results are then used to assess the entrainment of the instrumented particle for the six runs of the experiment by defining a threshold value separating the full entrainments from the twitching events (or the partial entrainments) that is validated by manual comparison to the video recordings. Additionally, the acceleration readings are linked to the velocities of the turbulent flow events via relevant theories of flow impulses (Valyrakis *et al.* 2010).

References

Al-Obaidi, K., and M. Valyrakis (2021), A sensory instrumented particle for environmental monitoring applications: development and calibration, *IEEE Sens. J.* **21**, 8, 10153–10166, DOI: 10.1109/JSEN.2021.3056041.

Al-Obaidi, K., Y. Xu, and M. Valyrakis (2020), The design and calibration of instrumented particles for assessing water infrastructure hazards, *J. Sens. Actuator Netw.* **9**, 3, 36, DOI: 10.3390/jsan 9030036.

Bagnold, R.A. (1966). *An Approach to the Sediment Transport Problem from General Physics*, Geophysical Survey Professional Paper 422-I, US Government Printing Office, Washington.

Buffington, J.M., and, D.R. Montgomery (1997), A systematic analysis of eight decades of incipient motion studies, with special reference to gravel-bedded rivers, *Water Resour. Res.* **33**, 8, 1993-2029, DOI: 10.1029/96WR03190.

Shields, A. (1936). Anwendung der Aehnlichkeitsmechanik und der Turbulenzforschung auf die Geschiebebewegung, Ph.D. Thesis, Technical University Berlin.

Valyrakis M., and A. Alexakis (2016), Development of a "smart-pebble" for tracking sediment transport, **In:** *Proc. 8th Int. Conf. Fluvial Hydraulics (River Flow 2016), St. Louis, USA.*

Valyrakis, M., and E. Pavlovskis (2014), "Smart pebble" design for environmental monitoring applications. **In:** *Proc. 11th. Int. Conf. Hydroinformatics (HIC 2014), New York City, USA*, 2684–2687.

Valyrakis, M., P. Diplas, C.L. Dancey, K. Greer, and A.O. Celik (2010), Role of instantaneous force magnitude and duration on particle entrainment, *J. Geophys. Res. Earth. Surf.* **115**, F02006, DOI: 10.1029/2008JF001247.

Received 22 March 2021
Accepted 12 April 2021

Publications of the Institute of Geophysics, Polish Academy of Sciences
Geophysical Data Bases, Processing and Instrumentation
vol. 434 (E-11), 2021, pp. 87-89
DOI: 10.25171/InstGeoph_PAS_Publs-2021-026
Webinar on Experimental Methods and Laboratory Instrumentation in Hydraulics, 13-15 April 2021

The Assessment of Acoustic Doppler Velocimetry Profiler from a User's Perspective

Da LIU, Khaldoon ALOBAIDI, and Manousos VALYRAKIS✉

Water Engineering Lab, School of Engineering, University of Glasgow, Glasgow, UK

✉ Manousos.Valyrakis@glasgow.ac.uk

A b s t r a c t

Acoustic Doppler velocimetry profilers (ADVPs) are widely used in both experimental and field studies because of their robustness in velocity measurements. The acquired measurements offer estimates of the instantaneous flow velocity at the interrogated measurement volume and can also be further processed for the estimation of the bed surface shear stresses and turbulent kinetic energy, thus finding a wide range of applications ranging from water engineering to geomorphology and eco-hydraulics. This study aims to evaluate the performance of an ADVP in obtaining hydrodynamics measurements under fixed flow conditions, with various probe configurations. Different assessment criteria are used for the evaluation including qualitative observations as well as quantitative error metrics to assess the uncertainties in the estimation of shear stresses using log Law of the Wall and turbulent kinetic energy due to the probe configuration settings. The methodology implemented herein, for a given flow, and the suggestions presented represent a generalized hierarchical framework which can find use from practitioners and researchers alike.

Keywords: acoustic Doppler velocimetry profilers, flow velocity, shear stress, turbulent kinetic energy, turbulence.

1. INTRODUCTION

Acoustic Doppler velocimetry (ADV) is widely used as one of the most versatile and robust flow diagnostics tools for both laboratory and field studies across a range of research and applied themes spanning engineering eco-hydraulics and geomorphology. A range of specific ADV probes with varying specifications are readily available for use by professionals and researchers. ADV measures the sampling volume of a water body in the water flow via the Doppler shift caused by the reflection of the pulse transmitted from the centre transducer (the centre beam) and received by the four receiving beams (Nortek 2012; Nortek AS 2015; Kraus et al.

1994). An acoustic Doppler velocimetry profiler (ADVP), i.e. Vectrino II, has the same working principle, but enables profile measurements, which may involve interrogating more than one measurement points, at the same time. Thus ADVPs, may typically have additional parameters that the user may need to define in the probe settings, which even though desirable, may leads to increased uncertainties if there is no generally acceptable guidance to enable their optimal use.

In this work, a series of laboratory experiments have been conducted, under the same open channel flow conditions, using a profiler (ADVP Vectrino II from Nortek®) aiming to cover the full range of probe configuration combinations that can be used in practice. Flow velocities have been measured via the software Nortek Multi-Instrument Data Acquisition System (Vectrino Profiler). The probe configuration in this software contains a few indexes which have some level of dependencies which are altered to identify their impacts on the velocity measurements, velocity profile and the estimated shear stress using these measurements.

2. EXPERIMENTS AND RESULTS

The experiment has been conducted in a rectangular horizontal recirculating flume in the Water Engineering Laboratory at the University of Glasgow. The flume is 1 m wide with glassed sidewalls, and the flume bed consists of a few centimetres high layer of sand with nominal diameter from 0.5 to 2.36 mm (d_{50} = 1 mm) covering the whole flume width. The probe is joined with a vertical gauge, which enables the probe to move vertically. The velocity profiles have been taken at the same lateral location (345 mm away from the sidewall) under the exactly same flow conditions, but different probe configurations. Examples of velocity profiles of selected experiments (different probe configurations) are shown in Fig. 1 below.

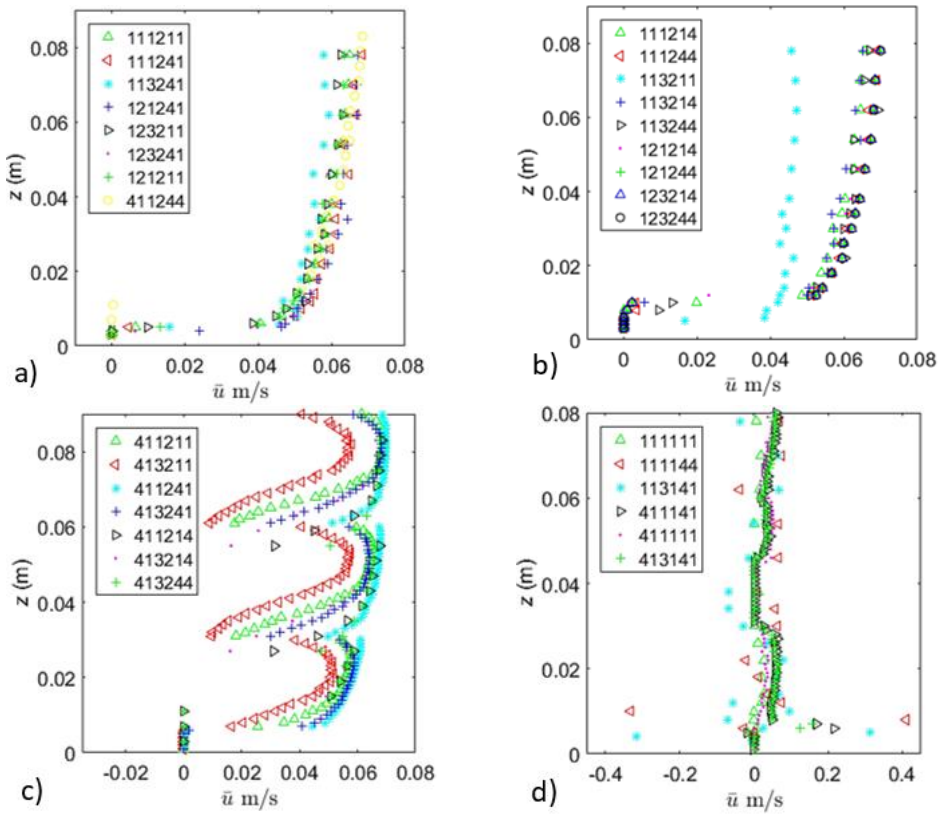

Fig. 1. Velocity profiles of selected experiments: a) “smooth” from visual check and good fit a logarithmic function, b) “smooth” from visual check, c) “curved” from visual check, and d) “random” from visual check.

3. CONCLUSIONS

Velocity profiles are taken at the same location and under the same flow condition with different probe configurations, and the result of mean velocity profile, shear stress estimated using turbulent kinetic energy and log Law of the Wall vary significantly, which clearly shows the dependency between the probe configuration and the results. Results show that overall, the accuracy of Vectrino-II is dependent on probe configurations, and this study provides a framework of preliminary test to find the best probe configuration for the given flow. The value of this research is independent of the exact software or the specific probe because it lays in the framework of optimizing the velocimetry results by tweaking the probe configuration parameters.

References

Nortek (2012), Vectrino profiler user guide, Nortek Scientific Acoustic Development Group Inc., Boston.

Nortek AS (2015), Comprehensive manual, available from: http://www.nortek-as.com/lib/manuals/the-comprehensive-manual (accessed: 22 October 2017).

Kraus, N.C., A. Lohrmann, and R. Cabrera (1994), New acoustic meter for measuring 3D laboratory flows, *J. Hydraul. Eng.* **120**, 3, 406–412, DOI: 10.1061/(ASCE)0733-9429(1994)120:3(406).

Received 22 March 2021
Accepted 12 April 2021

Publications of the Institute of Geophysics, Polish Academy of Sciences
Geophysical Data Bases, Processing and Instrumentation
vol. 434 (E-11), 2021, pp. 91-93
DOI: 10.25171/InstGeoph_PAS_Publs-2021-027
Webinar on Experimental Methods and Laboratory Instrumentation in Hydraulics, 13-15 April 2021

Automated Spectra Separation of Dye Mixtures

José Otávio Goulart PECLY[1,✉] and Carlos Henrique de Paula PAIVA[2]

[1]Federal University of Rio de Janeiro, PENO/COPPE, Rio de Janeiro, Brazil

[2]Federal University of Rio de Janeiro, EQ/POLI, Rio de Janeiro, Brazil

✉ pecly@ufrj.br

A b s t r a c t

Common practices related to the use of fluorescent tracers include multiple dyes in branches of convergent streams, and multiple dyes to compare the performance and to control the quality of the results. Although the control software of spectrofluorometers presents advanced features like multiple peak identification, a spectral separation function is usually not available. It is worth to note that a typical field campaign may result hundred or even a few thousand of samples whose tracers need to be identified and have its concentration measured. To deal with this issue, a set of Python scripts for background subtraction and spectra separation was tested with a dataset of samples with a single tracer and with mixtures of Eosin and Fluorescein. The uncertainty of the results is dependent on the concentration ratio of the tracers in the sample.

Keywords: fluorescence, spectral characteristic, separation method.

1. INTRODUCTION

Field campaigns employing fluorescent tracers provide data to estimate hydraulic parameters or to calibrate water quality models (Romanowicz et al. 2013).

As the spectra of tracers considered safe (Behrens et al. 2001) for application in inland, estuarine, and coastal water bodies present full width at half maximum (FWHM) relatively wide, the analysis of samples with mixture of tracers requires special attention (Käss 1967).

2. MIXTURE SEPARATION METHOD

Typical concentrations in field works are small, ranging from 1 to 20 mg m^{-3} at the sampling sites. These low concentrations, usually quantified by spectrofluorometers, present issues related to peak identification and separation by the instrument companion software or visual spectra inspection (see Fig. 1).

2.1 The experimental dataset

Laboratory work started with the preparation of standard solutions with concentrations of 1, 2, 5, 10, and 20 mg m^{-3} of Eosin and of Fluorescein followed by mixtures of these standards in destillated water. Sample analysis was carried out by the synchronous scanning method.

2.2 Spectra separation

A set of Python functions was built for adjusting Lorentz curves to the measured spectra for each selected tracer which is individually defined by a peak wavelength and by a FWHM.

The application used the least square fitting of the scipy.optimize.curve_fit function. Figure 1 depicts the result of the spectra separation for one sample with a mixture of 2 mg m^{-3} of Fluorescein with 20 mg m^{-3} of Eosin. The differences between the concentrations of the standard samples and those obtained from the adjusted spectrum were 19% for Fluorescein and 1.5% for Eosin, decreasing to 3.5% and 0.5%, respectively, after the application of the method.

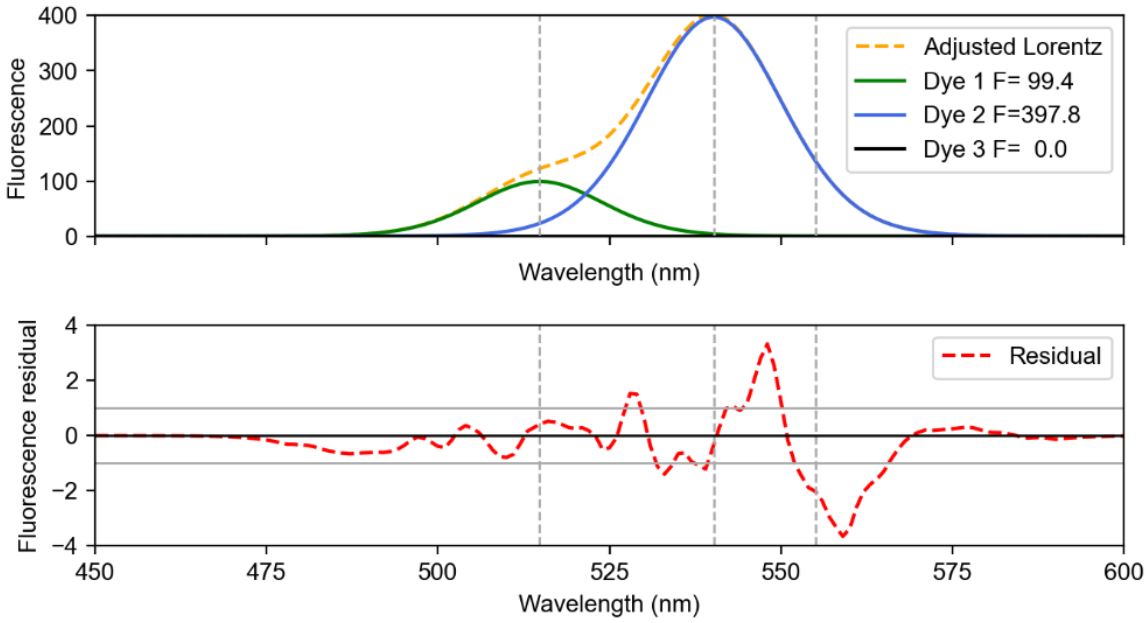

Fig. 1. Spectra of a sample with mixture of tracers: (above) adjusted spectrum by the sum of individual spectra; and (below) difference between the adjusted and the measured spectra.

The differences between the concentrations obtained from the adjusted spectra of samples with a single tracer and the mixture were 1.5% for Fluorescein and 1.0% for Eosin. For higher concentration ratios, e.g. a mixture of 20 mg m^{-3} of Fluorescein with 2 mg m^{-3} of Eosin, the differences between the concentrations of Eosin obtained from the adjusted spectrum were 100% and 6%, before and after the application of the separation method, respectively.

Acknowledgments. The second author acknowledges Fundação COPPETEC for the grants received along the development of this work.

References

Behrens, H., U. Beims H. Dieter, G. Dietze, T. Eikmann, T. Grummt, H. Hanisch, H. Henseling, W. Käss, H. Kerndorff, C. Leibundgut, U. Müller-Wegener, I. Rönnefahrt, B. Scharenberg, R. Schleyer, W. Schloz, and F. Tilkes (2001), Toxicological and ecotoxicological assessment of water tracers, *Hydrogeol. J*. **9**, 3, 321–325, DOI: 10.1007/s100400100126.

Käss, W. (1967), Erfahrungen mit Uranin bei Färbversuchen, *Steirische Beitr. Hydrogeol*. **1966/67**, 123–134.

Romanowicz, R.J., M. Osuch, and S. Wallis (2013), Modelling of solute transport in rivers under different flow rates: A case study without transient storage, *Acta Geophys*. **61**, 1, 98–125, DOI: 10.2478/s11600-012-0050-8.

Received 22 March 2021
Accepted 12 April 2021

Publications of the Institute of Geophysics, Polish Academy of Sciences
Geophysical Data Bases, Processing and Instrumentation
vol. 434 (E-11), 2021, pp. 95-96
DOI: 10.25171/InstGeoph_PAS_Publs-2021-028
Webinar on Experimental Methods and Laboratory Instrumentation in Hydraulics, 13-15 April 2021

Application of Digital Close-Range Photogrammetry to Determine Changes in Gravel Bed Surface due to Transient Flow Conditions

Leszek KSIĄŻEK[1], Bartosz MITKA[1], Magdalena MROKOWSKA[2], Michael NONES[2], Cong Ngoc PHAN[1,✉], Łukasz PRZYBOROWSKI[2], Andrzej STRUŻYŃSKI[1], Szymon WOJAK[1], and Maciej WYRĘBEK[1]

[1]University of Agriculture in Kraków, Faculty of Environmental Engineering and Land Surveying, Kraków, Poland

[2]Institute of Geophysics, Polish Academy of Sciences, Warsaw, Poland

✉ phancongngoc1402@gmail.com

Abstract

In this study, Digital Surface Model (DSM) was created to investigate to what extent unsteady flow affects gravel bed surface in laboratory conditions. Bed elevation was measured before and after the passage of unsteady flow using a Digital Close Range Photogrammetry (DCRP) technique and the processing of photographic data was performed using PhotoScan software. From these preliminary outcomes, it can be concluded that the DCRP technique can be considered as a complementary method to track the changes of gravel beds at the laboratory scale.

Keywords: Digital Close Range Photogrammetry technique, gravel bed surface, Digital Surface Models, transient flow.

1. HYDRAULICS LABORATORY EXPERIMENT SETUP

The experiment was performed in a flume with glass side walls, and bed slope equal to zero in the Laboratory of Faculty of Environmental Engineering and Land Surveying, University of Agriculture in Kraków, Poland. Before every test, the bed material was levelled for 7.5 m with a thickness of around 12 cm. A total of 9 experimental runs were carried out under unsteady flow conditions in a 12-m-long, 0.485-m-wide, and 0.60-m-deep flow-recirculating tilting

(20 Mpix), following a photogrammetry technique similar to one proposed by Faezal et al. (2016) and Stojic et al. (1998). The bed material was classified as average gravel (d_{50} = 3.52 mm). The spatial coordinates (X,Y,Z) of control points (14 CPs) were acquired with a Topcon OS-103 total station. The CPs data was later used to calibrate both the 3D model and the contour plots derived from the DCRP.

A unit of Sony DSC-RX10M4 camera was mounted on a steel bar centrally above the flume width to capture a series of digital images of the channel bed. The distance from the bed has been fixed to 1.4 m and the camera was moved along the longitudinal profile of the flume with a 10 cm interval to capture 64 digital frames of the bed surface.

2. RESULTS

Pre-flow and post-flow bed surface models were compared to each other to determine the bed surface changes. Figure 1 displays the changes of the bed surface between pre-flow and post-flow conditions, for a test with a water discharge Q_{max} = 180 m^3/hand duration of 9′20″.

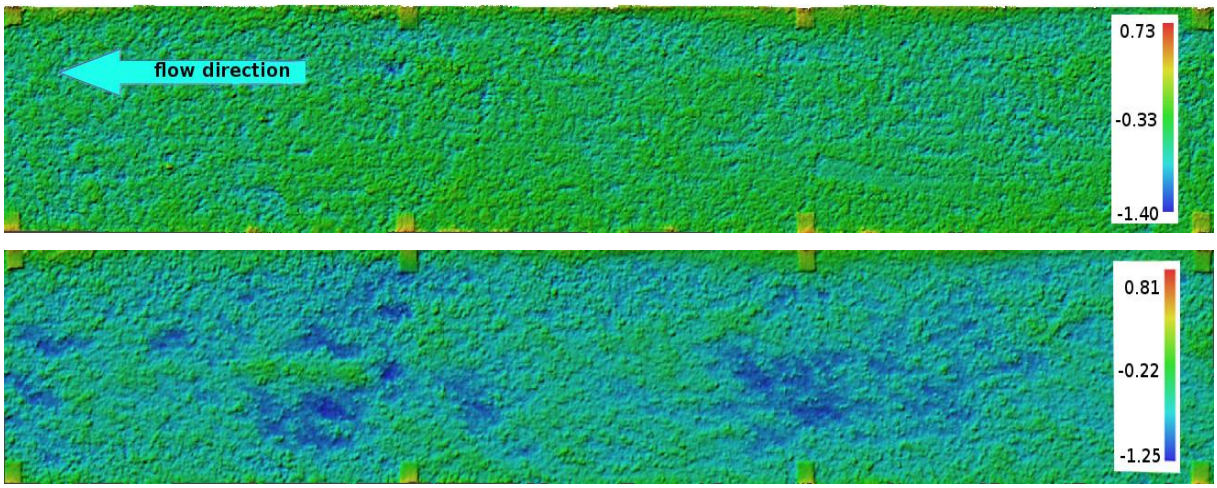

Fig. 1. The bed surface pre-flow (higher frame) and post-flow (lower frame), scale in cm.

The results show that the DCRP technique can be used to determine the bed surface changes, providing distributed information on erosion and accumulation zones. The comparison of pre- and post-flow DSM can also help in computing the total mass transport.

It is worth to note that the DSM have a sub-millimeter accuracy, while the flat sheets of paper used as CPs are reflected with very high accuracy.

References

Faezal, N., F.A.R. Mohd, L.R. Nurul, S. Radzuan, I. Zulkiflee, M. Mushairry, and A.H. Muhammad (2016), Monitoring laboratory scale river channel profile changes using digital close range photogrammetry technique, *Malay. J. Civil Eng.* **28**, 3, 252–266, DOI: 10.11113/mjce.v28.16012.

Stojic, M., J. Chandler, P. Ashrnore, and J. Luce (1998), The assessment of sediment transport rates by automated digital photogrammetry, *Photogramm. Eng. Rem. Sen.* **64**, 5, 387–395.

Received 22 March 2021
Accepted 12 April 2021

Publications of the Institute of Geophysics, Polish Academy of Sciences
Geophysical Data Bases, Processing and Instrumentation
vol. 434 (E-11), 2021, pp. 97-99
DOI: 10.25171/InstGeoph_PAS_Publs-2021-029
Webinar on Experimental Methods and Laboratory Instrumentation in Hydraulics, 13-15 April 2021

Comprehensive Testing of Suspended Sediment Analysis Techniques to Support Monitoring Activities in the Danube River

Flóra POMÁZI✉ and Sándor BARANYA

Budapest University of Technology and Economics,
Department of Hydraulic and Water Resources Engineering, Faculty of Civil Engineering,
Budapest, Hungary

✉ pomazi.flora@emk.bme.hu

Abstract

Establishing and operating a harmonised sediment monitoring system along large rivers such as the Danube is a challenging international task. Our objective is to develop a time- and cost-effective suspended sediment measurement protocol that can be easily carried out in the Upper-Hungarian Danube. In this study, we present the results of the comprehensive testing of direct and indirect (acoustic and optical) suspended sediment analysis methods, during which, we established moderate to strong relationships between the determined suspended sediment.

Keywords: acoustic backscatter, laser diffraction, suspended sediment, turbidimeter.

1. INTRODUCTION

Recent studies along the Danube (e.g. DanubeSediment 2019) pointed out the significance of harmonised suspended sediment (SS) monitoring system along large rivers. In the Upper-Hungarian Danube, the first Hungarian monitoring site with state-of-the-art instrumentation is currently under construction according to international guidelines and recommendations (e.g. Haimann et al. 2014). Our objective is to test different SS analysis methods in order to develop an integrated, time- and cost-effective SS measurement protocol, as the currently used monitoring method (pump sampling at 5 pre-fixed days per year; the suspended sediment concentration (SSC) determined by the evaporation method) is costly and time-consuming, and not suitable for detecting spatial and temporal variability of SS transport characteristics (i.e. SS load (SSL), SSC, particle size distribution (PSD)). As the monitoring site will consist of a near-

bank turbidimeter and a horizontal-looking Acoustic Doppler Current Profiler (ADCP), we tested different acoustic and optical instruments and compared them with the filtration method.

2. MEASUREMENT PROTOCOL

During the field measurements, we took samples with an US P-61-A1 isokinetic sampler according to the multi-point method (in 5 verticals, in 5 measurement points per each). Additionally, an Acoustic Backscatter Sensor (ABS), the LISST-ABS was fixed on the isokinetic sampler to collect acoustic backscatter data from the same point as the physical sampling. In order to calculate the SSL, we carried out flow measurements with a 1200 kHz ADCP instrument. This was supplemented with cross-sectional ADCP measurements. In order to determine the SSC, we tested different direct and indirect methods. We performed the followings: (i) positive pressure filtration (0.45 μm), (ii) laser diffraction analysis using the LISST-Portable|XR, (iii) turbidity measurement using the VELP TB1 portable turbidimeter, (iv) in-situ acoustic backscatter data collection with the LISST-ABS, and (v) calibration of the ADCP relative backscatter.

3. RESULTS AND DISCUSSION

Strong relationships could be established between the filtration method and both the optical methods (LISST-Portable|XR: $R^2 = 0.94$, VELP: $R^2 = 0.97$), and the acoustical LISST-ABS ($R^2 = 0.89$) which means that these indirect instruments can be calibrated with great reliability. However, we found that the reliability decreases above 150–200 mg/L (which occurs during high water regimes) in all three cases. The LISST-Portable|XR is an instrument that can provide information about the PSD as well. According to the results, at this section, the SS material is homogeneously distributed silt, with a mean size of 10–35 μm. Based on our previous study on another Danube section (Pomázi and Baranya 2020), only the LISST-ABS measurements are expected to be sensitive to size effects within this range of particle size.

We examined how the LISST-ABS would work as a near-bank turbidimeter, and established a strong connection ($R^2 = 0.96$) between the calibrated near-bank LISST-ABS concentration and the total cross-sectional SSL. It seems, that the future near-bank turbidimeter will be a suitable instrument of the SS monitoring indeed.

In case of the ADCP calibration, the established relationship is only moderate ($R^2 = 0.60$) and more scattered which could be explained by the calibration process (Gartner 2004) itself as many parameters are needed to be determined (instrument-specific constants and coefficients that depend on water and sediment characteristics). However, we believe that the calibration can be used for qualitative analysis and thus, the spatial and temporal variability of SS monitoring can be enhanced.

References

DanubeSediment (2019), Sediment monitoring in the Danube River, Interreg Danube Project Report, available from: http://www.interreg-danube.eu/uploads/media/approved_project_output/0001/27/659489792a6c2b58c4e322ac8c609943565c3095.pdf.

Gartner, J.W. (2004), Estimating suspended solids concentrations from backscatter intensity measured by acoustic Doppler current profiler in San Francisco Bay, California, *Mar. Geol*. **211**, 3–4, 169–187, DOI: 10.1016/j.margeo.2004.07.001.

Haimann, M., M. Liedermann, P. Lalk, and H. Habersack (2014), An integrated suspended sediment transport monitoring and analysis concept, *Int. J. Sed. Res.* **29**, 2, 135–148, DOI: 10.1016/S1001-6279(14)60030-5.

Pomázi, F.; and S. Baranya (2020), Comparative assessment of fluvial suspended sediment concentration analysis methods, *Water* **12**, 3, 873, DOI: 10.3390/w12030873.

Received 22 March 2021
Accepted 12 April 2021

Publications of the Institute of Geophysics, Polish Academy of Sciences
Geophysical Data Bases, Processing and Instrumentation
vol. 434 (E-11), 2021, pp. 101-103
DOI: 10.25171/InstGeoph_PAS_Publs-2021-030
Webinar on Experimental Methods and Laboratory Instrumentation in Hydraulics, 13-15 April 2021

Experimental Test Bench for Performance-Assessment of Large Submersible and Dry-Action Pumps Used in Waterways

Joris HARDY[1,✉], Pierre DEWALLEF[1], Sébastien ERPICUM[1], Michel PIROTTON[1], Darren PARKINSON[2], Nigel TAYLOR[2], Chris BARNET[2], Paula TREACY[3], Olivier THOMÉ[1], Pierre ARCHAMBEAU[1], and Benjamin DEWALS[1]

[1]Université de Liège, School of Engineering, Liège, Belgium
[2]Canal & River Trust (CRT), United Kingdom
[3]Waterways Ireland (WI), Ireland
✉ joris.hardy@uliege.be

A b s t r a c t

Pumping in waterways, particularly in artificial canals, is energy-intensive, costly and may be responsible for the emission of large quantities of CO_2. Innovative pumping technologies have the potential to reduce energy consumption; but their performance needs to be thoroughly assessed. This communication presents the design, sizing and construction of an experimental test bench for evaluating the performance of large submersible and dry-action centrifugal pumps typically used in waterways. It enables testing prototype-scale pumps and was designed in close collaboration with stakeholders such as canal operators. This experimental facility is challenging on many aspects given its size, as well as requirements for power supply and for measurement of system efficiency.

Keywords: experimental test bench, waterways, pumps, stainless steel pipe design, flow instrumentation.

1. DESIGN AND SIZING

The overall objective of the test bench is to enable monitoring the efficiency of submersible and dry-action centrifugal pumps under a broad range of operating conditions. The primary goal

being the assessment of pumps typically used for lifting water in artificial waterways, the capacity requirements for the test bench were defined in close collaboration with stakeholders, mostly canal operators. This lead to the following specifications: pressure up to 10 bars, flow rate up to 0.3 m³/s, power supply up to 300 kW and pumps of up to 2 tons in weight (Table 1). Given these specifications, various aspects of the test bench were designed and sized: layout of stainless steel pipes, pipe diameters, water supply system, regulating valve, energy dissipation system, power electronic boxes with safety and emergency systems, pressure measurement devices and release of entrapped air, among others. A closed-loop system was selected. The overall layout is represented in the CAD model shown in Fig. 1. The positioning of dry-action pumps to be tested is sketched on the right side of the figure, while submersible pumps to be tested shall be installed inside the large tank (visible on the left of the figure).

Table 1
Main characteristics of the test bench

Tank characteristics		Pump characteristics		Test bench characteristics	
Weight	3.5 T	Weight max	2 T	Sensors	10+
Capacity	30 m^3	Power max.	300 kW	Area	8 m × 10 m
Diameter	3 m	Flow rate max.	300 l/s	Piping weight	2 T
Height	4.5 m	Pressure max.	10 bar	Height max.	4.5 m

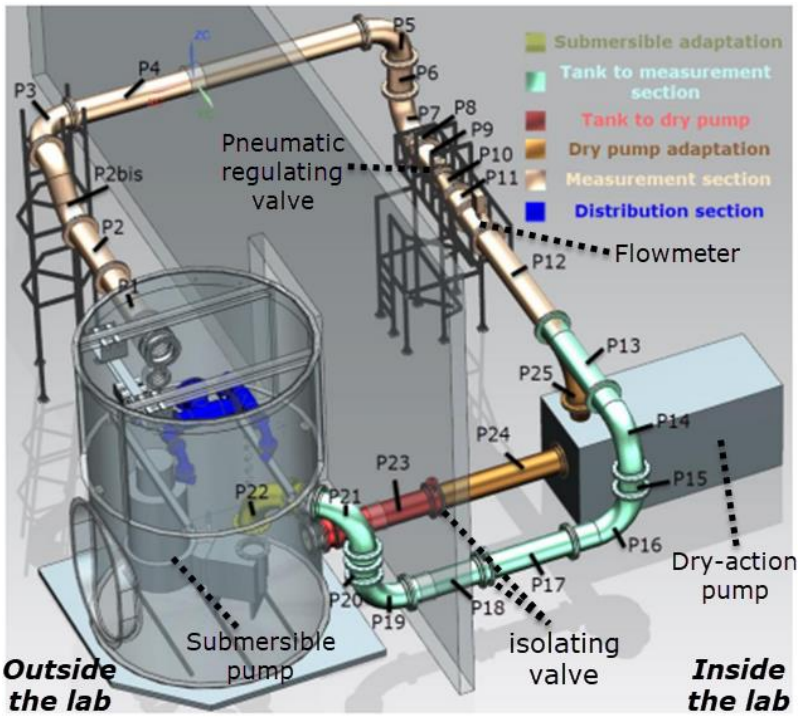

Fig. 1. Layout of the test bench.

The measurement system includes a flowmeter, a regulating valve (to adjust the head), pressure transducers as well as a power analyser and NI data logger. The main pipes have a diameter DN350, allowing friction losses to remain relatively low and ensuring that the diameter of the pump outlet is smaller than the pipe diameter. Sufficiently long straight pipe sections are placed

at the inlet of the flowmeter as well as for the suction pipe of dry-action pumps, to ensure uniform velocity distribution and equalised pressure on the considered section as this helps avoiding swirl conditions.

The diameter and the height of the main tank were determined to prevent swirl conditions at the inlet of the submersible pumps (Sulzer-Pumpen 2010). Given the resulting dimensions (3 m in diameter and 4.5 m in height), the main tank was not available off-the-shelf; but it was manufactured on purpose for the test bench. It is made of stainless steel and its sizing accounts for a variety of constrains, including mechanical strength (finite element simulations were performed to size the curved door and lid), manufacturing process, pump installation procedure and test operations. The door is curved to withstand the inside pressure when the tank is filled with water. The stainless steel sheets are all minimum 6 mm thick. An energy dissipation system, made of several distribution pipes (in dark blue in Fig. 1), is installed at the inlet of the tank to further contribute to avoiding swirl conditions close to the inlet of submersible pumps. A regulating valve is used to adjust the head losses in the hydraulic loop by varying the valve opening angle (between 30° and 70°). Given the specifications on the operation range of the pumps to be tested, a butterfly valve of diameter DN200 was selected.

2. OPERATION

Once a pump is installed, the operating procedure is the same for both submersible and dry-action pumps. The regulating valve and the rotation speed of the pump are electronically steered to browse a range of operating points. The pump is started at its nominal rotating speed, with the lowest opening angle of the regulating valve (30°). While the measurements in the bench are continuously recorded at a high frequency, the opening angle is increased by steps of 10°, up to the maximum flow rate of the pump or the valve maximum opening angle is reached. Then, the operation is repeated in reversed order, by decreasing the valve opening angle by steps of 10°. Next, the pump rotating speed is decreased by a predefined step and the whole operation is repeated again. This enables characterizing steady operating points of the pump for a representative range of heads and rotational several speeds. The characteristic curve of the pump can be redrawn with associated performance for nominal and non-nominal operation. Submersible pumps to be tested are placed inside the tank through the door using a fork truck lift machine and the bridge crane installed at the top of the tank while dry-action pumps are placed inside laboratory.

Acknowledgments. This research is partly supported by ERDF funding in the framework of the Interreg NWE project Green WIN. CRT and WI are gratefully acknowledged.

References

Sulzer-Pumpen (2010), Special data for planning centrifugal pump installations. **In:** Sulzer-Pumpen (eds.), *Centrifugal Pump Handbook*, 3rd ed., Elsevier Science, 91–97.

Received 22 March 2021
Accepted 12 April 2021

Publications of the Institute of Geophysics, Polish Academy of Sciences
Geophysical Data Bases, Processing and Instrumentation
vol. 434 (E-11), 2021, pp. 105-106
DOI: 10.25171/InstGeoph_PAS_Publs-2021-031
Webinar on Experimental Methods and Laboratory Instrumentation in Hydraulics, 13-15 April 2021

Effect of Orientation Angle on Flow Field around Submerged Vertical Square Cylinder Subjected to Steady Current Over Plane Bed

Krishna Pada BAURI and Arindam SARKAR

Indian Institute of Technology Bhubaneswar, Bhubaneswar, Odisha, India

✉ kb13@iitbbs.ac.in; asarkar@iitbbs.ac.in

A b s t r a c t

The experimental and numerical simulation of the three dimensional flow around fully submerged vertical aligned square and circular cylinder due to steady current over plane bed is reported. The focus of the present investigation is toward assessing the flow characteristics and reattachment length around these cylinders. Streamlines around these cylinders are obtained from normalized longitudinal velocity. In addition, power spectra are determined to explain the variation of dominant vortex shedding frequency around cylinders, which is employed to determine the entrainment of the bed sediment particles around these cylinders. The dominant shedding frequency is evident for circular than square cylinder. Results show that the magnitude of the normalized streamwise velocity is 20–40% less for square than circular cylinder. Further, scour prone zone is determined from the bed shear distribution around various cylinders. Bed shear stress is higher for circular than aligned square cylinder. Reattachment length is higher for higher size of the cylinders.

Keywords: alignment angle, fully submerged cylinders, bed shear stress, submergence ratio, reattachment length.

1. INTRODUCTION AND OBJECTIVES

A vertical cylinder turns into fully submerged when the depth of flow is above the cylinder's height. Various investigations were reported, which focus on the flow around the cylinders.

In addition, the majority of the investigations were carried out to measure the flow characteristics around the different shapes of fully submerged structures, but there is deficiency of data on the effect of alignment angle on the flow around square cylinder over plane bed. Moreover, the present study focuses on the variation of maximum bed shear stress around aligned square cylinder over plane bed.

2. MATERIAL AND METHODS

The study provides the measurements of the flow characteristics around submerged vertical cylinders in a rectangular open channel over the plane bed. Further, numerical simulations were carried out to validate the experimental results. Velocity measurement at different sections around the submerged cylinders were carried out using Acoustic Doppler Velocimeter (ADV). Numerical simulations were performed using COMSOL Multiphysics 5.0 with k-ω turbulence closure model. The simulations are also used to investigate the variations of flow characteristics and reattachment length around the submerged cylinders. The simulations show the variation of reattachment length with the variation of submergence ratio, velocity and orientation of the square cylinder. In this study, the steady-state Reynolds Averaged Navier-Stokes equation (RANS) with constant turbulence viscosity for the conservation of mass and momentum equations were used for the simulation of the recirculating flow around the submerged cylinders. The geometry boundary elements were distincted into triangular or quadrilateral. The grid spacing was considered adequate for the convergence of solution and resembled good agreement with the experimental results.

3. RESULTS

Results show that re-attachment length is higher for larger diameter of the cylinder as well as the square side of the square cylinder. Reattachment length is 10–35% more in the case of square cylinder compared to the circular cylinder. The higher recirculation zone is noticed in the mid-depth compared to near the bed and free surface for all the submerged cylinders, whereas the center of the eddy reduces due to increasing of submergence depth for all the submerged cylinders. The flow separation is evident at the top of the fully submerged cylinders below the free surface. Bed shear stress is found to be higher near to the submerged cylinders and it decreases away from the cylinder, which is shown in Fig. 1. Besides, the bed shear increases with alignment angle in the downstream, whereas it decreases in upstream and transverse directions of the square cylinders.

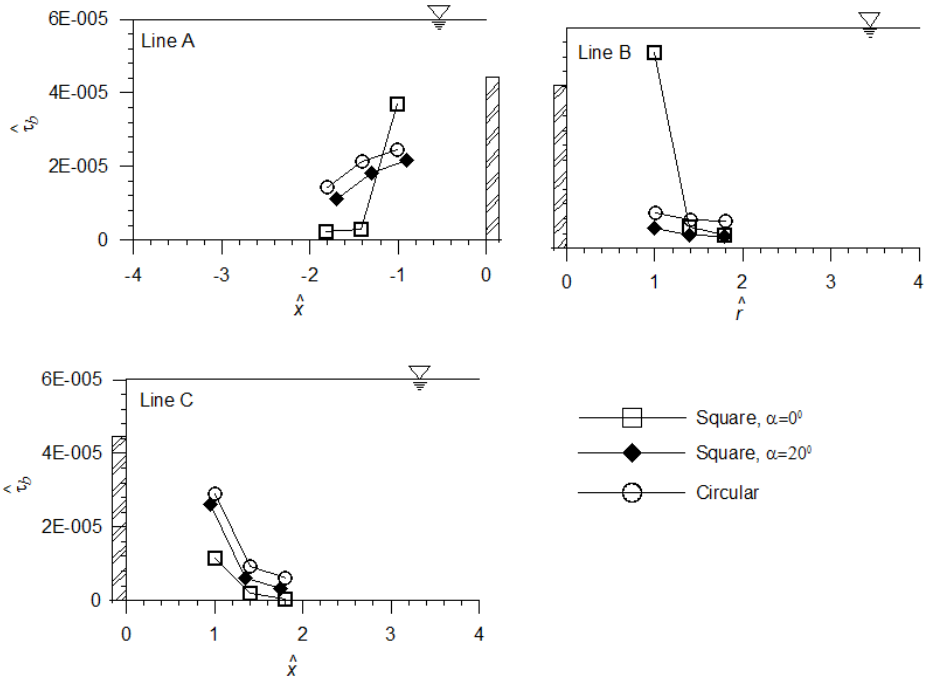

Fig. 1. Variations of normalized bed shear stress ($\hat{\tau}_b$) with $\hat{x}$ and $\hat{r}$: A ($\theta = 0°$), B ($\theta = 90°$), and C ($\theta = 180°$). The peak of power spectra is significant for circular cylinder than square and aligned square cylinder. The peak shows the strength of vortices to transport the bed sediments around the cylinders.

Received 22 March 2021
Accepted 12 April 2021

Publications of the Institute of Geophysics, Polish Academy of Sciences
Geophysical Data Bases, Processing and Instrumentation
vol. 434 (E-11), 2021, pp. 107-109
DOI: 10.25171/InstGeoph_PAS_Publs-2021-032
Webinar on Experimental Methods and Laboratory Instrumentation in Hydraulics, 13-15 April 2021

Assessing Underwater Visibility Conditions in a Large River

Alexander Anatol ERMILOV✉, Flóra POMÁZI, and Sándor BARANYA

Department of Hydraulic and Water Resources Engineering,
Budapest University of Technology and Economics,
Budapest, Hungary

✉ ermilov.alexander@emk.bme.hu

Abstract

In this study, the comparison of measured suspended sediment concentrations, calculated light transmissivity and underwater images was done in order to assess the visibility conditions in a large river and to investigate the opportunities of a possible forecasting methodology that could support diving operations and underwater image processing methods. Further discussion will be made based on the first set of results. The measurements were carried out in the Hungarian section of river Danube.

Keywords: suspended sediment, river, transmissivity, underwater camera.

1. INTRODUCTION

Underwater diving operations in rivers are always hazardous due to the limited visibility conditions and strong currents. Hence, pre-monitoring of the diving sites in terms of physical conditions is essential. Acoustic Doppler Current Profiler (ADCP) measurements not only give information about the flow velocities, but the suspended sediment concentration (SSC) can also be assessed (Pomázi and Baranya 2020), playing an important role in visibility. Moreover, SSC values can provide the so-called optical transmissivity parameter (i.e. the proportion of visible light transmitted through unit distance of the turbid medium) (McCarthy et al. 1974). This could give information for the divers about visibility distance. In this study, we used ADCP measurements to estimate SSC and optical transmissivity in a case study in the Hungarian Danube.

Nowadays, computer vision and image-processing methods are rapidly improving and spreading into more and more field of engineering, for instance, hydraulic engineering. In our earlier study of river Danube (Ermilov et al. 2020), underwater cameras were deployed on the

field to take images of the riverbed and bedload to quantify grainsize distributions and bedload transport rate. These images were used here to validate the calculated optical transmissivities.

2. METHODOLOGY

In a recent study (Pomázi and Baranya 2020), we tested a 1200 kHz ADCP to derive SSC distributions from acoustic backscatter. Time-averaged echo intensity (EI) profile (Fig. 1a) could be determined from fixed-boat ADCP measurement. We performed the calibration by the so-called sonar equation (Gartner 2004), establishing a relationship (R^2 = 0.60) between the relative backscatter and the measured SSC. An example for the calibrated SSC profile is shown on Fig. 1b. Additionally, we analysed the above-mentioned physical samples with the LISST-Portable|XR laser diffraction device applying the Mie-theory for quartz particles. Besides SSC, laser diffraction provides particle size distribution of the suspended sediment in the 0.34–500 μm size range, as well as the optical transmission (%) of the samples. Based on the relationship between the SSC and the optical transmission data, we estimated the vertical variation of transmissivity due to suspended sediment particles (Fig. 1c).

When measuring the sediment conditions along the water columns with ADCP and physical samplings, a camera was also lowered from the measurement vessel. The footages here were used to check the colour range of the infiltrating natural light, depending on the water depth and SSC. The changes in the colour are clearly visible in Fig. 1d. We found, that the boundaries are related to the inflexions of the optical transmission profile. Besides, estimation of visibility distances could also be done to validate the calculated optical transmissivity.

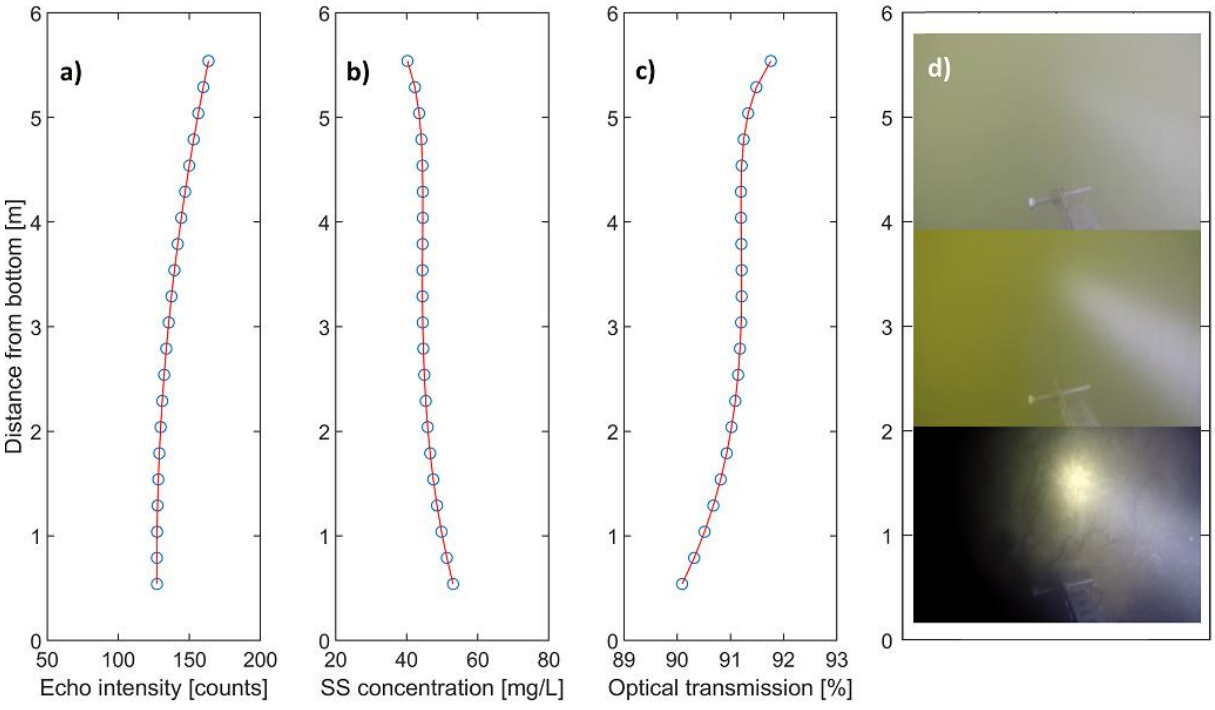

Fig. 1: a) Echo intensity profile, b) calibrated SSC profile, c) optical transmission along the vertical, d) example of images from one vertical, taken during the lowering of the camera (top: close to the water surface, bottom: riverbed).

References

Ermilov, A.A., S. Baranya, and G.T. Török (2020), Image-based bed material mapping of a large river, *Water* **12**, 3, 916; DOI: 10.3390/w12030916.

Gartner, J.W. (2004), Estimating suspended solids concentrations from backscatter intensity measured by acoustic Doppler current profiler in San Francisco Bay, California, *Mar. Geol*. **211**, 3–4, 169–187, DOI: 10.1016/j.margeo.2004.07.001.

McCarthy, J.C., T.E. Pyle, and G.M. Griffin (1974), Light transmissivity, suspended sediments and the legal definition of turbidity, *Estuarine Coast. Mar. Sci.* **2**, 3, 291–299, DOI: 10.1016/0302-3524(74)90019-X.

Pomázi, F.; and S. Baranya (2020), Comparative assessment of fluvial suspended sediment concentration analysis methods, *Water* **12**, 3, 873, DOI: 10.3390/w12030873.

Received 22 March 2021
Accepted 12 April 2021

Publications of the Institute of Geophysics, Polish Academy of Sciences
Geophysical Data Bases, Processing and Instrumentation
vol. 434 (E-11), 2021, pp. 111-113
DOI: 10.25171/InstGeoph_PAS_Publs-2021-033
Webinar on Experimental Methods and Laboratory Instrumentation in Hydraulics, 13-15 April 2021

Flow Characterization around Tandem Piers on Rigid Bed Channel

Laxmi Narayana PASUPULETI✉, Prafulkumar Vasharambhai TIMBADIYA, and Prem Lal PATEL

Sardar Vallabhbhai National Institute of Technology, Civil Engineering Department, Surat, India
✉ laxmiraagini@gmail.com

Abstract

The present study investigated flow characterization around tandem piers of circular shape having diameter (d = 8.8 cm) at different radial angles, θ = 0°, 45°, 90°, 135°, and 180° and compared with single pier of same diameter on rigid bed condition with identical flow conditions. The velocity fields at different depth around piers was measured using Acoustic Doppler Velocimeter (ADV). To characterize the flow, turbulence intensities, turbulence kinetic energy, and Reynolds shear stresses distributions are quantified and plotted for single and tandem piers. The Reynolds shear stresses are increased by 30% around the front pier and decreased by 30% around rear pier in tandem pier arrangement vis-à-vis single pier. In tandem case, turbulence intensity has shown 30% increase in front pier and 30% decrease in rear pier, as compared to the single pier. Further, in tandem arrangement, it has been found that there is significant decrease in the turbulence kinetic energy around the rear pier (≈ 50%) vis-à-vis single pier.

Keywords: tandem arrangement, rigid bed, turbulence intensity, reynolds shear stress.

1. INTRODUCTION

The flow characterization around tandem piers are important to understand flow field dynamics. Several researchers attempted to study the turbulence around tandem piers in the past (Ataie-Ashtiani and Aslani-Kordkandi 2013; Laxmi Narayana et al. 2020). Further, Ataie-Ashtiani and Aslani-Kordkandi (2013) explored turbulence parameters around tandem piers on rigid bed and found that all these parameters are decreasing in tandem case in comparison to isolated case. However, the turbulence characteristics around the tandem piers at different radial angles (θ = 0°, 45°, 90°, 135°, and 180°) was not studied in detail in past. This study is focussed on

characteriation of turbulence fields around tandem bridge front and rear piers on rigid bed condition.

2. EXPERIMENTATION AND METHODOLOGY

The experiments around the single and tandem piers are performed using steel pipe as pier, having diameter 8.8 cm (Fig. 1). The pier is placed at predefined location and water was released into channel using SCADA system; a calibrated flow meter was fitted to inlet pipe to measure the water discharge. At 1 m upstream of the pier, at centreline of the flume, instantaneous 3D velocities were measured using ADV at several vertical positions starting from 0.5 cm above the bed at sampling frequency 40 Hz over a period of 180 seconds. The collected raw signals were post processed to eliminate the possible noise in the signals using phase space threshold technique proposed by Goring and Nikora (2002). The processed velocity signals were checked on Kolmogorov's scale.

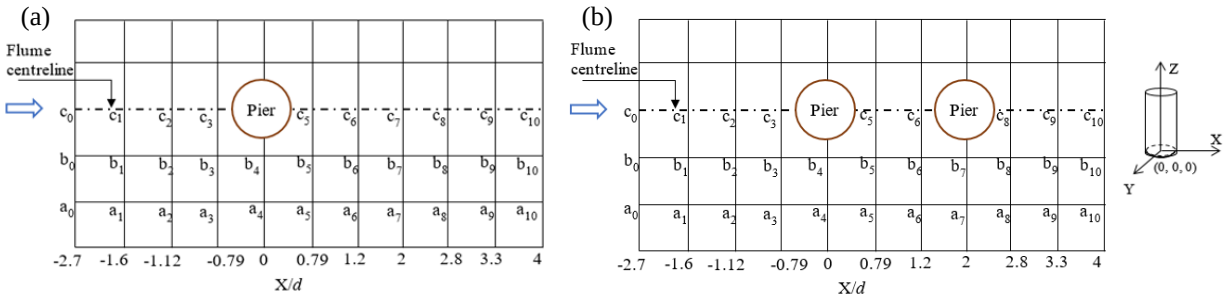

Fig. 1. Schematic of ADV data collection around the (a) single pier, and (b) tandem pier.

3. RESULTS AND DISCUSSIONS

The turbulence kinetic energy, turbulence intensity, and Reynolds shear stresses are computed as per studies of Ataie-Ashtiani and Aslani-Kordkandi (2013). The results revealed that the parameter has been found to increase around $X/d = 2$ in both configurations (X – distance from centre of pier in downstream, and d – diameter of the per). Further, higher turbulence kinetic energy has been found for single pier condition vis-à-vis tandem pier. Also, it is seen that, the parameter is maximum at $\theta = 180°$ (θ is measured from positive X-axis passing through centre of pier in anticlockwise direction).

The analysis of Reynolds shear stresses revealed that, as the flow approaches the pier, the component $\frac{-\overline{u'w'}}{U^2}$ is maximum at $\theta = 0°$ due to the downflow created just upstream of the pier. The Reynolds shear stresses have been found to decrease with increase in the angle with minimal value at $\theta = 90°$. The analysis also revealed that, shear stresses are 30% smaller in case of tandem pier vis-à-vis single pier condition.

The analysis of turbulence intensity revealed that, the parameter is increased with increase in the angle in both the cases. It was found that the turbulence intensities behind the single pier ($\theta = 180°$), were strong, due to flow separation. Further, turbulence intensities are found to decrease by 30% behind the front pier in tandem pier condition vis-à-vis single pier condition at the same location.

Acknowledgments. Authors are thankful to Centre of Excellence (CoE) on "Water Resources and Flood Management" of SVNIT Surat funded under TEQIP-II, Ministry of Education (MoE), Government of India, necessary infrastructure support for conducting the experiments.

References

Ataie-Ashtiani, B., and A. Aslani-Kordkandi (2013), Flow field around single and tandem piers, *Flow Turbul. Combust*. **90**, 3, 471–490, DOI: 10.1007/s10494-012-9427-7.

Goring, D.G., and V.I. Nikora (2002), Despiking acoustic Doppler velocimeter data, *J. Hydraul. Eng*. **128**, 1, 117–126, DOI: 10.1061/(ASCE)0733-9429(2002)128:1(117).

Laxmi Narayana, P., P.V. Timbadiya, and P.L. Patel (2020), Bed level variations around submerged tandem bridge piers in sand beds, *ISH J. Hydraul. Eng*., DOI: 10.1080/09715010.2020.1723138.

Received 22 March 2021
Accepted 12 April 2021

Publications of the Institute of Geophysics, Polish Academy of Sciences
Geophysical Data Bases, Processing and Instrumentation
vol. 434 (E-11), 2021, pp. 115-117
DOI: 10.25171/InstGeoph_PAS_Publs-2021-034
Webinar on Experimental Methods and Laboratory Instrumentation in Hydraulics, 13-15 April 2021

Bedload Transport Quantification using Image Processing Techniques

Alexander Anatol ERMILOV[1,✉], Slaven CONEVSKI[2,✉],
Massimo GUERRERO[3,✉], Sandor BARANYA[1], Nils RUTHER[2], and Gabor FLEIT[1]

[1]Department of Hydraulic and Water Resources Engineering,
Budapest University of Technology and Economics, Budapest, Hungary

[2]Department of Civil and Environmental Engineering,
Norwegian University of Science and Technology, Norway, Trondheim

[3]Department of Civil, Chemical, Environmental, and Materials Engineering, University of Bologna, Bologna, Italy

✉ ermilov.alexander@emk.bme.hu; slaven.conevski@ntnu.no; massimo.guerrero@unibo.it

A b s t r a c t

Image processing techniques we deployed to measure bedload transport characteristics. The bedload velocity was successfully measured and in some cases the bedload concentration and particle size were estimated. Two different approaches were used and good corelations were reported from both the laboratory and the field data. Comparing the field video results to conventional bedload sampling measurements showed promising results for further development of the image-based techniques. Moreover, the captured videos could help understanding the performance of the conventional samplers, pointing out typical sampling errors.

Keywords: sediment transport, image processing, bedload, image velocimetry, bedload monitoring.

1. INTRODUCTION

In the last few decades, various videography techniques have been developed to investigate the behavior of the bedload particles, mostly on a small scale and in controlled conditions. These techniques are usually applied for very weak transports and mostly to examine the incipient motion of the particles. The image processing techniques such as optical flow and image differencing have been successfully applied to calculate the mobile bed velocity, the surface concentration of mobile particles and the shape of the particles when gravel transport takes place, both in laboratory and field environment (Radice et al. 2006; Conevski et al. 2019; Ermilov et

al. 2020). In this study, two image-based methods are implemented and their applicability in various bedload transport conditions is discussed.

2. METHODOLOGY AND RESULT

2.1 Experimental set ups and data post- processing

GoPro cameras (4k, 2.7 k and 1080 p; 30 and 60 fps) were used to record videos for both laboratory and field measurements. In the laboratory the camera was mounted at the centre of the flume filled with sediment material which had a bedload trap at the end measuring the bedload mass at 1 Hz. Three different bedload transport conditions were performed with medium sand (0.35 mm) and fine gravel (7 mm). In the latter case, the device was fixed to a bedload sampler and was lowered from a boat to the riverbed. Underwater lights ensured adequate light source and visibility in both experiments.

The image data processing followed the same procedure as explained in Conevski et al. (2019), involving image enhancement, image de-blurring and applying the image subtraction method (i.e., two-frame change detection). The excluded changes are considered as single particles (e.g., gravel) or fluxes of particles movements.

The second method, applied for the field data, was based on the statistical background method extraction. The method is adaptive, e.g., when a particle settles the background will be updated. Then, the same procedure of subtracting and identifying the background and foreground pixels is applied in both methods. The false pixels were filtered out by using threshold and low pass filtering. Next, the velocities are calculated by using cross correlation methods (i.e., PIV methodology). A cut off velocities derived from the measured water velocities were used to screen the final velocity outputs. The particle size (e.g., gravel bed) and the bedload concentration (e.g., sandy bed and sand-gravel) were calculated based on the detected foreground pixels.

2.2 Results and discussion

Good correlation coefficients (Pearson), between bedload transport rate and the camera measured velocities, were observed in both lab ($r \sim 0.8$, Fig. 1a) and field study ($r \sim 0.6$). The measurement with sandy sediments gave higher deviation due to the random resuspension of particles from the bedload. By considering a characteristic sediment density and converting the particle size from pixel to millimetres, the mass of the bedload transport was estimated (Fig. 1b).

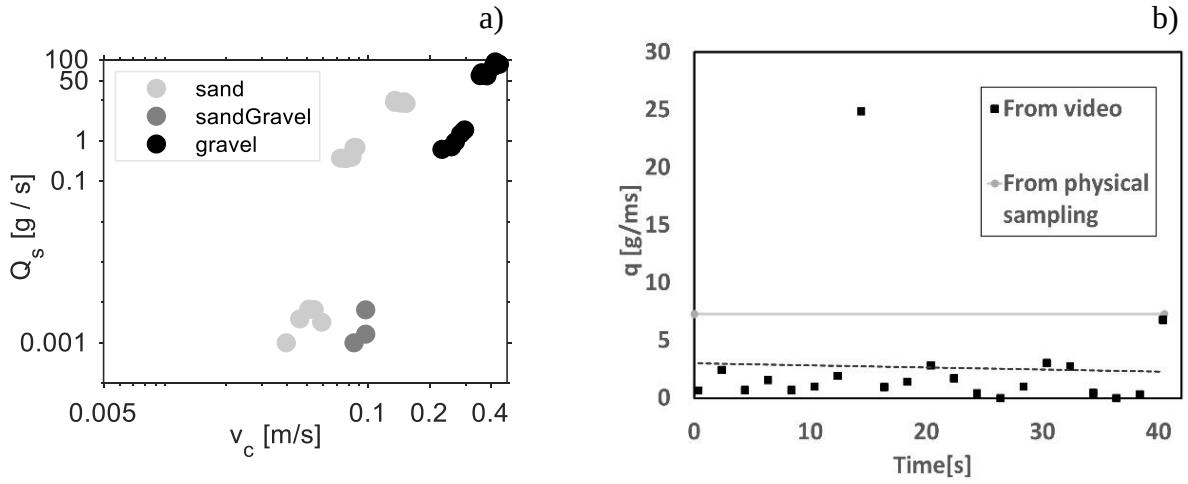

Fig. 1: a) Camera velocities vs bedload transport rate (lab), b) field data – calculated mass of bedload per unit width (field).

The different methods and their results highlighted the possible limitations (e.g. high suspended sediment concentration – poor visibility). Nevertheless, at lower sediment transport conditions, image-based techniques are for a good alternative and can significantly decrease the time- and labor demand of bedload sampling measurement campaigns.

References

Conevski, S., M. Guerrero, N. Ruther, and C.D. Rennie (2019), Laboratory investigation of apparent bedload velocity measured by ADCPs, *J. Hydraul. Eng.* **145**, 11, DOI: 10.1061/(ASCE)HY.1943-7900.0001632.

Radice, A., S. Malavasi, and F. Ballio (2006), Solid transport measurements through image processing, *Exp. Fluids* **41**, 5, 721–734, DOI: 10.1007/s00348-006-0195-9.

Ermilov, A.A., S. Baranya, G. Fleit, and G.T. Török (2020), Developing image-based methods for analysing morphodynamics in large rivers, *Hidrológiai Közlöny* **100**, 3, 74–86.

Received 22 March 2021
Accepted 12 April 2021

Publications of the Institute of Geophysics, Polish Academy of Sciences
Geophysical Data Bases, Processing and Instrumentation
vol. 434 (E-11), 2021, pp. 119-121
DOI: 10.25171/InstGeoph_PAS_Publs-2021-035
Webinar on Experimental Methods and Laboratory Instrumentation in Hydraulics, 13-15 April 2021

Riparian Plants' Morphometry Derived by RGB + Structured-light 3D Scanning within Real Vegetated Flows

Giuseppe Francesco Cesare LAMA✉ and Mariano CRIMALDI

University of Naples Federico II, Department of Agricultural Sciences, Naples, Italy

✉ giuseppefrancescocesare.lama@unina.it

Abstract

The knowledge of riparian vegetation bio-mechanical and morphometric features is one of the main topics in the analysis of the hydrodynamic interaction between riparian plants and water flow in vegetated streams. In this work, the scanning of real riparian plants was performed through a portable device composed of RGB sensors and structured-light 3D scanner, and the outcomes of the 3D image processing in terms of Plant Area Index (PAI) based on Digital Hemispherical Photography (DHP) were compared and then employed in real-scale hydraulic simulations. The results of this study furnish useful insights to ecohydraulic researchers dealing with ecohydraulic experimental analyses and numerical modeling of real vegetated flows.

Keywords: real vegetated flows, 3D scanning, riparian vegetation, morphometry, modeling.

1. INTRODUCTION

Predictive and numerical ecohydraulic modeling of vegetated channels aim at investigating the effect of flow – riparian vegetation interaction on their hydrodynamic behaviour, as pointed out by Lama et al. (2020). The Authors reported that one of the main challenges of ecohydraulics is the knowledge of riparian plants' bio-mechanical and morphometric features in the field. in this context, the easiest way to acquire these properties is embodied 3D scanning of riparian reed beds based on structured-light 3D scanner, a portable device which sensors measures the Near-InfraRed (NIR) pattern projected across reed canopy, while an additional InfraRed sensor captures the reflected light pattern.

2. PRELIMINARY RESULTS

The 3D scanning outcomes in terms of Plant Area Index (PAI) of 20 woody riparian vegetation stands were compared to those based on Digital Hemispherical Photography (DHP) processing. The preliminary results of this work will be employed to simulate a vegetated reclamation channel examined by Errico et al. (2019), which performed hydraulic and vegetation measurements at upstream channel's cross-section equipped with an acoustic Doppler velocimeter (ADV), to estimate the accuracy of the hydraulic simulations by comparing the experimental and modeled flow average velocities U and water levels h. Figure 1 shows the main processing steps of 3D scans for the examined woody riparian vegetation stands.

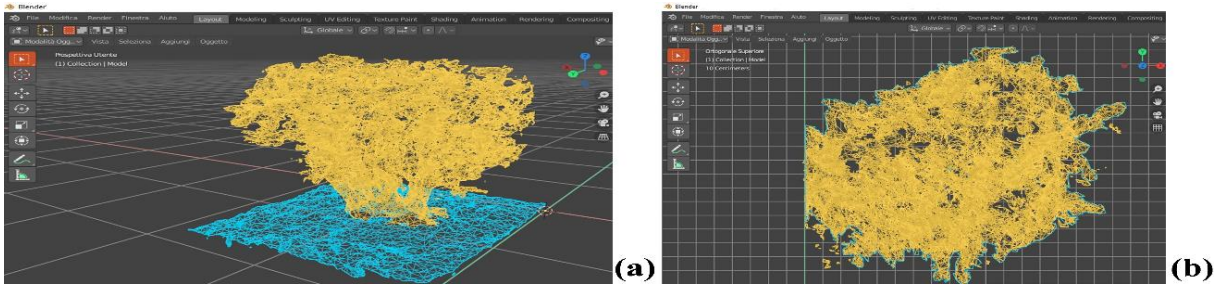

Fig. 1. Examples of 3D scan processing for: (a) soil detection, and (b) PAI estimations.

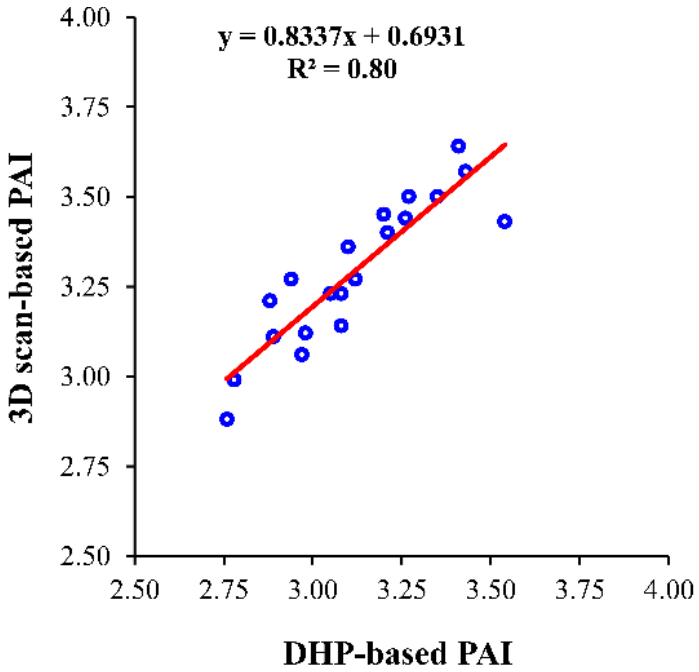

Fig. 2. Comparison of PAI derived by DHP and 3D scanner acquisitions corresponding to 20 woody riparian plants' stands.

In Fig. 2 are shown the accuracy of the hydraulic simulations, performed by comparing the experimental and modeled flow average velocities U and water levels h, expressed in m.

Figure 2 shows that DHP- and 3D scan-based PAI estimations of the 20 examined riparian samples are highly correlated, testified by a coefficient of determination $R^2 = 0.80$.

References

Lama, G.F.C., A. Errico, S. Francalanci, L. Solari, F. Preti, and G.B. Chirico (2020), Evaluation of flow resistance models based on field experiments in a partly vegetated reclamation channel, *Geosciences* **10**, 2, 47, DOI: 10.3390/geosciences10020047.

Errico, A., G.F.C. Lama, S. Francalanci, G.B. Chirico, L. Solari, and F. Preti (2019), Flow dynamics and turbulence patterns in a drainage channel colonized by common reed (Phragmites australis) under different scenarios of vegetation management, *Ecol. Eng*. **133**, 39–52, DOI: 10.1016/j.ecoleng.2019.04.016.

Received 22 March 2021
Accepted 12 April 2021

Publications of the Institute of Geophysics, Polish Academy of Sciences
Geophysical Data Bases, Processing and Instrumentation
vol. 434 (E-11), 2021, pp. 123-125
DOI: 10.25171/InstGeoph_PAS_Publs-2021-036
Webinar on Experimental Methods and Laboratory Instrumentation in Hydraulics, 13-15 April 2021

A Lightweight, Autonomous, Down-looking Wave Gauge Array in Shallow Lakes

Mariann SZILÁGYI[1,✉], Tamás KRÁMER[1], Tibor CINKLER[2], András REHÁK[1], János JÓZSA[1], Marcell CSONTHÓ[2], Zsolt NAGY[2], and Áron JÁSZBERÉNYI[2]

[1]Department of Hydraulic and Water Resources Engineering,
Budapest University of Technology and Economics, Budapest, Hungary

[2]Department of Telecommunications and Media Informatics,
Budapest University of Technology and Economics, Budapest, Hungary

✉ szilagyi.mariann@emk.bme.hu

A b s t r a c t

Spatially and temporally distributed in-situ wave data is difficult or expensive to collect, however, such a dataset is important for understanding wave propagation and validating numerical models. Here we explored an alternative to array of underwater pressure gauges, consisting of cheap and easy-to-install ultrasonic wave gauges mounted on tripods above the water surface, measuring the downward distance, equipped with telecommunication modules and solar panels. In a pilot application, these wave gauges were deployed in a shallow lake, and their data was compared to those collected simultaneously with an underwater, upward looking echosounder. The presented network proved to be able to provide an accurate picture of the sea state at a fraction of the cost of a "professional" instrumentation.

Keywords: wave gauge, acoustic surface tracking, ultrasonic distance measurement.

1. INTRODUCTION

In the presence of patchy emergent vegetation, for example, the wave field has a high spatial and temporal variability, as it is influenced by refraction and diffraction. In order to sample wave characteristics at many frequent combinations of wind and mean water level on the field with high enough likelihood, sufficiently long-term and spatially distributed measurements must be performed. In order to reduce the costs of such a survey, we developed solar-powered,

networked ultrasonic wave gauges, whose low cost make them affordable for array measurements, e.g. in a regular pattern just a few hundred meters from each other. The paper describes the technical details and the validation through a pilot study.

2. MEASURING INSTRUMENTS

Our wave gauges track the distance of the water surface from a fixed point above the water surface with a ubiquitous ultrasonic car parking sensor, same as those integrated into bumpers. The instrument is equipped with a battery, a solar panel, a microcontroller including a time module, an SD card and a radio communication module. Earlier the gauges were successfully operated at a frequency of 1 min^{-1} in order to observe slower wind-induced water level fluctuations in a channel system connected to a lake (Krámer et al. 2020). In this study, the gauges were adapted to measuring wave parameters using 5 Hz sampling frequency.

For validation, we carried out a pilot study in a bay of Lake Fertő (Austria/Hungary). The average water depth of the measurement area was only between 60 and 80 cm. The transducer of the gauges was placed above the water level, on aluminium tripods, looking down vertically towards the water surface. Moreover, a single Nortek Signature 100 acoustic Doppler current profiler placed on a cross-shaped platform on the lake bottom, was operated simultaneously to validate one of the down-looking gauges. Due to the constraining shallowness, the only useable information from this instrument was the ultrasonic surface tracking. Additionally, the wind was recorded close to measuring area by a sonic anemometer placed on a 4 m tall mast.

3. RESULTS

Figure 1 gives insight into the validation through the derived bulk wave parameters from spectra at one of the gauges for a three-day-long period. The Nortek Signature surface tracking was considered an accurate and detailed reference. The estimation of significant wave height H_{m0} from the down-looking gauges was found to be accurate and unbiased. Whereas the wave period

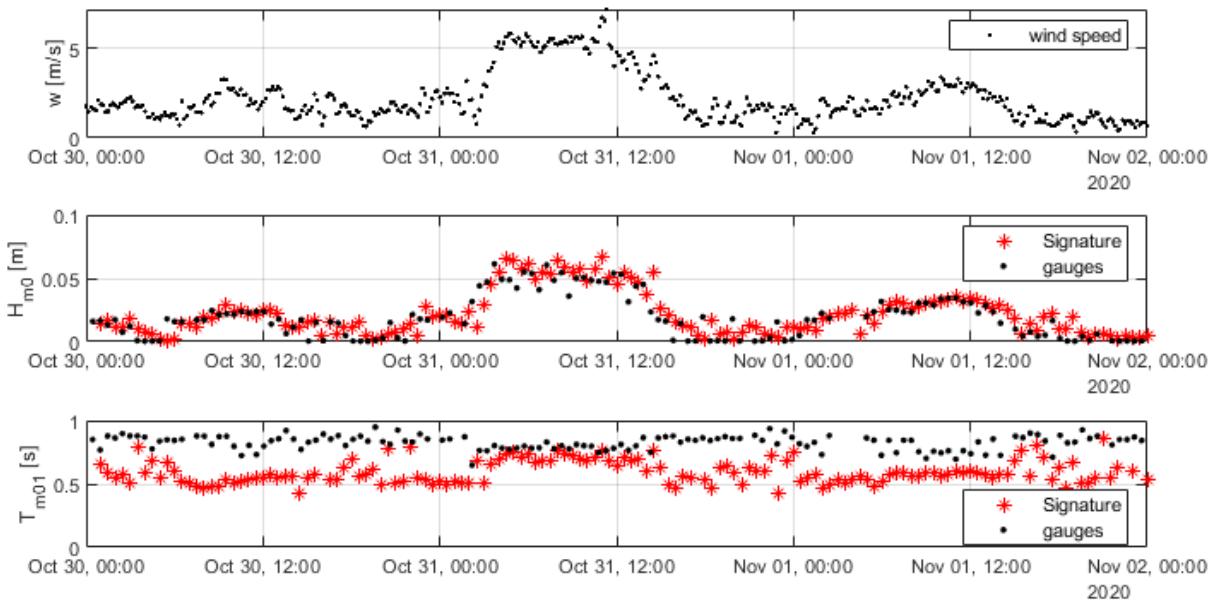

Fig. 1. Measured time series between 30 October and 2 November 2020. From top to bottom: wind speed, significant wave height H_{m0}, and wave period T_{m01}. Red – underwater surface tracking by the Nortek Signature, black – down-looking gauges.

T_{m01} was also quite well resolved during wind speeds exceeding 5 m/s, it was overestimated during calm periods. As is known, unlike H_{m0}, the wave period T_{m01} depends not only on the zero-order, but also on the first-order moment of the power spectrum, and so, it is sensitive to high-frequency noise. The low accuracy during weaker winds is not seen as a major drawback when the impact of waves on sediment motion must be characterised, as waves below 2 centimetres do not generate significant turbulence near the bed anyway.

4. OUTLOOK

The easy deployment and the successful validation of the lightweight down-looking wave gauges encourages their application in lake studies. Thanks to their low cost, the gauges can be deployed in large numbers in this shallow, fetch-limited environment. The solar panels ensure that their operation is autonomous, which helps lower total costs further. As the next step of the development, the low-power wide-area LoRa (Long Range) module installed on the gauges to provide online communication with the gauges will be tested, with the vision of real-time processing and visualisation of the sea state.

Acknowledgments. The research reported in this paper and carried out at BME has been supported by the NRDI Fund (TKP2020 IES, Grant No. TKP2020 BME-IKA-VIZ) and NKFIH-K 120551 of the National Research, Development and Innovation Office.

References

Krámer, T., A. Rehák, J. Józsa, T. Cinkler, M. Csonthó, Z. Nagy, and Á. Jászberényi (2020), Okos tavak [Smart lakes] *Híradástechnika*, **LXXV**, 47–52 (in Hungarian).

Received 22 March 2021
Accepted 12 April 2021

Publications of the Institute of Geophysics, Polish Academy of Sciences
Geophysical Data Bases, Processing and Instrumentation
vol. 434 (E-11), 2021, pp. 127-129
DOI: 10.25171/InstGeoph_PAS_Publs-2021-037
Webinar on Experimental Methods and Laboratory Instrumentation in Hydraulics, 13-15 April 2021

Laboratory Investigations into Stability and Breaching of Rockfill Dams

Geir Helge KIPLESUND✉ and Fjola Gudrun SIGTRYGGSDOTTIR

Norwegian University of Science and Technology,
Department of Civil- and Environmental Engineering, Trondheim, Norway

✉ geir.h.kiplesund@ntnu.no

A b s t r a c t

Laboratory investigations into the breaching of rockfill dams is an ongoing research at NTNU. The current model represents a full dam profile and is a development of earlier models used for investigating stability of rockfill dams and ripraps under throughflow and overtopping situations. Instrumentation of the model includes pore pressure measurements along the dam foundation, water level recording and video recording from multiple angles. Video is used to extract images at intervals throughout the breaching process and 3D models of the breach opening created using "structure from motion" and "multi view stereo" processing techniques. The overall aim is to enhance current knowledge on the breaching of rockfill dams. Modelling of the impervious element is a major challenge for the experiments and the process of finding an appropriate solution to this is described in the present study along with preliminary results.

Keywords: dam breach, rockfill dams, structure from motion.

1. INTRODUCTION

The current research is based on a continuous series of laboratory tests combined with some large-scale field tests and other field investigations starting in 2013. The original focus was on the stability of riprap on dams (Hiller et al. 2018, 2019). Further work was done on riprap stability as well as investigating throughflow in rockfill dams (Ravindra et al. 2019, 2020a,b), and how this affects overall stability and how different toe designs affect throughflow and stability (Kiplesund et al. 2021). One of the important outcomes of this research has been the description of failure mechanisms and quantification of the increased safety provided by dumped and placed ripraps as well as how the factor of safety is affected by the throughflow conditions in the downstream supporting fill. Present work is focused on breach initiation and development

in rockfill dams. To describe breach development beyond the initiation a redesign of the model to incorporate a breachable core element rather than a fixed core as in earlier experiments was necessary. This work discusses the challenge relating to acceptable modelling of the impervious element, i.e. the core, and provides related results from SWOT analysis and pilot experiments. Some observations on breach development can also be drawn at this early stage from the completed tests.

2. EXPERIMENTAL SETUP

The rockfill dam model is situated in a 25 m long flume in the hydraulic laboratories at NTNU. Figure 1 shows the model setup. The breaching process is recorded with strategically located video cameras for creating 3D models using "structure from motion" and "multi view stereo". Additionally, pore pressures along the base, upstream water levels and inflow are recorded. The dam body comprises about 5000 kg of well graded rockfill, scaled from observed rock gradations in existing dams. Two main materials have been tested for the core: a tiled extruded foam core and a rubber membrane. The experiments are ongoing but currently a total of six pilot tests have been carried out. Currently the first test with a riprap protection is about to be performed.

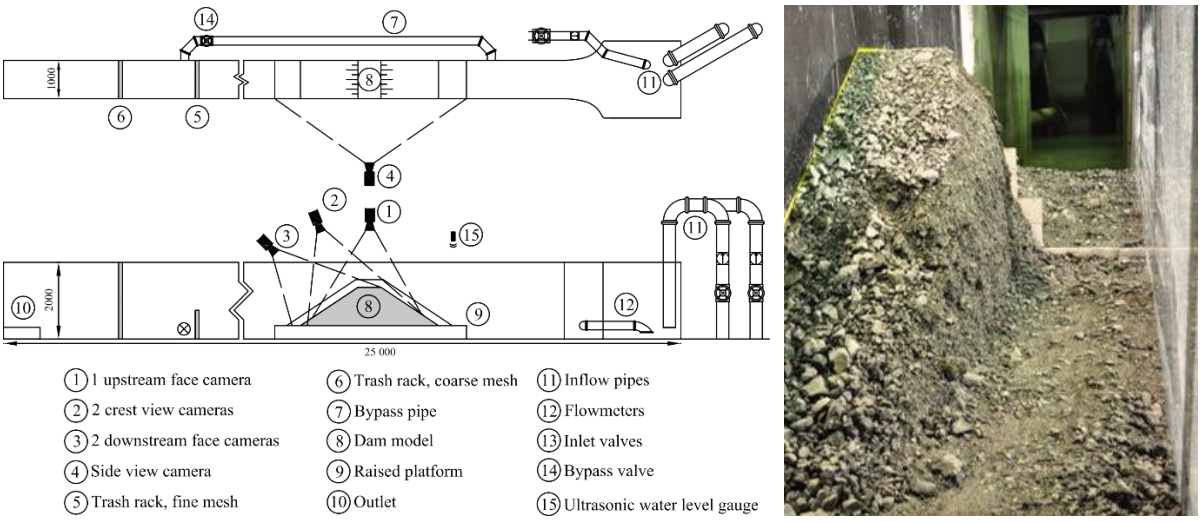

Fig. 1. Laboratory setup (left) and example of breached dam (right).

3. ANALYSIS

There are restrictions on the use of fines in the flume due to a circulation system. Consequently, the conditions do not allow for a realistic modelling of a clayey core. Hence, the main goal of the presented experiments is to realistically model the breach formation in the rockfill itself. Thus, different criteria for a successful test series were defined and included: a realistic phreatic line prior to and during the overtopping situation; reasonable effect of the watertight membrane on the breaching; and ease of separating the core material from the rockfill remains. A SWOT analysis was conducted in the selection process. Furthermore, a work process has been developed to analyse the breach process using 3D models created by extracting synchronized frames from the videos. Through this work many lessons have been learned on optimal camera settings, alignment, number of cameras, lighting, etc.

4. RESULTS

The SWOT analysis aided in modelling strategically the watertight membrane. Analysis of data and videos from the experiments supported the selected strategy and has proven to be important in analysis of the breach process. The main outcome is that the research can continue with the rockfill, adding riprap on the dam slopes to further investigate the effect of riprap erosion protection on the breaching process using the selected instrumentation and tools.

Acknowledgments. Financial support from HydroCen is acknowledged.

References

Hiller, P.H., J. Aberle, and L. Lia (2018), Displacements as failure origin of placed riprap on steep slopes, *J. Hydraul. Res*. **56**, 2, 141–155, DOI: 10.1080/00221686.2017.1323806.

Hiller, P.H., L. Lia, and J. Aberle (2019), Field and model tests of riprap on steep slopes exposed to overtopping, *J. Appl. Water Eng. Res*. **7**, 2, 103–117, DOI: 10.1080/23249676.2018.1449675.

Kiplesund, G.H., G.H.R. Ravindra, M.M. Rokstad, and F.G. Sigtryggsdottir (2021), Effects of toe configuration on throughflow properties of rockfill dams, *J. Appl. Water Eng. Res*., DOI: 10.1080/23249676.2021.1884615.

Ravindra, G.H.R., F.G. Sigtryggsdóttir, and Ø.A. Høydal (2019), Non-linear flow through rockfill embankments, *J. Appl. Water Eng. Res*. **7**, 4, 247–262, DOI: 10.1080/23249676.2019.1683085.

Ravindra, G.H.R., O. Gronz, J.B. Dost, and F.G. Sigtryggsdóttir (2020a), Description of failure mechanism in placed riprap on steep slope with unsupported toe using smartstone probes, *Eng. Struct*. **221**, 111038, DOI: 10.1016/j.engstruct.2020.111038.

Ravindra, G.H.R., F.G. Sigtryggsdottir, and L. Lia (2020b), Buckling analogy for 2D deformation of placed ripraps exposed to overtopping, *J. Hydraul. Res*. **59**, 1, 109–119, DOI: 10.1080/00221686.2020.1744745.

Received 22 March 2021
Accepted 12 April 2021

Publications of the Institute of Geophysics, Polish Academy of Sciences
Geophysical Data Bases, Processing and Instrumentation
vol. 434 (E-11), 2021, pp. 131-132
DOI: 10.25171/InstGeoph_PAS_Publs-2021-038
Webinar on Experimental Methods and Laboratory Instrumentation in Hydraulics, 13-15 April 2021

Assessing the Flow Field around an Oblong Bridge Pier. Vectrino Acquisition Time Sensitivity Analysis

Ana Margarida BENTO[1,2,✉], João Pedro PÊGO[2], Lúcia COUTO[1], and Teresa VISEU[1]

[1]National Laboratory of Civil Engineering, Lisboa, Portugal
[2]Faculty of Engineering of the University of Porto, Porto, Portugal
✉ ana.bento@fe.up.pt

A b s t r a c t

Local scour has been widely identified as one of the primary threats to bridge pier stability. To better understand how the turbulent flow field modified by bridge piers interacts with the bed surface, it is relevant to assess the flow structures that are potentially sufficient to remove the bed material. Thus, the accuracy and measurement quality in estimating the flow field is of primordial importance, mainly in a well-controlled laboratory environment. In the present study, time-averaged velocities and Reynolds shear stresses were measured by using a high-resolution acoustic velocimeter. Due to the highly turbulent nature of the flow, an assessment of the signal acquisition time's influence on the statistics of turbulent quantities is performed, including the inherent uncertainties regarding the flow field measurement technique. The results showed that the required sampling time for mean and fluctuation velocities, and the lateral Reynolds shear stress, differ by one order of magnitude.

Keywords: acquisition time, downlooking vectrino, statistical parameters, velocity measurements.

1. INTRODUCTION

The presence of a scour hole at the vicinity of a pier radically alters the turbulent flow field and its hydrodynamic characteristics. For instance, the bed shear stress and turbulence quantities are strengthened, which induces further sediment transport and scour development at the pier vicinity. The increased horseshoe vortex and the turbulent energy indicate that different mechanisms trigger the flow field structure when a scour hole is present, requiring further research to deepen the understanding of the pier scouring process (Li et al. 2020).

The measurement quality of the turbulent flow field around a bridge pier model, using a high-resolution acoustic velocimeter (also called vectrino), is strongly influenced by three main factors: (i) the signal acquisition time, (ii) the type of seeding particles, and (iii) the alignment of the probe. The current work focuses on the assessment of the signal acquisition time for measuring the flow field and its influence on the statistics of turbulence characteristics.

2. ACQUISITION TIME INFLUENCE

Flow and turbulence characteristics at an eroded bed stage around a 0.14 m wide oblong pier at the flume mid-plane surface were assessed, with respect to the vectrino signal acquisition time, in order to check the time needed to get stable time-averaged values. The local scouring experiment belongs to a campaign composed of six fixed bed experiments performed in a recirculating tilting flume, located in the National Laboratory of Civil Engineering (LNEC), in Lisbon, Portugal (Bento 2021). An acquisition of 30 min with a 4-beam down-looking probe, with 200 Hz of sampling frequency (totalizing 1800 data samples), in a point situated at an upstream distance of 0.09 m from the front edge of the bridge pier (0.20 L and 1.5 W, being L the total pier length, perpendicular to the main flow direction, and W the effective pier width), and at a distance of 0.223 m from the bed surface, were used for this work. The experiment was performed at steady flow conditions and with the introduction of seeding particles into the flow.

Measurements were filtered using ExploreV to reject points with a correlation coefficient less than 70% and signal-to-noise ratio (SNR) less than 15 dB for ensuring the reliability of instantaneous velocity data (Beheshti and Ataie-Ashtiani 2010). The recorded signals were characterized by a mean correlation value of 90% and a mean SNR of 22 dB. A sensitivity analysis of the sampling time for measuring the time-averaged streamwise velocity and fluctuation ($\bar{u}$ and $\overline{u'}$, respectively), and the lateral Reynolds shear stress ($\overline{u'v'}$) was undertaken.

The time needed for the stabilization of $\bar{u}$ and $\overline{u'}$ was lower than one order of magnitude for $\overline{u'v'}$. After 10 seconds, $\bar{u}$ indicated a relative difference of less than 2%, when compared with the time-average value for 0.5 hours of the down-looking vectrino acquired signal. For $\overline{u'}$, a relative difference of 2% was attained after 88 seconds. The variable that required longer time to stabilize was the lateral Reynolds shear stress. For this case, a relative difference of 5% was ensured after 297 seconds of acquisition. These values are in line with studies in the literature, which acquisition times range from 60 to 300 seconds (Li et al. 2020, among others).

Acknowledgments. We express our gratitude to the Portuguese Foundation for Science and Technology (FCT) for their financial support through the Ph.D. scholarship PD/BD/127798/2016 of the first author in the framework of INFRARISK Doctoral Program.

References

Beheshti, A.A., and B. Ataie-Ashtiani (2010), Experimental study of three-dimensional flow field around a complex bridge pier, *J. Eng. Mech.* **136**, 2, 143–154, DOI: 10.1061/(ASCE)EM.1943-7889.0000073.

Li, J., Y. Yang, and Z. Yang (2020), Influence of scour development on turbulent flow field in front of a bridge pier, *Water* **12**, 9, 2370, DOI: 10.3390/w12092370.

Bento, A.M. (2021), Risk-based analysis of bridge scour prediction, Ph.D. Thesis, Faculdade de Engenharia da Universidade do Porto, Porto, Portugal.

Received 22 March 2021
Accepted 12 April 2021

"Publications of the Institute of Geophysics, Polish Academy of Sciences: Geophysical Data Bases, Processing and Instrumentation" appears in the following series:

A – Physics of the Earth's Interior

B – Seismology

C – Geomagnetism

D – Physics of the Atmosphere

E – Hydrology (formerly Water Resources)

P – Polar Research

M – Miscellanea

Every volume has two numbers: the first one is the consecutive number of the journal and the second one (in brackets) is the current number in the series.